WORKSHOP ON

LUNAR VOLCANIC GLASSES: SCIENTIFIC AND RESOURCE POTENTIAL

Edited by

John W. Delano and Grant H. Heiken

Held at

Lunar and Planetary Institute

Houston, Texas

October 10 - 11, 1989

Sponsored by

Lunar and Planetary Institute

Lunar and Planetary Sample Team

Lunar and Planetary Institute 3303 NASA Road 1 Houston, Texas 77058-4399

LPI Technical Report Number 90-02

Compiled in 1990 by the
LUNAR AND PLANETARY INSTITUTE

The Institute is operated by Universities Space Research Association under Contract NASW-4066 with the National Aeronautics and Space Administration.

This report may be cited as:
Delano J. W. and Heiken G. H., eds. (1990) *Workshop on Lunar Volcanic Glasses: Scientific and Resource Potential.* LPI Tech. Rpt. 90-02. Lunar and Planetary Institute, Houston. 74 pp.

Papers in this report may be cited as:
Author A. A. (1990) Title of paper. In *Workshop on Lunar Volcanic Glasses: Scientific and Resource Potential* (J. W. Delano and G. H. Heiken, eds.), pp. xx-yy. LPI Tech. Rpt. 90-02. Lunar and Planetary Institute, Houston.

This report is distributed by:

ORDER DEPARTMENT
Lunar and Planetary Institute
3303 NASA Road 1
Houston, TX 77058-4399

Mail order requestors will be invoiced for the cost of shipping and handling.

Contents

Preface

This report documents the "Workshop on Lunar Volcanic Glasses: Scientific and Resource Potential" that was held at the Lunar and Planetary Institute on October 10-11, 1989. This workshop on lunar mare volcanism was the first since 1975 to deal with the major scientific advances that have occurred in this general subject, and the first ever to deal specifically with volcanic glasses. Forty-five scientists attended and made 26 presentations.

Lunar volcanic glasses are increasingly being recognized as our best geochemical and petrologic probes into the lunar mantle. Lunar volcanic glasses, of which 25 compositional varieties are presently known, appear to represent primary magmas that were produced by partial melting of differentiated mantle source regions at depths of perhaps 400-500 km. These high-magnesian picritic magmas were erupted onto the lunar surface in fire fountains associated with the release of indigenous lunar volatiles. The cosmic significance of this volatile component, in an otherwise depleted Moon, remains a lingering puzzle. The resource potential, if any, of the surface-correlated volatile sublimates on the volcanic glass spherules had not been systematically addressed prior to this workshop.

The Organizing Committee consisted of Grant H. Heiken, Los Alamos National Laboratory, and John W. Delano, State University of New York at Albany, chairmen; B. Ray Hawke, University of Hawaii; Chuck Meyer, NASA Johnson Space Center; Paul Spudis, U.S. Geological Survey at Flagstaff; and G. Jeffrey Taylor, University of New Mexico. Logistics and administrative support were provided by the Program Development Office at the

Lunar and Planetary Institute. Special recognition is due LeBecca Simmons, Pam Jones, and the staff of the Publications Services Department at the LPI, as well as Diana Paton at SUNY Albany, for efficiency, professionalism, and good humor during the organization of this important workshop.

John W. Delano and Grant H. Heiken

Program

Tuesday Morning, October 10

8:00 - 9:00	Registration
9:00 - 9:30	Lunar Volcanic Glasses: What Do We Know About Them From Sample Studies? *J. W. Delano*
9:30 - 10:00	Lunar Explosive Volcanism: The Remote Sensing Perspective *C. R. Coombs B. R. Hawke*

TOPIC 1 - GEOLOGIC SETTING
Chairman: Paul Spudis
Summarizer: A. Basu

10:00 - 10:30	Apollo 17 Orange Soil: Interpretation of Geologic Setting *H. H. Schmitt*
10:45 - 11:15	Pyroclastic Volcanism in the Alphonsus Region *C. R. Coombs B. R. Hawke S. Zisk P. Lucey*
11:15 - 11:30	DISCUSSION AND WALK-ON CONTRIBUTIONS

TOPIC 2 - ERUPTION MECHANISMS
Chairman: B. Ray Hawke
Summarizer: Cassandra Coombs

11:30 - 12:00	Origin of Lunar Basalts: A Geophysical Interpretation *J. Arkani-Hamed*

Tuesday Afternoon, October 10

TOPIC 2 - ERUPTION MECHANISMS, Continued

1:30 - 2:00	Phenocryst Content of Mare Volcanics: Inferences for Magma Migration Mechanisms on the Moon *G. J. Taylor*
2:00 - 2:15	DISCUSSION AND WALK-ON CONTRIBUTIONS

TOPIC 3 - PETROLOGY AND GEOCHEMISTRY
Chairman: Arch Reid
Summarizer: John Jones

2:15 - 2:45 Lunar Pyroclastic Soils of the Apollo 17 Double Drive Tube 74001/2
A. Basu D. S. McKay S. J. Wentworth

2:45 - 3:05 Apollo 15 Green Glass I: New Compositional and Petrographic Insight
A. M. Steele R. L. Korotev L. A. Haskin

3:05 - 3:25 Apollo 15 Green Glass II: The Elusive Complete Database
A. M. Steele R. L. Korotev L. A. Haskin

3:45 - 4:15 In Search of Ancient Lunar Pyroclastics
S. J. Wentworth D. J. Lindstrom D. S. McKay R. M. Martinez

4:15 - 4:45 Pristine Glasses of Mare Fecunditatis
Y. Jin L. A. Taylor

4:45 - 5:15 DISCUSSION AND WALK-ON CONTRIBUTIONS

Wednesday Morning, October 11

TOPIC 4 - LUNAR VOLATILES
Chairman: Chuck Meyer
Summarizer: Tammy Dickinson

9:00 - 9:15 Literature Review of Observations Pertaining to Condensed Volatile Coatings on Lunar Volcanic Glasses
C. Meyer

9:15 - 9:45 Thermodynamic Calculations of Trace Species in Volcanic Gases: The Possible Applications of New Computer Models to Lunar Volcanic Gases and Sublimates
R. B. Symonds W. I. Rose

9:45 - 10:15 Thermodynamic Models of Trace Metal and Volatile Element Transport by Lunar Volcanism
B. Fegley D. Kong

10:15 - 10:45 DISCUSSION AND WALK-ON CONTRIBUTIONS

TOPIC 5 - RESOURCE POTENTIAL
Chairman: Jack Schmitt
Summarizer: John Delano

11:00 - 11:30 The Optimal Lunar Resource: Ilmenite-Rich Regional Pyroclastic Deposits
C. R. Coombs B. R. Hawke B. Clark

11:30 - 12:00 Resource Potential of Lunar Sulfur
D. T. Vaniman G. H. Heiken

Wednesday Afternoon, October 11

TOPIC 6 - PETROLOGY AND GEOCHEMISTRY
Chairman: Jeff Taylor
Summarizer: John Jones

1:30 - 2:00 — The Source of the Mare Basalt Europium Anomaly: REE Distribution Coefficients for Pigeonite
G. McKay J. Wagstaff L. Le

2:00 - 2:30 — Differentiates of the Picritic Glass Magmas: The Missing Mare Basalts
J. Longhi

2:45 - 3:15 — Secondary Ion Mass Spectrometric Analysis of Glasses: Trace Element Characteristics of Lunar Picritic Glasses and Implications for the Mantle Sources of Lunar Picritic Magmas
C. K. Shearer J. J. Papike K. C. Galbreath H. Yurimoto N. Shimizu

3:15 - 3:45 — Pristine Lunar Glasses: A "Window" Into the Moon's Mantle
J. W. Delano

3:45 - 4:00 — DISCUSSION AND WALK-ON CONTRIBUTIONS

TOPIC 7 - RETURN TO THE MOON
Chairman: Jack Schmitt
Summarizer: B. Ray Hawke

4:00 - 4:30 — Future Geologic Exploration of the Moon
G. J. Taylor P. D. Spudis

4:30 — ADJOURN

Summary of Technical Sessions

TOPIC 1: GEOLOGIC SETTING

Summarized by Abhijit Basu

Three presentations were made dealing with the geologic setting of lunar volcanic deposits. On a global scale, P. Spudis proposed that some dark pyroclastic materials associated with mare basaltic volcanism were deposited on the Moon as recently as 10^9 years ago. C. Coombs focused on localized dark mantle deposits, which are associated with fractures on the floor of the 118-km-diameter Alphonsus Crater. H. (Jack) Schmitt discussed a possible sorting mechanism that may have caused separation of the orange glass spherules from the denser crystal-laden black spherules on the rim of the 80-m-diameter Shorty Crater at the Apollo 17 landing site.

Dark mantle deposits, which are generally believed to have been produced by volcanic fire-fountaining, are not only widespread on the Moon but also appear to span a large age range. Since these unconsolidated deposits cause craters to degrade rapidly, crater counting is not reliable for estimating the ages of these deposits. However, Spudis argued that superposition of dark mantle deposits on datable mare basalt flows establishes a minimum age. He used a calibration curve correlating crater counts on basalt flows with absolute ages. He showed that in Mare Smythii dark mantle deposits are interbedded with basalts that are about 1.5×10^9 years old. In addition, dark mantle deposits with associated basalts occurring on the floor of the crater Taruntius clearly postdate this $\sim 10^9$-year-old crater. According to Spudis, the geomorphologic similarity of all dark mantle deposits, both young and old, suggests that the styles of eruption on the Moon did not change appreciably through time. In response to a question from L. Taylor, Spudis said that Pb and Ar ages of Apollo 12 breccias, as well as the landslide ages of Apollo 17 regolith, constrained the absolute ages of Copernicus (0.9×10^9 years) and Tycho (0.1×10^9 years) in the calibration curve. C. Wood observed that crater counts on the floors of Copernicus and Tycho agree with these ages.

Dark-halo craters and localized dark mantle deposits inside the 118-km-diameter pre-Imbrian Alphonsus Crater in south-central lunar highlands were examined in detail by Coombs and coworkers. Weak echoes in the 3.0-cm radar data indicate that the surfaces of these localized dark mantle deposits are smooth. The dominance of "red" in the UV-visible (0.3-1.1 μm) reflectance spectra suggests a basaltic composition. Moderately deep (~6%) asymmetrical absorption bands in the 1.0 μm region of the near-infrared (0.6-2.5 μm) reflectance spectra indicate dominance of olivine and low-Ca pyroxene in these deposits. Individual deposits are small (~450 km^2) and are associated with prominent fractures and endogenic craters on the floor of Alphonsus. Coombs and coworkers suggest that magma emplacement at depth after crater formation caused uplift of the crater floor and the ensuing violent volcanism. In response to J. Longhi's question, Coombs said that it is not yet possible to determine whether the lava flows and pyroclastic deposits were petrogenetically related.

Schmitt drew attention to the sharp contact between the orange soil (mostly orange glass spherules and clasts, ~35 cm thick) and the black soil below (mostly olivine- and ilmenite-rich spherules and clasts, >45 cm thick) at the rim of the Shorty Crater (station 4, Apollo 17 site). Only the uppermost 10-15 cm show any evidence of surface exposure. The glasses, which are pyroclastic in origin and about 3.6×10^9 years old, must have been buried almost immediately after eruption. Schmitt assumed that the orange and black spherules, and fragments thereof, were homogeneously mixed in the original pyroclastic deposit, which was produced by volcanic fire-fountaining associated with the release of volatiles. He postulated that about 19×10^6 years ago, the Shorty Crater event instantaneously released these trapped volatiles causing fluidization of the buried pyroclastic deposits. Remobilization of these deposits through impact-generated fractures was envisaged by Schmitt as having led to an efficient sorting between the less dense orange glass spherules and the denser crystal-laden black spherules. This scenario might explain the observed sharp contact between these two components at station 4, Apollo 17 site.

TOPIC 2: ERUPTION MECHANISMS

Summarized by Cassandra Coombs

Eruption mechanisms and conditions on the Moon differ from those found on Earth. In addition, the conditions under which an eruption occurs may be locally variable. This session addressed some of these differences and pointed out just how variable the conditions and mechanisms for lunar pyroclastic eruptions may be.

Three presentations were made in this session. The first of these was an invited talk by J. Arkani-Hamed in which he discussed the geophysical state of the Moon and what it implies for the origin and source regions of mare basalts. He began by stating that the major basaltic eruptions on the Moon were not triggered by the impacts that formed the large basins; rather, the

major flows occurred ~100 m.y. after the formation of the major basins.

Arkani-Hamed discussed the asymmetry between the volume of basalts present on the near- and farsides of the Moon and their absence on the southeast side. From the discrepancy between the near- and farside basalts, it was determined that the mare basalts were partially melted at a depth greater than that of the base of the crust and that the farside basalts should be much more viscous than those found on the nearside. A negative Bouguer gravity anomaly present below the nearside highlands units indicates that no mascon is present beneath them.

Electrical conductivity measurements, heat flow experiments, seismic data, and magnetic field measurements were used to model the temperature of the lunar interior. From the model it was determined that the temperature of the upper 300 km of the lunar lithosphere is at present between 400°-800°C. From models of thermal evolution, it appears that the upper 300 km cooled in the last 3 b.y. and that the heat was transported by conduction. The magma was transported through cracks created by global stress and local tension in the viscous upper 400 km of the Moon. Arkani-Hamed ended his presentation with a discussion of the magma source and lateral magma migration.

Schmitt asked about the difference in formation between most of the large basins, which are irregular in shape, and Fecunditatis and Nectaris, which appear to be almost circular. Arkani-Hamed responded that the differences are most likely due to readjustments after impact. Schmitt also mentioned that according to most of the structural data he has seen, there is little or no evidence for compression (or shearing) on the surface. Arkani-Hamed said that many thrust faults have been identified, and therefore compression did occur. M. Cintala asked what Schmitt would call the Lee-Lincoln scarp. Schmitt responsed that he did not know. J. Jones made the final observation that, if Arkani-Hamed is correct, the young volcanic deposits described by Spudis come from a deep source, and he asked whether there is a need to sample these areas. Arkani-Hamed replied that he thought there was a strong, thick column of this "volcanic" material below the mantle.

The second talk was presented by J. Taylor who observed that, in general, phenocrysts grow at depth; however, there are few phenocrysts in lunar samples. As an example, Taylor presented a slide of 14053 and mentioned that it was hard to see large phenocrysts that grew at depth. Why is there such a contrast between the lunar basalts where virtually no phenocrysts are found, and the terrestrial basalts where phenocrysts are abundant? It appears that (1) mare basalt magmas had quite different thermal histories than their terrestrial counterparts; (2) lunar magmas spent less time in magma chambers; and (3) lunar magmas traveled more rapidly from their source regions and/or through hotter rock.

The magma migration rate is 50% faster on the Moon than on Earth due to the reduced gravitational field and lower viscosity of the lunar magmas. Crack propagation rates within the conduit are proportional to one-third the gravity and inversely proportional to magma viscosity. Lunar magma cooling rates also differ from those on Earth. Wider conduits on the Moon would lead to greater eruption rates and imply slower cooling with more material flowing through the channels and more heating of the surrounding wall rock, all of which results in fewer phenocrysts and less fractionation. Fractional crystallization most likely occurred in one or two places: (1) along the walls of the main conduit or (2) in the flows.

Taylor concluded that (1) magma recharge was less effective on the Moon than on Earth due to the rarity of magma chambers; (2) no ilmenite-rich cumulates of any significance were produced in mare lava flows, except possibly in lava lakes; (3) one should look for mantle xenoliths near vents; and (4) perhaps Mg-suite rocks did not form in magma chambers either.

Schmitt started the discussion following Taylor's presentation with a question regarding crack propagation and magma migration rates on the Moon. Taylor responded that since the viscosity of the magma is lower on the Moon, the rates of migration would be faster. Schmitt commented that one should not underestimate the degree of differentiation among the Apollo 12 and 15 rock suites where there is a remarkable amount of olivine present. Longhi noted that there is only one mare basalt (74275) with true xenolith in it, a microdunite. J. Delano mentioned that the high-titanium Apollo 17 station 4 sample, 74275, has a microdunite fragment and olivine megacrysts. A high-resolution microprobe analysis of these olivines by Delano showed that the microdunite was a cognate xenolith that appeared to preserve some information about the pre-eruptive history of the 74275 magma. Schmitt asked if any petrogenetic relationship could be made between the microdunite xenolith and the orange glass, such that 74275 may be from the flow that buried and protected the orange glass. In reply, Delano said that the Fe and Sc in 74275 and 74220 are so different that they appeared not to be petrogenetically related. Longhi suggested that maybe 74275 started off as an orange glass, to which Delano reiterated that the geochemical data suggest 74275 is unrelated to the 74220 orange glass. Spudis asked about the polygonal texture of the olivines in the microdunite, and whether that texture indicated metamorphism. J. Taylor responded that it is possible to recrystallize crystals with strain and generate the observed texture.

The rates and directions of propagation of dikes and magma injection were then discussed. W. Phinney

pointed out that in terrestrial examples dikes may propagate laterally for hundreds of kilometers. Also, evidence shows that (1) dikes radiate outward from the center, and (2) whenever/wherever one finds phenocrysts, the dikes are offset. The phenocrysts tend to pond on one side of the dike and are always on the same side as the constrictions. Furthermore, trace element abundances in samples collected from the chilled margin over a 200-km span are identical. Cintala commented that when one takes a megacryst and recrystallizes it in a strain field it will have the same orientation as the strain field. L. Taylor asked what factors lead to low viscosity. J. Taylor replied that bulk composition and liquidus temperature were the principal factors affecting viscosity. On average, terrestrial basalts are 10 times more viscous than lunar mare basalts. A. Basu then asked what criteria are used to accept a megacryst as a phenocryst. J. Taylor said that it is hard to tell which is which with some skeletal grains. Schmitt questioned if it was worth doing a systematic analysis of the vesicle assemblages in the samples. J. Taylor said that the presence of the vesicles was noted but as yet has not been studied in detail.

Schmitt presented a short walk-on discussion of some of his original lantern slides of the Apollo 17 orange glass deposit displaying the subtle color differences that he had personally observed on the lunar surface at station 4, Shorty Crater.

TOPICS 3 and 6
PETROLOGY AND GEOCHEMISTRY

Summarized by John Jones

A. Basu and coworkers presented new data on the petrology and geochemistry of pyroclastic soils in the double drive tube 74001/2 at station 4, Apollo 17. As shown by earlier workers, a layer of pyroclastic orange glass (74220) overlies, and is in sharp contact with, a layer that is dominated by vesicular, black spherules. These black pyroclastic spheres owe their opacity to tiny crystals that nucleated during quenching of the melt. Basu noted that many of the black spheres display crystallites that grow inward from the periphery, perhaps due to a high amount of dust during the eruption that stuck to the spherules' surfaces creating nucleation sites. These observed differences in the petrologic nature of the pyroclastic deposits were interpreted as being due to variations in volatile abundances, dust content, and plume geometry during the fire-fountaining event(s). Observations by electron microprobe analysis showed the compositional variation among these glasses to be the result of olivine fractionation.

A. Steele and coworkers presented INAA data collected on more than 360 individual spheres of Apollo 15 green glass. In addition to confirming the existence of several compositionally distinct groups of Apollo 15 green glass identified by earlier investigators, Steele discovered systematic geochemical trends (e.g., a strong positive correlation between Co and Sm) for which no interpretations were readily available. This work provided compelling evidence that the petrogenesis of these glasses was more complex than previously appreciated and that much work and thought remained to be done.

S. Wentworth and coworkers had been searching for ancient mare pyroclastics that might occur in old Apollo 16 regolith breccias. Ultra Mg' compositions occur as a rare suite of glasses in these breccias. Although these unusual samples differ strongly from typical mare glasses of volcanic origin, available criteria for distinguishing impact glasses from volcanic glasses are presently inadequate for deciding the origin of these Apollo 16 glasses.

Y. Jin and L. Taylor presented the results of a laborious study that they have conducted on 116 glasses from the Luna 16 landing site. Although most of these glasses were concluded to be of impact origin, Jin and Taylor proposed that a compositionally varied assortment of their glasses may be volcanic. This subset of glasses was observed to be chemically unlike any of the volcanic glasses identified at the Apollo landing sites. As previously noted with respect to the study by Wentworth and coworkers, it was concluded that as more detailed searches are made for extremely rare varieties of volcanic glass, additional criteria must be developed to distinguish impact glasses from volcanic glasses.

G. Ryder showed geochemical data that he had recently collected on a large (i.e., 6-mm diameter) glass spherule from the Apollo 15 Apennine Front. This sample consists of chemically homogeneous orange/brown glass with crystal and lithic fragments embedded in its exterior surface. Based upon measured abundances of siderophile elements such as Ni, Ir, and Au, there is no detectable chondritic contamination and hence this glass may be volcanic. Ryder planned to perform more analyses on this intriguing sample to better constrain its origin.

G. McKay and coworkers presented new experimentally derived partition coefficients for rare earth elements between low-Ca pyroxene and mafic melt. In support of the concept recently advanced by C. Shearer and J. Papike, McKay's results demonstrated that low-Ca pyroxene can have a significant negative Eu anomaly. This added further constraints to the hypothesis of Shearer and Papike that the negative Eu anomaly commonly observed among mare magmas (i.e., mare basalts and volcanic glasses), which reflects Eu depletion in the mantle source regions, may not be the result of plagioclase flotation in the magma ocean forming the highlands crust but rather is due to pyroxene accumulation during the magma ocean event that formed the mantle source regions. Basu disagreed with the Shearer/Papike hypothesis by claiming that in

order to explain both (1) the negative Eu anomaly and (2) the high absolute abundance of Eu and the other rare earth elements in mare magmas, extremely low percentages of partial melting are required if plagioclase played no role. In response, Shearer stated that low degrees of partial melting to produce mare magmas was feasible. L. Nyquist agreed with Shearer by noting that the Apollo 17 high-Ti mare basalts appeared to be products of low percentage partial melting. J. Taylor countered that the mare volcanic glasses have high Mg's that seem best explained by high percentages of partial melting. The issue was left unresolved.

Longhi showed results of calculations that indicate little, if any, petrogenetic link between the picritic volcanic glasses and the less magnesian mare basalts. Specifically, the mare basalts do not, in general, appear to have been produced by fractional crystallization at low pressure of known picritic magmas. Although this apparent absence of a petrogenetic link between these two categories of mare magmas (i.e., basalts and picritic volcanic glasses) may be due merely to incomplete sampling of mare magmas, it might also indicate a real dichotomy of source regions. In support of this latter notion, Delano showed a plot of Sc vs. FeO illustrating that the mare basalts and picritic volcanic glasses define different trends that are suggestive of different mantle reservoirs.

Shearer and coworkers provided a summary of their latest geochemical data acquired on the mare volcanic glasses by ion microprobe. Their trace-element data on the Apollo 15 green glasses were in agreement with those presented in an earlier talk by Steele. A large dataset was also presented on about a dozen other varieties of mare volcanic glass indicating, for example, that the Apollo 14 glasses were derived from deep mantle source regions where small quantities (<1%) of a KREEP-like component had been present. Solid-state convection (i.e., mixing) of the differentiated lunar mantle after the magma ocean event was suggested as a possible mechanism for carrying KREEP into the deep lunar interior.

Delano presented experimental results intended to constrain the oxidation state of the lunar mantle. The strategy involved calibrating the abundance of Cr in lunar melts at spinel saturation as a function of temperature and oxygen fugacity. As shown for terrestrial basalt compositions by earlier investigators, and now for lunar magmas, the abundance of Cr in the melt at spinel saturation is systematically dependent upon T, fO_2. These new data were used to argue that the high Cr abundances observed in mare volcanic glasses could best be explained if the lunar mantle had a low redox state, in contrast to an earlier view by M. Sato that the lunar mantle is relatively oxidized.

TOPIC 4:
LUNAR VOLATILES

Summarized by Tammy Dickinson

A review talk by C. Meyer addressed the following questions: (1) What elements are enriched on the surfaces of the glasses? (2) What was the condensate? (3) Are these elements a possible lunar resource?

Numerous volatile elements are enriched on the glass bead surfaces relative to local basalts and relative to the interior of the glass beads. Elements Zn, Ge, Cd, Tl, Ag, and Br are enriched by a factor of about 100 over local mare basalts; Ga, Pb, Sb, In, Au, Se, and Te are enriched by factors of about 10. Fluorine and Cl are also enriched on the surfaces of the glass beads, but S is not greatly enriched. These observations, along with boiling point data, suggest that the surface-correlated deposits on the volcanic glasses are mixed salts of metal sulfides and halides.

Although the lunar volcanic glass beads are enriched in volatile metals, the glass coatings are depleted relative to typical terrestrial basalts. Thus, it is unlikely that the lunar glass deposits would provide a useful volatile resource for a lunar base. However, the glass beads themselves could be a potential source for ceramics and fiberglass, among other things.

Several questions remain concerning the origin of the volatiles on the lunar glass spheres. A mechanism is needed for enriching some, but not all, volatile elements in these glasses. For instance, why is Ni not enriched on the surfaces of the lunar glasses? Also, the composition of the condensate and the composition of the gas that formed the condensate need to be determined.

The two contributed talks in this session investigated thermodynamic modeling of possible lunar volcanic gases and sublimates. R. Symonds reviewed the modeling of metal transport in high-temperature, terrestrial volcanic fumaroles. The authors have successfully predicted the compositional zoning of the sublimates from the Merapi Volcano in Indonesia and Augustine Volcano in Alaska using their SOLVGAS and GASWORKS models. Their models were applicable to a variety of lunar volcanologic problems: (1) the speciation of major and trace components in lunar volcanic gases; (2) prediction of trace-element concentrations in lunar volcanic gases; and (3) the speciation and origin of lunar volcanic sublimates. However, in order to attack these problems they need additional data that are not yet available for the Moon. For instance, they would like to know the composition of lunar volcanic gases, as well as the composition and mineralogy of lunar volcanic sublimates. They also need to know the pressure and temperature of degassing and the oxygen fugacity.

D. Kong described another thermodynamic model that employed a similar approach to that of Symonds, except that it did not consider fractional condensation. The results showed that, for terrestrial volcanic systems, halides are the most important species for the transport of metals. Also, the calculations suggested that the oxidation state of the assumed gas becomes more reducing with decreasing temperature. Again, in order to apply their model to lunar volcanic gases, more data were needed on the composition of the lunar gas.

The discussion following this session centered on possible ways to obtain the data required to apply these thermodynamic models to lunar volcanic glasses. Some felt that it may be possible to better measure the composition of the sublimates. One might be able to estimate the composition of the gas phase from sealed vesicles within lunar volcanic glasses. It was pointed out that the models would need to be improved to take into account expansion of the gas phase into a vacuum. Additional important questions include (1) What is the source of the volatiles? and (2) Did the volatiles originate from the evolved lunar mantle, or from primitive undifferentiated material deep within the lunar interior?

TOPIC 5: RESOURCE POTENTIAL

Summarized by John Delano

B. R. Hawke and coworkers proposed that regional dark mantle deposits (e.g., Sinus Aestuum), which consist of high-Ti pyroclastic materials tens of meters thick, may have resource potential. In addition to being areally extensive and thick, these deposits are (1) essentially uncontaminated with highlands and other mare components, (2) generally devoid of blocks, (3) well sorted, and (4) loose, unconsolidated material that would allow relatively easy mining. In addition, these thick, unconsolidated materials would be useful for shielding habitation modules to the required depth of about 5 m. Reduction of ilmenite crystals contained in these high-Ti pyroclastics would yield oxygen, iron, and titanium that would be valuable to operations on the lunar surface and in low Earth orbit. Hawke further hypothesized that He^3 and other volatiles might also be present in these deposits in sufficient quantities for utilization. G. Heiken pointed out that since the grain size of the ilmenite crystals in these pyroclastic deposits was probably on the order of only 1 μm, physically concentrating these tiny crystals for an ilmenite reduction process would be difficult.

Heiken and coworkers discussed the resource potential of lunar sulfur, which is known to occur in high-Ti mare regoliths at abundances of about 0.1 wt.%. Since crushing of high-Ti mare basalt is energy intensive, thermal extraction of S from regolith would be preferable. Up to 90% of total S could be extracted by heating to a temperature of 1100°C. The resource potential of S derives largely from its special electrical, chemical, and fluid properties. For example, a sulfur concrete could be a valuable construction material. Liquid SO_2 is a low-temperature, low-viscosity fluid that might be feasible for use in hydraulic systems and as a heat-exchange fluid, despite its extreme toxicity. Batteries using a Na-S electrolyte might also prove to be useful.

J. Jordan discussed the resource potential of He^3 as a fuel for nuclear fusion. He concluded that lunar pyroclastic glasses would, in general, be poor in He^3 due to their lack of exposure to solar wind. In order to identify locations on the Moon having He^3 enrichments, Jordan observed that an excellent correlation existed between ppm He^4 and the product of $\%TiO_2$ and Is/FeO. This indicated that areas consisting of old, high-Ti regoliths that had been extensively exposed to the solar wind would be promising areas of He^3 enrichments.

TOPIC 7: RETURN TO THE MOON

Summarized by B. Ray Hawke

The final topic discussed at the workshop was one close to the hearts of most, if not all, attendees. G. J. Taylor and P. D. Spudis presented a well-received talk concerning the future geologic exploration of the Moon. They described a number of unanswered lunar questions and outlined a strategy for lunar geologic exploration designed to resolve these issues. The plan involved four kinds of geoscience research activities: orbiting spacecraft, global geophysical networks, reconnaissance missions with automated spacecraft that return samples to Earth, and geological field investigations. Special emphasis was placed on the capabilities of robotic field geologists.

The workshop participants agreed that detailed sampling and analysis of lunar pyroclastic deposits would almost certainly provide answers to a variety of major questions concerning the volcanic history of the Moon and the nature of the lunar interior. For example, it should be possible to determine the source of the volatile substances that are present on the surfaces of lunar pyroclastic debris. In addition, many attendees expressed the view that the pyroclastic deposits might prove to be excellent sites for permanent lunar bases.

ABSTRACTS

ORIGIN OF LUNAR BASALTS: A GEOPHYSICAL INTERPRETATION Jafar Arkani-Hamed, Department of Geological Sciences, McGill University, Montreal, Quebec, Canada

Introduction:

Lunar basaltic lava covers about 17% of the Moon's surface with an average thickness of about 1 km, constituting less than 1% of the mass of the lunar crust. Nevertheless, initiation of basaltic volcanism, its duration and spatial distribution, and persistence of lunar mascons for over 3 G.y. provide strong constraints on the thermal evolution of the lunar interior in the last about 4 G.y. This paper reviews the main constraints of the models proposed for the source of the basaltic magma.

Constraints:

Dating of lunar basaltic rocks [e.g. 1] and crater counts [e.g. 2] indicate that basaltic flow on the moon was a very slow process, taking from 300 to about 700 M.y. in a given mare. Existence of flooded craters, such as Archimides, and lack of ejecta of Imbrium and Orientale impacts on the older mare surfaces imply that major mare fillings lagged the respective impact events by about 100 to 200 M.y. The surface topography of mare Tranquillitatis prior to its filling by basaltic lava is satisfactorily explained by slow rising of the impact basin for about a few hundred million years [3]. Detailed analysis of rills and ridges of maria suggest that major basaltic flow was around 3.8-3.6 G.y. ago [4], though basaltic volcanism continued up to about 2.5 G.y. ago These evidence suggest that basaltic magmatism was not an instantaneous response of the lunar interior to large impacts.

Surface distribution of mare basalts [5], positive gravity anomalies over circular basins [6] negative Bouguer anomalies of highlands [7], negative gravity of unfilled basins [8], and lack of shallow moonquake sources beneath the far-side and the SE near-side highlands [9] suggest a close correlation between basaltic flow and large impacts, and lack of significant mascons beneath the highlands. This indicates that basaltic sources in the lunar mantle were activated by impact events and not by local concentrations of radioactive heat sources. Local concentrations of heat sources possibly created through initial differentiation of the Moon and/or by impacts of large planetesimals during the last stages of the lunar accretion [10] should in principle have a random distribution which does not necessarily correlate with the locations of the later event impacts which produced mare basins. Basaltic magmatism generated by such concentrations would result in randomly distributed intrusives and extrusives, and thus mass concentrations which have not yet been observed. Also, localized high concentrations of radioactive elements in the upper 400 km are not supported by either magma ocean or completely molten moon hypothesis both of which produce a spherically symmetric layered moon more efficiently than a laterally heterogeneous one.

The power spectra of the lunar gravity field [7], the physical

liberation of the Moon [11] and the hypocenters of shallow moonquakes [9] imply that major lateral variations of density occur within the upper 400 km and produce shear stresses of about 50-100 bars at these depths [12]. To support lunar mascons and the lateral density variations in the upper mantle for about 3.3 G.Y., the upper 400 km of the lunar mantle requires a minimum viscosity of about 10^{27} poise [13]. Viscosities of about 10^{25}-10^{26} poise were cited for this region during mare filling [14], i.e. period between 4.1 to 3.3 G.y. ago. Bearing in mind the strong temperature dependence of viscosity, these viscosity values provide essential information about the thermal evolution of the Moon, the upper about 400 km of the Moon beneath circular basins has been cold and strong in the last 3.3 G.y.

Electrical conductivity and heat flow measurements [15] indicate a cold lunar upper mantle with temperatures less than 0.75 times the melting temperature in the upper 400 km. Thermal evolution models of the moon calculated on the basis of thermal conduction [16], thermal convection [17] and thermal conduction with simulated convection effects [18] also result in a cold lunar upper mantle. The cold upper mantle prevents diapirism, basaltic magma has reached to the surface through existing cracks or crack propagation a transport which is mainly governed by the stresses in the medium. The major basaltic flow around 3.7 G.y. is interpreted in terms of global expansion of the Moon due to heating of its deep interior [19]. This is based on the assumption that the Moon was formed by accretion of cold planetesimals and that heat transfer in the Moon was by the conduction mechanism. However, a detailed study of global expansion due to thermal evolution and phase changes [20] shows that the time of maximum expansion is not well constrained, it depends on many parameters such as the heat transfer mechanism, the chemical composition, and phases of material constituting the Moon. Furthermore, an initially molten moon model is always in contraction since it cools monotonically [21]. It is therefore plausible to suggest that local expansion induced by local partial melting in the upper 400 km provides a transport mechanism for basaltic volcanism.

Source of Basaltic Magma:

Any model suggested for the origin of basaltic volcanism should satisfy the foregoing criteria. Geochemical analysis of lunar rock samples suggests that basaltic magma was produced by partial melting somewhere in the upper 400 km [22]. It requires about 20-30% partial melting to account for major chemical composition [23]. Such an extensive partial melting may not have taken place in the upper mantle directly beneath circular maria because it reduces the viscosity of this region drastically and the mascons associated with these maria can not be supported for long periods. For example, the mascon associated with mare Serenitatis is due to about 3-4 km basaltic lava, say a cylinder of about 400 km diameter and 3-4 km thickness. Assuming that the extruded lava was the access volume produced due to partial melting, a cylinder of a similar diameter but about 30-40 km thick is needed in the

upper mantle to become 30% partially molten. A gradual heating of such a large region to its melting temperature tends to heat up the surrounding area and thus reduce its viscosity by many orders of magnitude. Furthermore, there is no obvious source of heat generation directly beneath the basins. These regions tend to cool faster than their surroundings [24].

Figure 1 shows a model for the generation of basaltic magma triggered by a large impactor [25]. A large impactor producing circular mare basins excavated the lunar crust down to a depth of 20-40 km and deposited the material on the surrounding area as a loosely bound, highly porous ejecta blanket. The immediate rebound of the upper mantle implaced a plug of about 10-30 km thickness directly beneath the basin, upward displacing the radioactive-rich upper-most part of the upper mantle. The heat produced by the radioactive elements of the plug was conducted to the surface and was lost more efficiently, resulting in a fast decrease of temperature there. However, the loosely bound, porous ejecta blanket with a low thermal conductivity [26] provided a thermal blanket and hampered heat loss. The heat produced by radioactive heat sources in the upper-most part of the upper mantle beneath the ejecta blanket enhanced the temperature and partially melted this region. The resulting basalts transported upward and filled the basin. This simple model accounts for 1) delay in basaltic volcanism relative to impact event, 2) impact triggered lava flow, 3) support of the associated mascon by the cold and strong upper mantle directly beneath the mascon, and 4) local expansion required for magma transport.

References:

[1] Wasserburg, et al. (1977) Phil. Trans. R. Soc. Lond., Series A, 285, 7-21; [2] Baldwin, R.B. (1987) Icarus, 71, 1-18; [3] Solomon, S.C., et al. (1982) J. Geophys. Res., 87, 3975-3992; [4] Solomon, S.C. and J. W. Head (1980) Rev. Geophys. Space Phys., 18, 107-141; [5] Head, J.W. (1976) Rev. Geophys. Space Phys., 14, 265-300; [6] Muller, P.M. and W.L. Sjogren (1968) Science, 161, 680-684; [7] Bills, R.G., and A.J. Ferrari (1980) J. Geophys. Res., 85, 1013-1025; [8] Sjogren, W.L. (1977) Phil. Trans. R. Soc. Lond. Series A, 285, 219-226; [9] Lammlein, D.R. (1977) Phil. Trans. R. Soc. Lond., Series A, 285, 451-461; Goins, N.R. et al. (1981) J. Geophys. Res., 86, 5061-5074; [10] Taylor, S.R. (1982) Planetary Science: A Lunar Prespective; [11] Koziel, K. (1967) Icarus, 7, 1-28; [12] Arkani-Hamed, J. (1973) The Moon, 7, 84-126; [13] Arkani-Hamed, J. (1973) The Moon, 6, 100-111; [14] Baldwin, R.B. (1987) Icarus, 71, 1-18; [15] Hood, L.L. et al. (1982) J. Geophys. Res., 87, A109-A116; Langseth, M.G. et al. (1972) Apollo 15 Prel. Sci. Rept., 11-1, 11-20; [16] Solomon, S.C., and M.N. Toksoz (1973) Phys. Earth Planet. Inter., 7, 15-38; [17] Schubert, G. et al. (1977) Phil. Trans. R. Soc. Lond., Series A, 285, 523-536; Arkani-Hamed, J. (1979) Geophys. J. R. Astron. Soc., 56, 63-80; [18] Tokzos, M.N. et al. (1978) Moon Planets, 18, 281-320; [19] Solomon, S.C. (1978) Geophys. Res. Letters, 5, 461-464; [20] Kirk, R.L., and D.J. Stevenson (1989) J. Geophys. Res., 94, 12,133-12,144; [21] Binder, A.B., and J. Oberst (1985) Earth Planet. Sci.

Letters, 74, 149-154; [22] Taylor, S.R. (1987) American Scientists, 75, 469-477; [23] Binder, A.B. (1982) J. Geophys. Res., 87, A37-A53; [24] Arkani-Hamed, J. (1974) The Moon, 9, 183-209; [25] Arkani-Hamed, J. (1974) Proc. of the Fourth Lunar Sci. Conf., 2673-2684; [26] Huang, J.H. (1971) J. Geophys. Res., 76, 6420-6427.

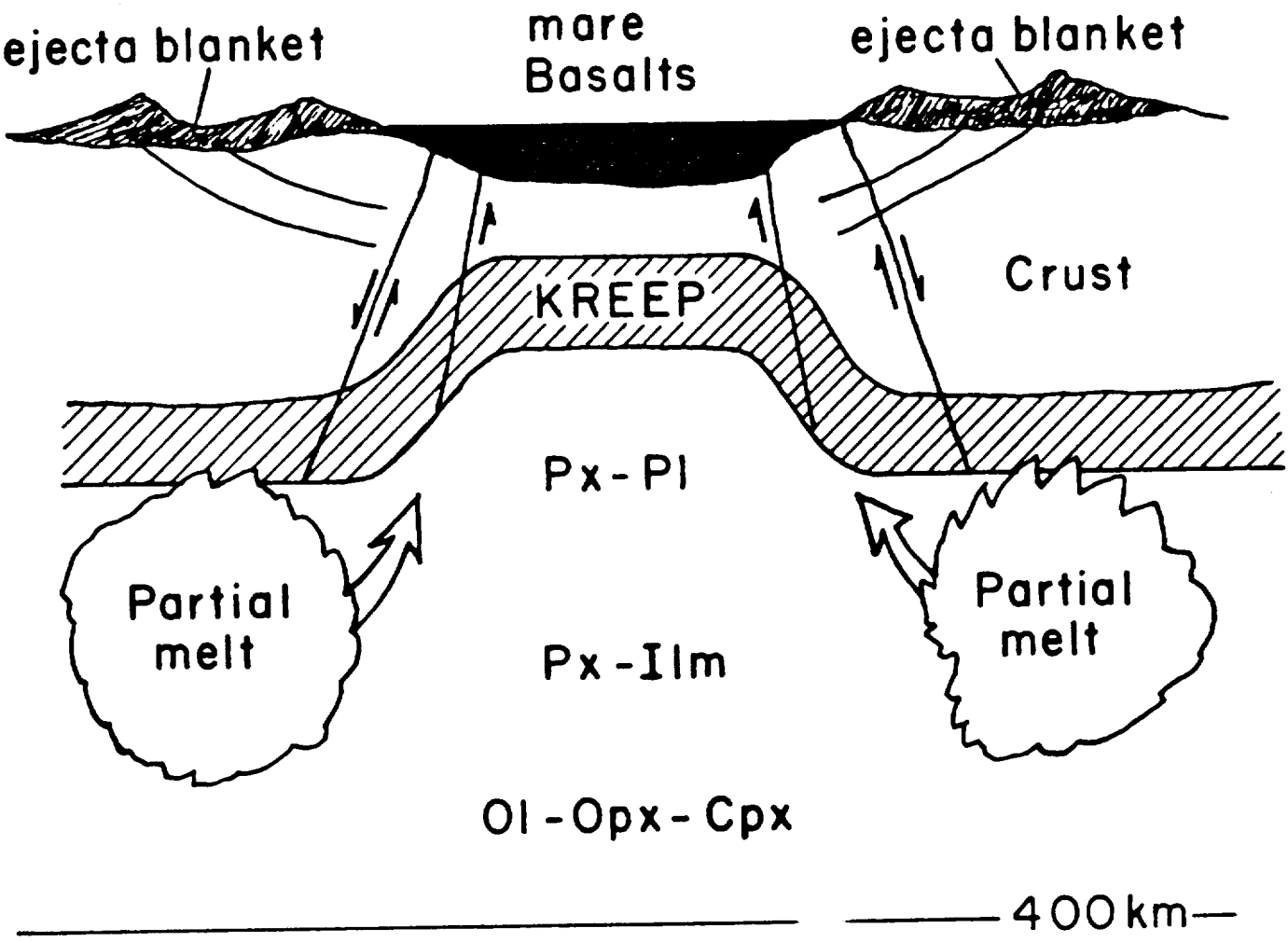
ejecta blanket
mare
Basalts
ejecta blanket
Crust
KREEP
Px-Pl
Partial
melt
Partial
melt
Px-Ilm
Ol-Opx-Cpx
400km

LUNAR PYROCLASTIC SOILS OF THE APOLLO 17 DOUBLE DRIVE TUBE 74001/2

Abhijit Basu, Indiana University, IN. 47405, D.S. McKay, NASA-JSC, and S.J. Wentworth, Lockheed, Houston, TX. 77058

The soils of the double drive tube core 74001/2 below ~5 cm do not contain any agglutinate and are apparently devoid of any measurable surface exposure; they must have erupted and then buried within a matter of hours [1,2,3] and are unique samples of pure lunar pyroclastic material. Only one pair of initial petrologic study of this soil has been carried out [1,2]. The purpose of this note is to present some new data on this soil.

The soil 74001/2 consists of spheres and broken spheres of black, brown, and yellow-orange crystal-laden and crystal-free glass. The black spheres contain many crystallites of ilmenite attached on the external surfaces of euhedral, skeletal and dendritic crystals of olivine. The brown spheres contain crystallites of olivine and most are free from ilmenite. Crystal-free spheres are generally yellow-orange in color as are the glassy parts of crystal-laden varieties. Intermediate varieties are common. Modal analysis shows that the black variety is the most abundant (black: 74%; brown: 20.3% and yellow-orange: 5.6%) and is also largest in size incorporating larger phenocrysts (Table 1). Many spheres contain vesicles and many have crystallites growing inward from the periphery. Such inclusions are much less common in other lunar pyroclastic glasses (Table 2). This suggests that more volatiles (to make gas bubbles) and dust (to provide nucleation sites at the surfaces of droplets) were available during the eruption of 74001/2 than during the eruption and emplacement of orange glass soil (74220) or the green glass soils (15401, 15411, etc.).

Major variations in the chemical compositions of the yellow-orange glass are controlled by olivine fractionation. Glass spheres without olivine crystals have higher Mg/(Mg+Fe) than those with olivine. A plot of calculated Ol-An-Qz proportions shows an olivine fractionation trend (Fig. 1), which does not cross over into the pyroxene field although pyroxene crystals are reported to have crystallized in these droplets. In addition, a plot of TiO_2 *vs.* Mg/(Mg+Fe) does not show sufficient depletion of Fe simultaneously with that of Ti suggesting that ilmenite fractionation has not been significantly responsible for variations in glass compositions (Fig. 2). This interpretation is compatible with the petrographic observation mentioned above. If olivine were to have crystallized in equilibrium with the liquids of the glass compositions, their Fo content would have varied from about 82 to 59 percent (K_D = 0.3 as an approximate average; note that TiO_2 in glass does vary considerably [4]). Interestingly, this is exactly the range of olivine composition reported earlier [2].

Analysis of phenocrysts and skeletal crystals of olivine in the black spheres show a variation of Fo content from about 83% to about 70% with an average CaO content of about 0.3%. Although much of this variation is related to crystal size, some of the phenocrysts show substantial zoning in the Fe/Mg ratio. The zoning is not necessarily concentric in the euhedral phenocrysts where "sector zoning" is more common. Large euhedral phenocrysts (Fo≈80) could be equilibrium crystallization products of the more primitive glass compositions. We envisage that these phenocrysts crystallized in the magma chamber before eruption and were caught, - both intact and fractured, - in the spray of a fire fountain event. The ilmenite attached to these phenocrysts are dendritic in morphology and may have

crystallized, along with dendritic and feathery olivine, even during the flight of the glass droplets [5].

In summary, we find evidence of probably the most volatile-rich and dust-rich eruption on the moon in this pyroclastic soil. Eruption of a mixture of early phenocrysts and the lava must have been rapid and the pyroclasts were covered very quickly. This scenario is essentially compatible with that proposed by Heiken and McKay [6].

REFERENCES : [1] McKay et al., PLSC 9, 1913-1932, 1978; [2] Heiken and McKay, PLSC 9, 1933-1943, 1978; [3] Morris et al., PLSC 9, 2033-2048, 1978; [4] Longhi et al., GCA, 42, 1545-1558, 1978; [5] Arndt and Engelhardt, PLPSC 17, E372-E376, 1987; [6] Heiken and McKay, PLSC 8, 3243-3255, 1977.

Table 1. Modal abundance of glass-sphere-sizes in soil 74001,6038.

Micron Range	Black	Brown	Yl-Orange
<4.7	0	0	0
4.7-9.3	0	3	1
9.3-18.6	0	10	10
18.6-37.2	10	28	29
37.2-74.4	21	40	36
74.4-148.8	50	17	24
148.8-297.6	14	2	0
297.6-595.2	3	0	0
>595.2	2	0	0

Table 2. Glass spheres with and without vesicles and crystals growing from edge inward.

	Crystals		Vesicles	
	Present	Absent	Present	Absent
A.	70	30	42	58
B.	3	39	1	41
C.	0	36	0	36
D.	4	13	0	17
E.	4	49	0	53

A. 74001,6038 (all size); B. 74220,6 (90-150μm); C. 15401,14+16 (250 - 500μm); D. 15411,42 (250-500μm); E. Green Glass (C+D)

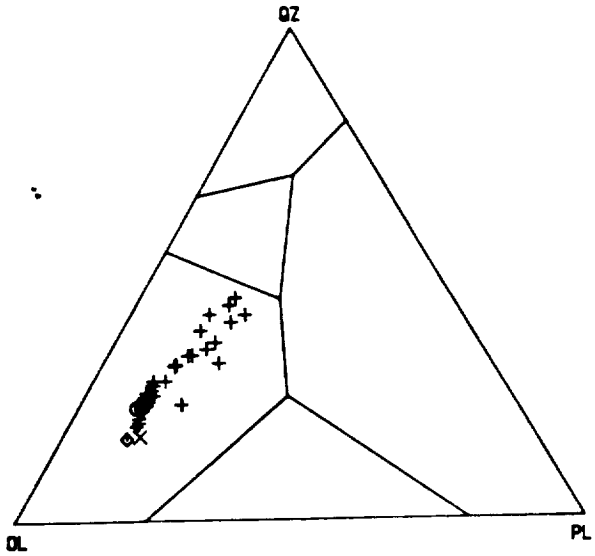

Fig. 1. Recalculated compositions of yellow-orange glass in 74001,6039 plotted in a Qz-Fo-An space; also plotted are compositions of orange glass (74220; ⊙), and the bulk compositions of top (◇) and bottom (X) soils of 74001/2.

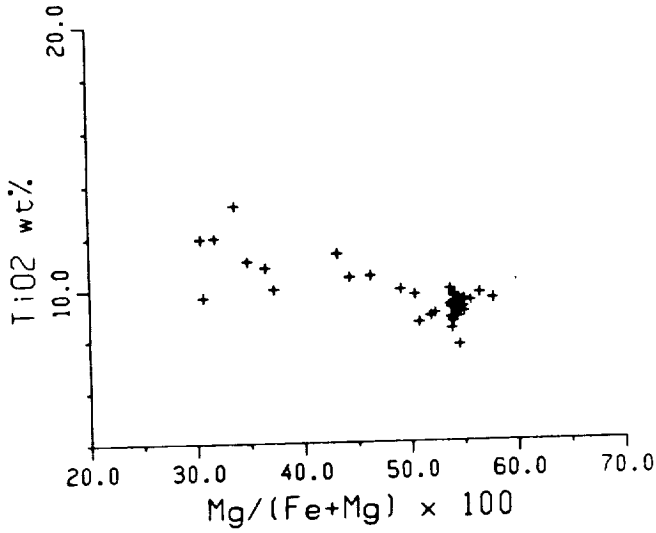

Fig. 2. Plot to show that TiO_2 in the yellow-orange glass in 74001, 6039 does not decrease significantly with an increase in Mg/(Mg+Fe).

LUNAR EXPLOSIVE VOLCANISM: THE REMOTE SENSING PERSPECTIVE

Cassandra Runyon Coombs, SN15, Johnson Space Center, Houston, TX, 77058, B. Ray Hawke, Planetary Geosciences Division, Hawaii Institute of Geophysics, 2525 Correa Rd., Honolulu, HI, 96822.

INTRODUCTION Prior to the Apollo missions our knowledge of lunar pyroclastic deposits was limited. The recent aquisition of remote sensing and geologic data has helped increase our understanding of these deposits and the role they played in resurfacing large portions of the Moon. Two genetically distinct types of pyroclastic deposits have been identified: regional and localized. Eruption mechanisms and emplacement styles for both the regional and localized deposits have been inferred from their source vent morphology, distribution, and the composition and geometry of their mantling deposits. Apollo and Lunar Orbiter photographs, UV-VIS, and near-IR reflectance spectra, albedo maps, multispectral images, 3.0, 3.8, and 70-cm radar images, and compositional data from the returned lunar samples have all been used to compile this summary of what is known to date about the lunar pyroclastic deposits.

REGIONAL PYROCLASTICS Regional dark mantling deposits (RDMD) are located in lunar highland areas adjacent to many of the major maria. These extensive deposits are relatively fine textured with a smooth, velvety appearance,[1,2,3] have a low albedo (0.079-0.096; 4), and typically cover 10's of 1,000's of km^2. RDMD formed as products of fire-fountaining that occurred in association with basaltic eruptions,[e.g., 5] and may have been associated with some of the early mare-filling episodes.[6,7] Depressions at the head of associated sinuous rilles and/or irregular depressions are the probable source vents for these deposits.[e.g., 8,9] Depolarized 3.8-cm radar maps of these features acquired by Zisk *et al.* [8] exhibit weak to nonexistent echoes. These low radar returns are believed to be due to a lack of surface scatterers (i.e., rocks and boulders) in the 1-50 cm size range.[e.g., 11]

Reflectance spectra (0.3 - 1.1 μm, 0.6 - 2.5 μm) and multispectral imagery were obtained for a large number of the RDMD. Analysis and interpretation of the near-infrared spectra indicate that some of these mantling units (i.e., Mare Humorum and Aristarchus) contain a significant Fe^{2+}-bearing glass component. Other regional deposits (i.e., Taurus-Littrow and Rima Bode) appear to be dominated by a mixture of orange and black spheres similar to those returned from the Apollo 17 landing site. [9,10] The Apollo 17 orange glass and their "quench-crystallized" equivalent, the black spheres, are thought to be relatively unfractionated samples of the deep lunar interior(>300 km).[5] These spherules, collected from the distal portion of the Taurus-Littrow RDMD, have a volatile-rich coating. Presumably condensed from gases involved in an explosive eruption, these glass coatings strongly suggest the existence of a volatile gas phase in their source magmas.

Studies have shown that the RDMD were most likely formed as a result of strombolian (continuous) eruption activity rather than the coalescence of localized pyroclastic deposits,[1,12] and that the lunar equivalent of strombolian activity is likely to sort and disperse the pyroclasts over a wide area. Hence, course material would be concentrated in a zone peripheral to the vent while finer debris would be more spread out.

LOCALIZED PYROCLASTICS Localized dark mantle deposits (LDMD) are relatively small (typically <250-550 km^2), low albedo units that are also of pyroclastic origin. These deposits, too, are concentrated about the perimeters of the major lunar maria and are commonly found in the floors of large Imbrian and pre-Imbrian aged impact structures.[e.g.,11,13,14] The LDMD are generally associated with small (< 3 km) endogenic dark-halo craters that are

aligned along crater floor-fractures and/or regional faults. These source craters typically are non-circular in shape and lack obvious crater rays. Morphometric analyses of the LDMD "haloes" suggest a vulcanian-type eruption mechanism, whereby gas accumulates in a capped magma chamber and eventually leads to an explosive eruption and the emplacement of pyroclastic material about the source vent. For these types of eruptions, the maximum range of all pyroclasts much larger than 1 cm is up to 4 km, while the smaller clasts may be thrown up to 10's of kms. Spectral reflectance studies have shown that the LDMD are spectrally distinct[e.g., 13, 14,15] Three general compositional types of LDMD have been identified on the basis of the depth, center and overall shape of the ~1.0 μm absorption features and continuum slopes. ***Group 1:*** Spectra in this group have a "checkmark-like" shape, similar to those obtained for typical lunar highlands areas. A strong feldspar-bearing mafic (orthopyroxene) assemblage is indicated. However, in addition to the highlands spectral geometry of the 1.0 μm band, these Group 1 spectra indicate an additional component of volcanic glass, olivine, and/or clinopyroxene. Multispectral images of this group indicate the presence of an exotic non-highlands component. The Group 1 pyroclastic deposits are most likely composed of a mixture of highlands-rich wall rock and glass-rich juvienile material with lesser amounts of basaltic cap-rock. ***Group 2:*** Spectra of the Group 2 pyroclastic deposits (i.e., from Rima Fresnel, Vitruvius) are deeper and more symmetrical than those in Group 1. A Ca-rich clinopyroxene composition is inferred. These spectra most closely resemble spectra obtained for mature mare areas.[16] Similarly, multispectral images obtained for the Group 2 deposits indicate that they are composed predominately of fragmented basaltic plug rock with much lesser amounts of highlands debris and juvenile material. ***Group 3:*** Spectra from this group include the Alphonsus LDMD as well as J. Herschel and other localities. These broad, asymmetrical and moderately deep spectra are characteristic of a composite feature produced by olivine and pyroxene. The olivine is thought to have been emplaced with the juvenile material while the bulk of the orthopyroxene was emplaced as a component in the highlands-rich wall rock. The basaltic plug rock may also have contributed minor amounts of olivine and pyroxene.

CONCLUSION Eruption mechanisms and emplacement styles for both the regional and localized lunar pyroclastic materials have shown that they are genetically different. A strombolian, or continuous, eruption origin is consistent with the unfractionated, volatile-coated glass samples returned by Apollo 17 and the idea that these originated deep in the lunar interior (> 300 km). The lack of associated lava flows and the small radial extent of the dark-halos around the localized dark mantle deposits suggests that they were formed during a short-lived (vulcanian) explosive eruption. The explosive origin of these volatile-rich pyroclastic materials stands in striking contrast to the massive outpouring of volatile-depleted low-viscosity magma which formed the lunar maria. Thus, lunar pyroclastic mantling deposits are unique among lunar volcanic materials.

REFERENCES (1) Cernan E.A. et al. (1972) *MSC-07629.* (2) Lucchita B.K. (1972) *U.S.G.S. Map I-725.* (3) Lucchita B.K. and Schmitt H.H. (1974) *PLPSC 5th*, pp. 223-234. (4) Pohn H.A. and Wildey R.L. (1970) *U.S.G.S. Prof. Pap. 599-E.* Plate 1. (5) Heiken G.H. et al. (1974) *Geo. Cosm. Acta, 38*, 1703-1718. (6) Howard K.A. et al. (1973) *NASA SP-330*, pp. 29-1 to 29-12. (7) Head J.W. (1974) *PLPSC 5th*, pp. 207-222. (8) Zisk S.H. (1974) *The Moon, 17*, 59-99. (9) Gaddis L.R. et al. (1985) *Icarus, 61*, 461-489. (10) Pieters C.M. et al. (1973) *J.G.R., 78*, 5867-5875. (11) Head J.W. and Wilson L. (1979) *PLPSC 10th*, pp. 2861-2897. (12) Wilson L. and Head J.W. (1981) *J.G.R., 78*2971-300. (13) Coombs C.R. et al. (1987) *HI Sym. on How Volc. Work.* (14) Coombs C.R. and Hawke B.R. (1989) *Proc. Kagoshima Int'L Conf. on Volc.*, 416-419. (15) Hawke B.R. et al. (1989) *PLPSC 19th*, pp. 255-268. (16) McCord T.B. et al. (1981) *J.G.R., 86*, 10883-10892.

THE OPTIMAL LUNAR RESOURCE: ILMENITE-RICH REGIONAL PYROCLASTIC DEPOSITS

Cassandra Runyon Coombs, SN 15, Johnson Space Center, Houston, TX, 77058; Bernard Ray Hawke and Beth Clark, Planetary Geosciences Division, Hawaii Institute of Geophysics, 2525 Correa Rd., Honolulu, HI, 96822.

INTRODUCTION

With the onset of a new space era for the U.S. and a committment to establish a lunar base, the need for lunar resources has increased dramatically. It has been suggested that titanium production might be a profitable activity for a lunar base, and that lunar material would be useful for shielding space habitats and military facilities in orbit. Recently, attention has focused on the production of oxygen propellant and He-3 as nuclear fusion fuel (e.g., 1). Ilmenite-rich material is the preferred source of these substances. Efforts to locate ilmenite-rich deposits thus far have focused on the high-titanium mare basalts present on the lunar nearside. Instead, we suggest that large, ilmenite-rich pyroclastic deposits would make an excellent source. Not only would these deposits provide useful by-products, but they would be easy to mine as they are relatively thick and unconsolidated and have a block-free surface.

DISCUSSION

Direct sampling and remote sensing studies have indicated that major deposits of high-Ti mare-basalt exist on the Moon. Spectral reflectance and orbital geochemical data indicate that Mare Tranquilitatis contains the largest expanse of high-Ti basalt on the eastern nearside (e.g., 2,3). The orange glasses and black spheres sampled at Shorty Crater and elsewhere at the Apollo 17 site are fine grained droplets. Their chemical compositions are indistinguishable; the only difference being that the black spheres are largely crystallized. The black quench-crystallized spheres are rich in TiO_2 (9 - 10 %) and ilmenite and are similar in composition to the Apollo 17 mare basalts. Nearly all ilmenites identified in the Apollo 17 orange glass spheres are fine-grained and have dendritic shapes (4). One of the most unique features of the these and other lunar pyroclastics are the sublimates that coat the individual grain surfaces. These consist of sulfur compounds and include elements such as Zn, K, Cl, Na, Ga, Ni, Cu, and Pb (5). These sublimates most likely were emplaced on the pyroclast surfaces during lava fire-fountaining. A large deposit of these pyroclastic spheres exists 50 km west of the Apollo 17 site at Taurus Littrow. This deposit extends over 4000 km^2 and is 10's of meters thick. Other large ilmenite-bearing regional pyroclastic deposits also occur at Rima Bode, S. Sinus Aestuum, and S. Mare Vaporum.

Another lunar product with a potentially large market that would require minimal processing is O_2 for use as spacecraft propellant (6). Lunar oxygen may also prove to be a viable export for sustaining operations in low-Earth orbit (LEO) and elsewhere in near-Earth space. A variety of methods for producing oxygen from lunar rocks and soils have been investigated. After extensive research, however, the reduction of ilmenite seems to be the preferred method (e.g., 6). In addition, potentially useful by-products such as Fe and Ti are produced by the reduction of ilmenite. Lunar He-3 supplies originate from solar wind

materials that are embedded in near-surface regions of fine grained regolith particles.The utilization of lunar He-3 as a nuclear fusion fuel would dramatically improve our energy future (7). Helium and other solar wind gases can easily be extracted from the lunar regolith by the relatively simple procedure of heating the soil to temperatures of 700C or higher. Cameron (8,9) noted that mare regoliths rich in titianium, hence ilmenite, exhibit high helium contents. During the course of operations to extract He-3 from the regolith, other valuable volatiles implanted by the solar wind such as H_2, N_2, CO_2, CH_4, and the noble gases, could be collected with relatively small mass and power penalties (10,11).

CONCLUSION

Numerous ilmenite-rich regional pyroclastic deposits have been identified on the lunar surface (i.e., Taurus Littrow, Rima Bode). The large areal extent of these deposits as well as their relatively great thicknesses (10's m's) make them excellent sites for mining operations. In addition to the production of oxygen and He-3, the pyroclastic deposits could provide by-products such as Fe and Ti in addition to S, Cu, Ni, Pb, Zn, and Cd which are present on the surface of the pyroclastic spheres. Also, other volatile elements implanted by the solar wind, such as H_2, N_2, and CO_2, may be recovered. In addition to the above mentioned elements, the unconsolidated, thick pyroclastic deposits would provide a ready source of shielding material against meteorite impact and space radiation. In short, the resource potential of the lunar RDMD should not be taken lightly when deciding where to locate a permanent lunar base.

REFERENCES

(1) Kulcinski G.L. ed. (1988) *Astrofuel for the 21st Century.* College of Engineering, University of Wisconsin, Madison. 20 pp. (2) Pieters C.M. (1978) *Proc. Lunar and Planet. Sci. Conf. 9th*, pp. 2825-2849. (3) Johnson T.V., Mosher J.A. and Matson D.L. (1977) *Proc. Lunar Planet. Sci. Conf. 8th*, pp. 1013-1028. (4) Heiken G.H. and McKay D.S. (1977) *Proc. Lunar Planet. Sci. Conf. 8th*, pp. 3243-3255. (5) Meyers C., Jr., McKay D.S., Anderson D.H. and Butler P. (1975) *Proc. Lunar Sci. Conf. 4th*, pp. 1625-1634. (6) Mendell W.W., ed., (1985) *Lunar Bases and Space Activities of the 21st Century.* Lunar and Planetary Institute, Houston, TX, 866 pp. (7) Wittenberg L.J., Santarius J.F., and Kulcinski G.L. (198€ *usion Technology, 10,* 167-178. (8) Cameron E.N. (1987) WCSAR-TR-AR3-8708, Wisconsin Center for Space Automation and Robotics (WCSAR), Madison, WI. (9) Cameron, E.N. (1988) In *Papers Presented to the Symposium on Lunar Bases and Space Activities of the 21st Century*, p. 47. Lunar and Planetary Institute, Houston. (10) Crabb T.M. and Jacobs M.K. (1988) In *Papers Presented to the Symposium on Lunar Bases and Space Activities of the 21st Century*, p. 62. Lunar and Planetary Institute, Houston. (11) Haskin L.A. (1989) In *Lunar and Planetary Science XX*, pp. 387-388. Lunar and Planetary Institute, Houston.

PYROCLASTIC VOLCANISM IN THE ALPHONSUS REGION *Cassandra Runyon Coombs, SN15 Johnson Space Center, Houston, TX 77058; B. Ray Hawke, Stan H. Zisk, and Paul G. Lucey, Planetary Geosciences Division, Hawaii Institute of Geophysics, Honolulu, HI, 96822.*

INTRODUCTION

Alphonsus, a slightly elongate, 118-km, pre-Imbrian crater located in the south-central lunar highlands, has long been of interest to lunar scientists. Floor fractures, dark halo craters (DHC's) and a north-south trending central ridge within Alphonsus distinguish it from other highland craters of similar size. The majority of the work done on Alphonsus has centered around the dark halo craters scattered about the periphery of its floor. Suggested origins for these deposits have varied from tephra deposits due to maars (1) to pyroclastic deposits from a central vent (2). Vulcanian eruption models developed by (3) and (4) support the pyroclastic nature of the localized dark mantle deposits (LDMD), as do recent spectral and geologic investigations (e.g., 5, 6, 7, 8). This study, in particular, takes a closer look at the spectral signatures of the Alphonsus DHC's and their adjacent features in an effort to address some outstanding questions: (1) What is the composition of the dark mantling material surrounding the endogenic craters? (2) What is the origin of the light plains material on the crater floor? (3) How was the central ridge formed and is it related to the formation of the central peak and DHC's? (4) What caused the crater floor uplift and is it related in any way to the deposition of the dark mantling material?

METHOD

Spacecraft and Earth-based photographs, topographic maps, UV-visible (0.3 - 1.1 μm) and near-infrared (0.6 - 2.5 μm) reflectance spectra as well as newly obtained 3.0-cm radar data were used in this study. Spectra were collected for three of the localized dark mantle deposits within Alphonsus, the central peak, the light plains mantling the floor, and a variety of other features associated with Alphonsus.

RESULTS AND DISCUSSION

The radar, UV-visible and near-IR reflectance data collected for this study have helped greatly in unravelling the geologic and stratigraphic history of the Alphonsus region. Weak echoes in the new 3.0 cm radar indicate that the surfaces of the Alphonsus LDMD are smooth. The UV-VIS spectra for the Alphonsus features vary somewhat. Spectra collected for a portion of the northeast floor (light plains material) indicate a highlands composition similar to that of the Apollo 16 site. In contrast, the spectra taken of the western LDMD are "red", indicating a basaltic composition. One group of spectra collected and analyzed for another LDMD, Alphonsus R, in southeast Alphonsus, suggest that it may have a different compostion than the western LDMD.

The near-infrared reflectance spectra collected of these Alphonsus features, on the other hand, are more consistent. The spectra of the LDMD indicate a basaltic composition

rich in olivine and have been classified as being typical of the Group 3 spectral class of Hawke et al. (7,9). These spectra exhibit broad, moderately deep (5 - 7 %) asymmetrical absorption bands in the 1.0 μm region. The broad nature and asymmetrical shape are indicative of composite features with band centers in the 1.0 μm region. Most often, this type of band indicates the presence of both olivine and orthopyroxene (10,11). While in theory this band could be produced by the combination of clinopyroxene, orthopyroxene, and Fe^{2+}-bearing glass, the analyses presented by McCord et al. (10) and Hawke et al. (7) indicate that this is unlikely.

Some of the olivine may have come from the basaltic rock, however, it is thought that the majority was emplaced with the juvenile material brought up from depth. Also, it seems likely that the bulk of the orthopyroxene in the Alphonsus DHC deposits was present as a component in the highlands-rich wall rock and that it was eroded and emplaced during the explosive eruptions which produced the LDMD. Spectra of the light plains deposits on the crater floor exhibit a noritic composition, different from the other locally derived Alphonsus features. The origin of this deposit is still uncertain, however, these deposits are thought to be related to the Imbrium impact event that resurfaced the Alphonsus region. Spectra collected of the central ridge and peak of Alphonsus indicate that they are non-basaltic in composition. Rather, the central ridge appears to be composed of Imbrium-related material and the central peak is composed of pure anorthosite.

CONCLUSIONS

Vulcanian-type eruptions deposited several localized dark mantle deposits on the floor of Alphonsus. Associated with prominent floor fractures and endogenic source craters, the individual deposits cover areas less than 450 km^2, while the largest coalesced deposit is nearly 800 km^2. The reflectance spectra collected for the LDMD indicate that the Alphonsus pyroclastics are rich in olivine and pyroxene and contain lesser amounts of fragmented basaltic plug-rock and highlands-rich wall rock. The central ridge appears to have an origin related to the Imbrium impact event and is not related to the formation of the DHC's or the central peak. The central peak is composed solely of anorthosite, suggesting that a lens of the material must have been present at depth below the target site Floor uplift within Alphonsus most likely is the result of magma emplacement at depth well after the crater had formed.

REFERENCES

(1) Howard K.A. and Masursky H. (1968) *U.S.G.S. Map I-566.* (2) Carr M.H. (1969) *U.S.G.S. Map I-599.* (3) Head J.W. and Wilson L. (1979) *PLPSC 10th*, pp. 2861-2897. (4) Wilson L. and Head J.W. (1981) *J.G.R., 78*, 2971-3001. (5) Gaddis L.R., Pieters C.M., and Hawke B.R. (1985) *Icarus, 61*, 461-489. (6) Coombs C.R., Hawke B.R. and Gaddis L.R. (1987) *LPSC XVIII*, pp. 197-198. Lunar and Planetary Institute, Houston, TX. (7) Hawke B.R. Coombs C.R., Gaddis L.R., Lucey P.G. Owensby P.D. (1989) *PLPSC 19th*, pp. 255-268. (8) Coombs C.R., Hawke B.R., Lucey P.G., Head J.W. (1989) *LPSC XX*, pp. 185-186. (9) Hawke B.R. , Lucey P.G., Bell J.F., Owensby P.D. (1985) *LPSC XVI*, pp. 329-330. (10) McCord T.B., Clark R.N., Hawke B.R. McFadden L.A. , Owensby P.D. (1981) *J. G.R., 86*, 10883-10892. (11) Singer R.B. (1981) *J.G.R., 86*, 7967-7982.

PRISTINE LUNAR GLASSES: A 'WINDOW' INTO THE MOON'S MANTLE. J.W. Delano, Dept. of Geological Sciences, State University of New York, Albany, NY 12222

Pristine lunar glasses are a suite of twenty-five, high-Mg magmatic compositions that were erupted onto the Moon's surface in fire fountains [e.g. 1-3]. Since these magmas appear to be geochemically less evolved than the crystalline mare basalts [e.g. 4-7], they provide our best 'window' into the Moon's mantle. Specific constraints are furnished on the following topics: (a) oxidation state of the Moon's mantle [e.g. 8]; (b) compositional heterogeneity of the Moon's differentiated mantle [e.g. 6]; (c) depths of mare source-regions [e.g. 10,11]; (d) residual mineralogy in mantle source-regions [6,10,11]; (e) composition of the Moon [12]; and (f) the possible role of melt/solid density-crossovers in the Moon's geochemical evolution [9].

Oxidation State of the Moon's Mantle

Although the lunar science community appears to implicitly believe that the oxidation state of the Moon's mantle is strongly reducing, the most careful study conducted thus far on pristine lunar glasses by M. Sato [8] concluded something quite different. Sato [8] proposed that the oxidation state of the lunar mantle may be controlled by the so-called 'graphite surface' involving chemical equilibrium with C (graphite) + CO + CO_2 + O_2. If correct, owing to the large pressure-dependence on this redox reaction [e.g. 13-15], the oxidation state prevailing in the source-regions of the mare magmas at a pressure of about 20-25 kilobars [10,11] would be near the fayalite + magnetite + quartz (FMQ) buffer (highly oxidizing). Although this hypothesis [8] has had major implications for the petrogenesis of mare magmas, it has gone unchallenged.

The low abundance of Cr (<700 ppm) in terrestrial basalts (e.g. MORB's) is known to be caused in part by the elevated redox states (~FMQ) in the mantle source-regions. The Cr abundance of the melt is controlled by spinel saturation [16]. Importantly, the Cr abundance in a mafic melt at spinel saturation is known to be a function of temperature and oxygen fugacity. For example, with decreasing oxidation state (at constant temperature), the abundance of Cr in the melt required for spinel saturation increases sharply [e.g. 17,18,19]. This raises a decisive question: If, as proposed by [8], the lunar mantle at 20-25 kilobars is relatively oxidizing (~FMQ), why do mare basalts and pristine glasses contain high abundances (~4000 ppm) of Cr compared to terrestrial basalts? (Figure 1) Experiments designed to measure the Cr abundance in the melt at spinel saturation as a function of temperature and oxygen fugacity in a pristine glass composition should clarify this question bearing on the oxidation state of the lunar interior.

Isothermal (1260°C) subliquidus experiments have been performed on a synthetic Apollo 15 yellow/brown volcanic glass composition [6,7] for a range of oxygen fugacities. One hundred milligram pellets were suspended on Pt-wire loops [e.g. 20] in a Deltech furnace where the oxygen fugacity was controlled by CO + CO_2 gas mixtures and continuously monitored with a yttria-doped zirconia sensor. Equilibrium was verified based on reversibility of the results plotted in Figure 2. Note that at constant temperature (1260°C), the abundance of Cr in the melt at spinel saturation decreases by a factor of 4 in the redox range between the iron/wustite (IW) and nickel/nickel oxide (NNO) buffers. This is a manifestation of the marked change in valence state of Cr occurring within that interval of oxygen fugacity [e.g. 21] from about 30% Cr (III) at IW to about 90% Cr (III) at NNO [e.g. 17]. The partitioning behavior of Cr between spinel and melt is therefore strongly dependent on the valence state. These preliminary data from a lunar composi-

tion (Figure 2) imply that mare magmas having Cr abundances of ~4000 ppm were derived from mantle source-regions having a low redox state, rather than the high redox state proposed by Sato [8].

Compositional Heterogeneity of the Moon's Mantle

Petrologists have constrained the composition of a primary picritic MORB (mid-ocean ridge basalt) that helps to better define the composition and mineralogy of the Earth's upper mantle beneath mid-ocean ridges [e.g. 18,19]. This notion of one primary magma has proven successful largely due to the limited compositional (major elements) variability in fertile regions of the Earth's upper mantle. In stark contrast, the Moon's mantle appears to be so heterogeneous that no one primary magmatic composition is universally applicable. Instead, the twenty-five pristine glasses, which span a remarkable range from 0.4 to 16.4 weight % TiO_2, are all primary magmas [6]. Continued discovery of additional varieties of pristine lunar glass [e.g. 5] will provide further constraints on the nature and causes of this extraordinary variability in the lunar mantle.

REFERENCES: [1] Heiken et al. (1974) Geochim. Cosmochim. Acta, 38, p. 1703-1718; [2] Wilson and Head (1981) J. Geophys. Res., 86, p. 2971-3001; [3] Gaddis et al. (1985) Icarus, 61, p. 461-489; [4] Longhi (1987) PLPSC 17, p. E349-E360; [5] Shearer et al. (1989) Geochim. Cosmochim. Acta, in press; [6] Delano (1986) PLPSC 16, p. D201-D213; [7] Hughes et al. (1988) Geochim. Cosmochim. Acta, 52, p. 2379-2391; [8] Sato (1979) PLPSC 10, p. 311-325; [9] Delano (1989) PLPSC 20, in press; [10] Green et al. (1975) PLPSC 6, p. 871-893; [11] Delano (1980) PLPSC 11, p. 251-288; [12] Jones and Delano (1989) Geochim. Cosmochim. Acta, 53, p. 513-527; [13] Brett and Sato (1984) Geochim. Cosmochim. Acta, 48, p. 111-120; [14] French and Eugster (1965) J. Geophys. Res., 70, p. 1529-1539; [15] Woermann et al. (1978) EOS, 59, p. 813; [16] Langmuir et al. (1977) Earth Planet. Sci. Lett., 36, p. 133-156; [17] Barnes (1986) Geochim. Cosmochim. Acta, 50, p. 1889-1909; [18] Murck and Campbell (1986) Geochim. Cosmochim. Acta, 50, p. 1871-1887; [19] Hill and Roder (1974) J. Geol., 82, p. 709-729; [20] Donaldson et al. (1975) Amer. Mineral., 60, p. 324-326; [21] Schreiber (1977) PLSC 8, p. 1785-1807; [22] Green et al. (1979) The Earth: Its Origin, Structure, and Evolution (M.W. McElhinny, ed.), p. 265-290. Academic Press, London; [23] Stolper (1980) Contrib. Mineral. Petrol., 74, p. 13-27.

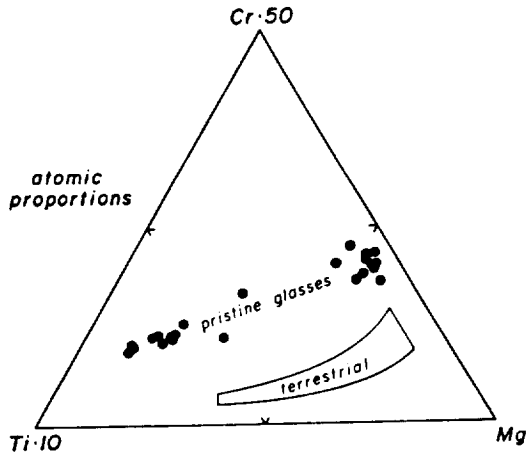

Figure 1

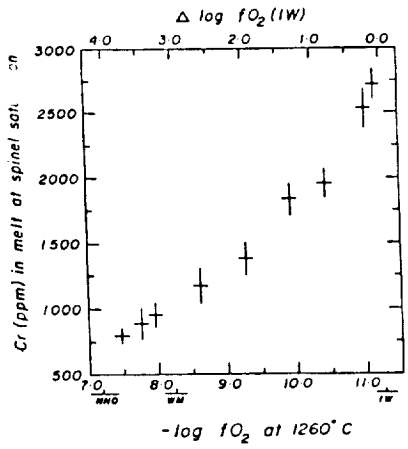

Figure 2

PRISTINE MARE GLASSES AND MARE BASALTS: EVIDENCE FOR A GENERAL DICHOTOMY OF SOURCE REGIONS. J.W. Delano, Department of Geological Sciences, State University of New York, Albany, NY 12222

Mare volcanic (i.e. pristine) glasses are generally regarded as being better candidates for primary, mantle-derived magmas than most, if not all, of the crystalline mare basalts [1]. Although this might be taken to imply that the crystalline mare baslats are fractional differentiates from high-MgO parental magmas represented by the pristine glasses, such does not appear to be the case [2-4]. Despite general similarities between calculated differentiates from pristine glasses and mare basalts [5, 6], no mare basalts can yet be attributed to any of the pristine glasses via low-pressure crystal/liquid fractionation [2-4]. While this may only indicate that mare basalts have been subjected to fractionation processes that were more complex than the low-pressure crytal/liquid differentiation that has been modelled, other possibilities exist. For example, the picritic magmas represented by the pristine glasses may have been derived from different regions of the lunar mantle than those magmas represented by the majority of mare basalts in the present sample-collection. This hypothesis seems to be supported by the relationships illustrated in Figure 1. Mare basalts (open circles) define two main trends on this diagram of Sc vs FeO. Most mare basalts (Apollo 14 groups 1-5; Apollo 17 VLT; Apollo 11 high-Ti basalts A, B1, B2, B3, D; Apollo 17 high-Ti basalts A, B, C; and Apollo 12 high-Al mare basalt) plot along a high-Sc trend in Figure 1. The other group of mare basalts (Apollo 12, 15, and Luna 24 low-Ti) have a FeO/Sc ratio close to a value of 5400. Note that <u>all</u> of the pristine mare glasses (black boxes) analyzed thus far [4-7] also occur in the same grouping as the Apollo 12, 15 and Luna 24 low-Ti magmas. Each of the two groupings of mare magmas in Figure 1 contain low- and high-Ti compositions. Since experimental pertrology suggests that olivine ± clinopyroxene were the sole residual phases in most, if not all, of the mantle source-regions for mare magmas, the bulk partition coefficients for FeO and Sc during partial melting may have been near unity. If so, the dichotomy apparent in Figure 1 was inherited from the mantle sources, in which the majority of mare basalts came from different reservoirs than the pristine glasses. Hubbard and Rhodes [8] were the first to suspect this relationship by noting that the Apollo 17 orange, high-Ti pristine glass (74220) had a closer compositional resemblance to the Apollo 12 ilmenite basalts than to the Apollo 11, 17 high-Ti mare basalts.

In summary, the picritic magmas represented by the pristine mare glasses may have been derived from different mantle source-regions than the majority of sampled mare baslats.

REFERENCES: [1] Delano J. W. (1986) PLPSC 16, p. D201-D213; [2] Longhi (1987) PLPSC 17, p. E349-E360; [3] Longhi (1989), this volume; [4] Shearer et al. (1989) Geochim. Cosmochim. Acta, in press; [5] Hughes et al. (1988) Geochim. Cosmochim. Acta, 52, p. 2379-2391; [6] Hughes et al. (1989) PLPSC 19, p. 175-188; [7] Hughes et al. (1990) PLPSC 20, in press; [8] Hubbard and Rhodes (1976) Lunar Sci-VII, p. 390-392.

DICHOTOMY OF SOURCE REGIONS: Delano J. W.

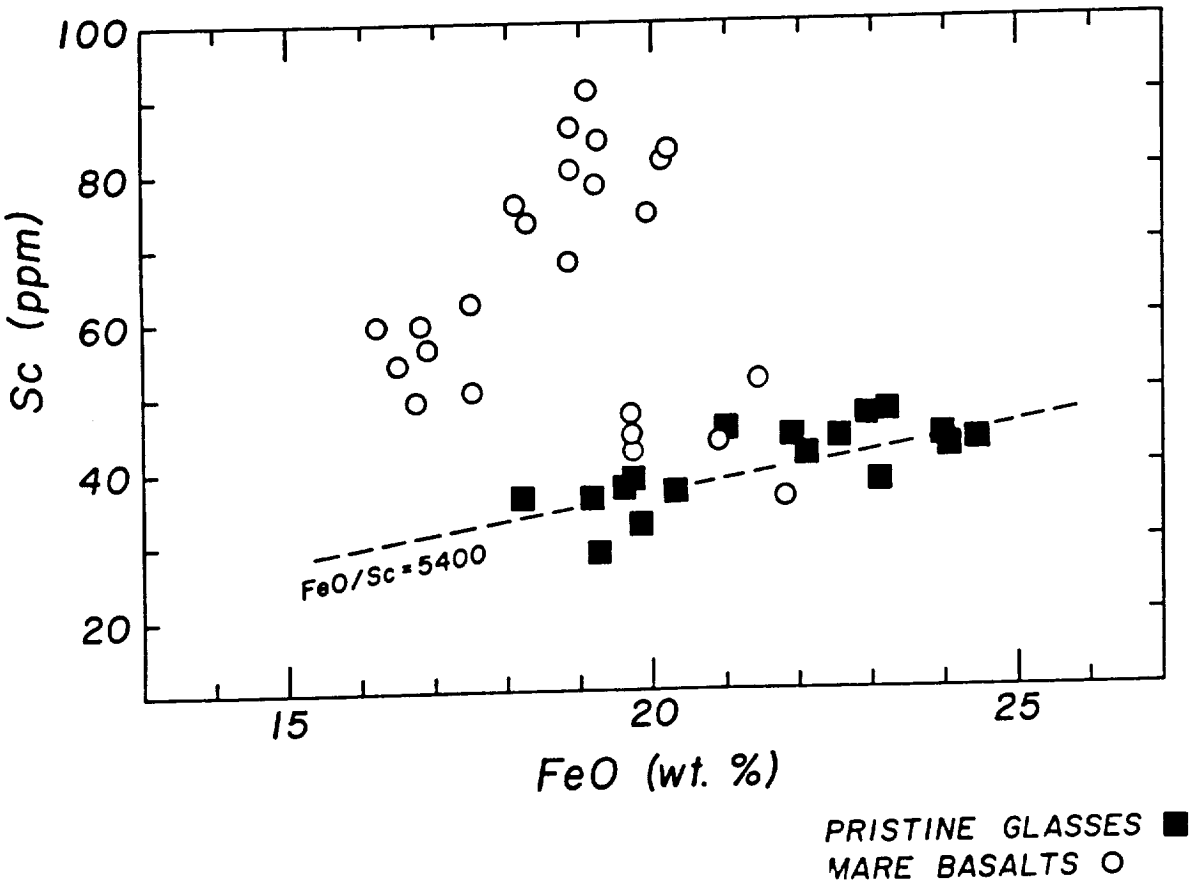

THERMODYNAMIC MODELS OF TRACE METAL AND VOLATILE ELEMENT TRANSPORT BY LUNAR VOLCANISM Bruce Fegley Jr. and Derrick Kong, Department of Earth, Atmospheric and Planetary Sciences, Massachusetts Institute of Technology, Cambridge, MA 02139

Introduction. In this abstract, we present preliminary results of the first set of comprehensive chemical equilibrium calculations on the gas phase chemistry of trace metals and volatile elements (e.g., B, C, F, Na, S, Cl, Cu, Zn, Ga, Ge, Br, Ag, Cd, In, Sb, Te, I, Au, Hg, Tl, Pb, Bi, etc.) associated with lunar glasses (1). These results are important for identifying the major gas phase species of these elements and for modelling the transport mechanisms for trace metals and volatile elements in lunar volcanic gases.

Calculations. A revised and expanded version of the TOP20 code was used for the ideal gas chemical equilibrium calculations. This code uses the dual constraints of mass balance and chemical equilibrium to solve the molecular composition (at a specified temperature, pressure, and set of elemental atomic abundances) of a gas phase containing over 1000 gases of over 70 elements. The thermodynamic data used in the calculations come from standard compilations such as the JANAF Tables (2,3). The computational method used in the TOP20 code has been schematically described by Barshay and Lewis (4).

Results. A preliminary subset of our results for the gas phase chemistry of sulfur, copper, sodium, and potassium is illustrated by the figures on the next page. These calculations were done at a total pressure of 1 bar and with an "average" terrestrial fumarolic gas composition having the following normalized elemental atomic abundances: N=1.0, F=6.8, S=21.8, Cl=36.1, C=163, O=3982, and H=7417. The Br and I elemental abundances were determined by assuming Cl/Br and Cl/I atomic ratios appropriate for seawater (5). The abundances of other elements such as copper, sodium, and potassium were deliberately set at 1 part per billion. By doing this, their chemistry can be calculated without affecting the overall mass balance of the gas phase.

Discussion. An important result of the calculations is that halides are important species for the transport of metals such as copper, sodium, and potassium. This is also true for several other metals including Fe, Mg, Ca, Ni, Ti, Cr, Mn, and Co. For copper, sodium, and potassium, a chloride is the dominant gas over a wide temperature range. The elemental abundances of the other halogens (F, Br, I) will be an important factor for determining the relative importance of gaseous bromides, fluorides, and iodides. A second important result is that more complex species such as dimers and trimers become important at low temperatures (e.g., see the graphs for copper and potassium). If no Al remains in the gas at low temperatures, dimeric halides will also be the dominant sodium-bearing gases. Third, the oxidation state of this assumed gas composition becomes more reducing at lower temperatures. This is reflected by the decreased abundances of oxidized sulfer gases and by the increased abundances of reduced sulfur gases at low temperatures.

Summary. Preliminary ideal gas chemical equilibrium calculations illustrated here show that even in water-rich gases, halides are an important species for the transport of metals including Cu, Na, and K. Calculations done with drier assumed volcanic gas compositions reinforce this conclusion.

Acknowledgements. This work was supported by grants from the NASA Planetary Materials and Geochemistry Program and the Planetary Atmospheres Program to MIT. The MIT UROP Program also provided partial support for DK.

References. (1) J.W. Delano 1986 *Proc. 16th LPSC J. Geophys. Res.* **91**, D201-D213, (2) *JANAF Tables* 3rd. edition, (3) *Thermodynamic Properties of Individual Substances*, 4 vols., High Temperature Institute, Moscow, USSR, (4) S.S. Barshay and J.S. Lewis 1978 *Icarus* **33** 593-607, (5) *Handbook of Chemistry and Physics*, 55th ed., p. F190.

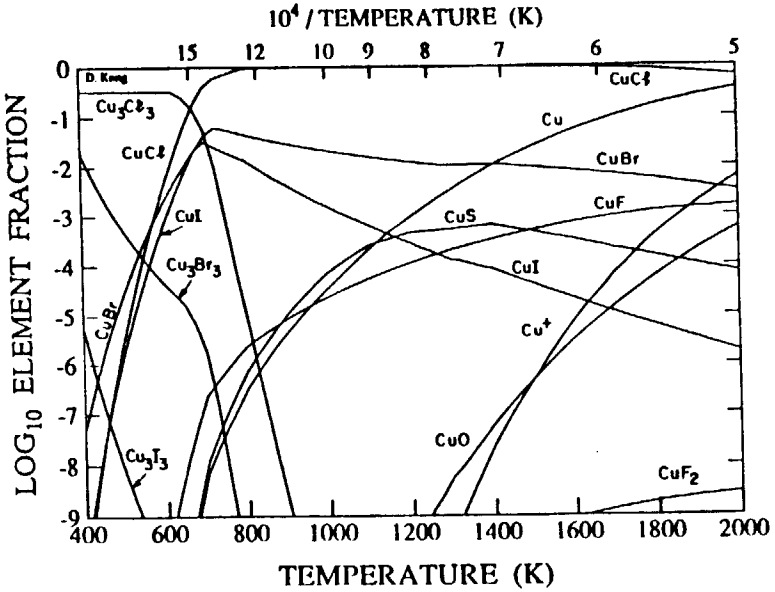
10⁴ / TEMPERATURE (K)
15 12 10 9 8 7 6 5
D. Kong
Cu₃Cl₃
CuCl
CuI
Cu₃Br₃
CuBr
Cu₃T₃
CuCl
Cu
CuBr
CuF
CuS
CuI
Cu⁺
CuO
CuF₂
LOG₁₀ ELEMENT FRACTION
0 -1 -2 -3 -4 -5 -6 -7 -8 -9
400 600 800 1000 1200 1400 1600 1800 2000
TEMPERATURE (K)

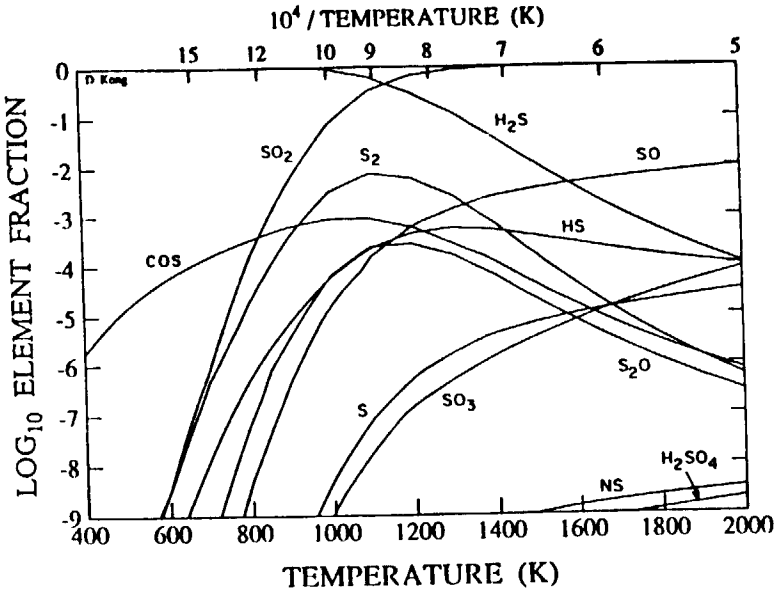
10⁴ / TEMPERATURE (K)
15 12 10 9 8 7 6 5
D Kong
H₂S
SO₂
S₂
SO
HS
COS
S₂O
S
SO₃
H₂SO₄
NS
LOG₁₀ ELEMENT FRACTION
0 -1 -2 -3 -4 -5 -6 -7 -8 -9
400 600 800 1000 1200 1400 1600 1800 2000
TEMPERATURE (K)

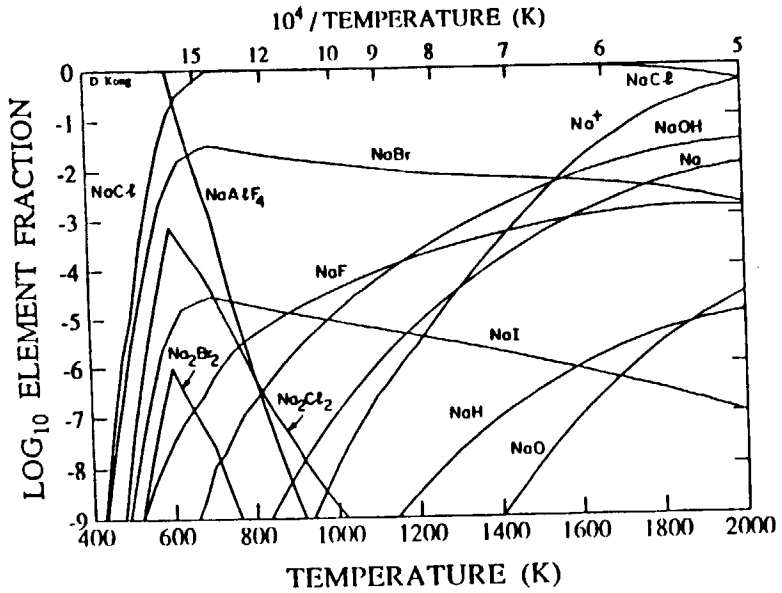
10⁴ / TEMPERATURE (K)
15 12 10 9 8 7 6 5
D Kong
NaCl
Na⁺
NaOH
NaBr
Na
NaCl
NaAlF₄
NaF
NaI
Na₂Br₂
Na₂Cl₂
NaH
NaO
LOG₁₀ ELEMENT FRACTION
0 -1 -2 -3 -4 -5 -6 -7 -8 -9
400 600 800 1000 1200 1400 1600 1800 2000
TEMPERATURE (K)

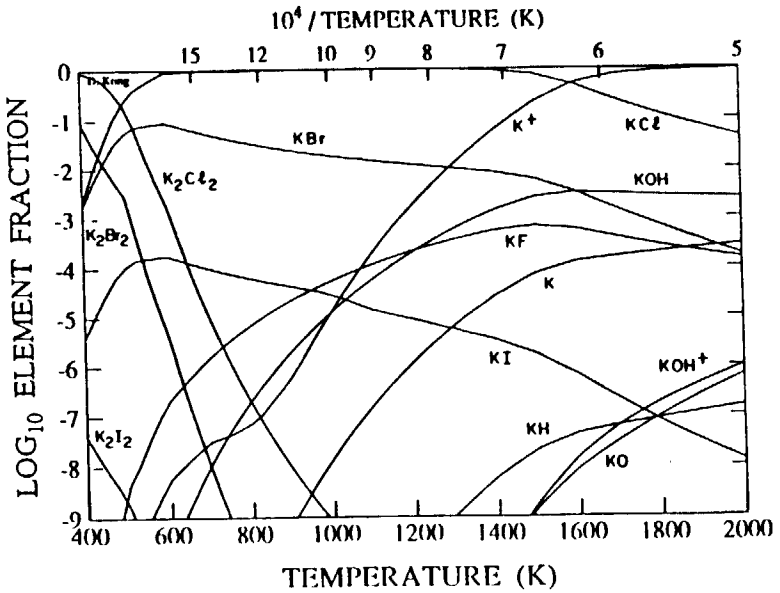
10⁴ / TEMPERATURE (K)
15 12 10 9 8 7 6 5
D Kong
K⁺
KCl
KBr
K₂Cl₂
KOH
K₂Br₂
KF
K
KI
KOH⁺
KH
K₂I₂
KO
LOG₁₀ ELEMENT FRACTION
0 -1 -2 -3 -4 -5 -6 -7 -8 -9
400 600 800 1000 1200 1400 1600 1800 2000
TEMPERATURE (K)

REMOTE SENSING AND GEOLOGIC STUDIES OF LUNAR DARK MANTLE DEPOSITS: A REVIEW. B. R. Hawke, Planetary Geosciences Division, Hawaii Institute of Geophysics, University of Hawaii, Honolulu, HI 96822.

INTRODUCTION: In recent years, interest in lunar dark mantle deposits of pyroclastic origin has dramatically increased. Dark mantle deposits are low-albedo surface units that mantle and subdue subjacent terrain. They vary in area from a few square kilometers for those surrounding endogenic dark halo craters to tens of thousands of square kilometers for the extensive regional deposits. In the pre-Apollo era, opinions differed concerning the nature and origin of dark mantle deposits. Some correctly suggested that the dark haloes surrounding certain small, irregular craters were produced by explosive volcanism. However, the regional dark mantle units were often interpreted as dark facies of basin ejecta or as dark volcanic constructs. A variety of pyroclastic debris was returned from the Apollo landing sites. Intensive study of these samples, e.g., 1, 2, 3, as well as remote sensing and geologic studies of dark mantle deposits during the post-Apollo era e.g., 4, 5, 6, 7 have resulted in a greatly improved understanding of explosive volcanism on the Moon. In the past decade, almost all lunar scientists have accepted the pyroclastic origin of dark mantle deposits 7, 8, 9.

Two genetically distinct types of pyroclastic deposits have been recognized on the lunar surface: regional and localized 8. Compositions, eruption mechanisms, and emplacement styles for both regional and localized dark mantle deposits have been determined, based on their distribution, geometry, and source vent morphology as well as a variety of remote sensing data 7,8,9. These remote sensing data included near-infrared reflectance spectra, multispectral images, albedo maps, 3.8- and 70- cm radar images, and Apollo orbital geochemistry data. The purpose of this paper is to summarize the results of remote sensing and geologic studies of lunar dark mantle deposits and to present an overall picture of explosive volcanism on the Moon.

REGIONAL DARK MANTLE DEPOSITS: Regional dark mantle deposits (RDMD) cover many thousands of square kilometers and are generally considered to be the products of fire-fountaining that occurred in association with basaltic eruptions e.g., 1,8,9. These regional pyroclastic deposits commonly occur in lunar highlands areas adjacent to many of the major maria; their emplacement may have been associated with some of the early mare-filling volcanic episodes 10,11. Depressions at the heads of associated sinuous rilles and other related irregular depressions are the probable source vents for the RDMD e.g., 9,12. Characteristically, the regional pyroclastic deposits are low-albedo (0.079 - 0.096 13) units that appear to cover and subdue the features of the underlying terrain. Visual observations as well as photographs obtained during the Apollo missions indicated that the surfaces of lunar pyroclastic deposits are very fine-textured and exhibit an extremely smooth, velvety appearance 14,15,16. All of the RDMD exhibit very weak to nonexistent echoes on the depolarized 3.8- cm radar maps of *Zisk et al.* 17. A lack of surface scatterers (rocks, blocks, etc.; 1-50 cm in size) is believed to be responsible for the low radar returns 4,9,12.

The material which comprised a major regional pyroclastic deposit was sampled at the Apollo 17 landing site. One of the major objectives of the Apollo 17 mission was to characterize the "dark mantle" unit at the site; premission analysis had indicated that this was a relatively young deposit of pyroclastic origin 5,6,9,15. After the mission, it was considered surprising that no obvious evidence was found of a young dark mantling material component in the returned samples 6. The regolith samples collected from the low-albedo unit on the valley floor are composed largely of ancient (~3.76 b.y.) high-titanium mare basalt 18. However, subsequent research identified the orange glass droplets and the chemically - equivalent, partially crystallized black spheres as pyroclastic components in the Apollo 17 soil 1,5,6. The chemical compositions of the orange and black spheres are indistinguishable, the only difference being that the black spheres are largely crystallized. The quench-crystallized black spheres are rich in TiO_2 (9 - 10%) and ilmenite and they are similar, though not identical, in composition to the Apollo 17 mare basalts. The pyroclastic debris is slightly younger (~3.6 b.y.) than the mare basalts at the site (~3.7 - 3.8 b.y.) 18.

Although the orange and black pyroclastic spheres are not abundant at the Apollo 17 site, there is a major regional pyroclastic deposit (Taurus-Littrow dark mantle deposit) just over 50 km west of the site. A comparison of reflectance spectra obtained for the Taurus-Littrow dark mantling deposit (DMD) with laboratory and telescopic reflectance measurements have demonstrated that the Apollo 17 black spheres are the characteristic ingredient of the Taurus-Littrow pyroclastic mantling deposit 4,5,6,9,19. The thickest part of the Taurus-Littrow DMD has an areal extent of just over 4000 km^2. However, the thinner portions of the deposit blanket a much larger area. Both geological and radar studies of the Taurus-Littrow DMD indicate that the core

portion of the deposit has a thickness of many tens of meters. The deposit exhibits very weak to nonexistent echoes on the depolarized 3.8-cm radar maps produced by *Zisk et al.* [17]. These very low depolarized radar returns are generally attributed to the lack of scatterers (1-50 cm) on the smooth surface of the pyroclastic mantling deposits [4,9,17]. A very low degree of small-scale surface roughness and a relatively block-free surface are indicated. Areas of enhanced-return, high-albedo material exposed by small impact craters which have penetrated this pyroclastic mantling unit are very rare. The 70-cm radar data obtained by Thompson [20] shows that the Taurus-Littrow DMD is deficient in large (~1-2 m) blocks.

Several other major occurrences of regional pyroclastic mantling deposits have been documented [9,21], including those at the following locations: Rima Bode, Aristarchus Plateau, Sulpicius Gallus, Montes Harbinger, southern Sinus Aestuum, southwestern Mare Humorum, and southern Mare Vaporum. These units have been characterized as extensive deposits of low-albedo (0.079-0.096) material which appear to subdue and mantle underlying terrain, are relatively fine-textured, and exhibit a smooth, velvety appearance. The low returns on Earth-based 3.8-cm depolarized radar back scatter maps confirm these observations of mantled areas and indicate an absence of surface scatters in the 1 to 50-cm size range. The surfaces of the regional pyroclastic deposits are rock-free.

Spectral reflectance studies have provided important information concerning the composition of regional pyroclastic (DMD) deposits [8,9,10,22]. Near-infrared spectra for a large number of regional pyroclastic deposits were obtained at the 2.2-m University of Hawaii telescope facility on Mauna Kea, Hawaii. As discussed above, the Taurus-Littrow DMD is dominated by ilmenite-rich black spheres. The spectra obtained for the Rima Bode pyroclastic deposits are almost identical to those collected for various positions of the Taurua-Littrow deposit. A similar composition is indicated. The reflectance and continuum-removed spectra obtained for the DMD on the Aristarchus Plateau and southwest of Mare Humorum exhibit broader, longer-wavelength absorption bands than those which can be attributed to pyroxenes alone in highland and mare soils. As noted by *Gaddis et al.*[9] and *Lucey et al.*[22], there must be additional Fe-bearing soil components which have both modified the "1 μm band" and maintained the low albedo of the materials observed. The presence of Fe^{2+}-bearing volcanic glasses in the mantling deposits from which the spectra were obtained is most consistent with the available spectral evidence [9,19,22]. The Aristasrchus Plateau and Mare Humorum pyroclastics appear "red" (low 0.40/0.56 μm values) in multispectral images [12,22,24].

The UV-VIS spectra (0.3-1.1μm) presented by *Pieters et al.*[4,6] and *Adams et al.*[5] have demonstrated that several DMD on the lunar nearside contain a significant component of ilmenite-rich spheres of pyroclastic origin. These include the following deposits; 1) Taurus-Littrow, 2) Rima Bode, 3) Southern Mare Vaporum, and 4) Southern Sinus Aestuum. The spectra (0.3-1.1 μm) for all of these deposits exhibit similar characteristics. For example, they exhibit very high 0.40/0.56 μm values and the deposits appear "blue" in 0.40/0.56 μm multispectral ratio images presented by *Pieters et al.*[6] and *McCord et al.*[23].

As mentioned previously, all of the regional pyroclastic deposits exhibit very low values on depolarized 3.8-cm radar images [4,9,12,17]. Low values are also commonly seen on 70-cm radar images [20]. 3.8-cm and 70-cm radar demonstrate that the regional pyroclastic debris is apparently unwelded or annealed. Otherwise, small craters in these dark mantle deposits would have excavated welded blocks. The deposits cover very large areas (up to 30,000 km^2) and both geologic and radar data indicate that the[illegible]ave thicknesses of tens of meters. Most of the regional pyroclastic deposits overlie highlands terrain but a few (e.g., Taurus-Littrow) were emplaced on a mare substrate.

The results of studies conducted by *Head and Wilson* [12,26] indicated that RDMD are likely to have been produced by eruption conditions such as those characteristic of strombolian or continuous eruptions, and that it is unlikely that these extensive dark mantle units are the results of coalescing deposits of localized pyroclastics (i.e. Alphonsus-Type dark halo craters). The results of their calculations indicate that the lunar equivalent of strombolian activity is likely to lead to the dispersal of pyroclasts over a wide area, with extreme sorting of particles. More specifically, clasts greater than a few centimeters in diameter would remain within several tens of meters of the vent, while clasts much smaller than 1 mm may be projected for many tens to hundreds of kilometers.

LOCALIZED DARK MANTLE DEPOSITS: Localized lunar dark mantle deposits (LDMD) are small (typically <250-550 km^2), low-albedo units of pyroclastic origin that are commonly located in the floors of large Imbrian to pre-Imbrian-aged (i.e., >3.4 b.y.) impact structures and are concentrated around the perimeters of the major lunar maria [8, 9, 25, 26, 27, 28, 29]. These deposits, typified by the Alphonsus dark halo craters, are generally

associated with endogenic dark halo craters within large highland impact craters. Characteristically, these dark halo craters are small in size (>3 km), aligned along crater floor fractures, have a noncircular shape, and lack obvious rays. The source craters are surrounded by peripheral deposits of smooth, block-free, low-albedo material that composes the dark halo. Though endogenic dark halo crater deposits are by far the most common mode of occurrence of LDMD, other types of localized deposits have also been identified. These include deposits found (1) as isolated patches in the highlands with no obvious source vents, (2) as isolated patches on the maria, and (3) as isolated patches in the highlands adjacent to the mare deposits. The source vents for these deposits may have been obscured by pyroclastic debris or by flooding with mare basalt. Sizes of the LDMD vary. Individual (i.e., from one source vent) LDMD typically are <100km^2, while larger coalesced LDMD are in general <1000 km^2 (most fall between 250-550 km^2). A few exceptional deposits are as large as 2100 km^2. This variation in size is in part a result of the number of coalesced deposits at each locality.

Morphometric analyses of these "haloes" and their associated source vents have led investigators to suggest an eruption mechanism for the LDMD analogous to that of terrestrial vulcanian explosive eruptions [25]. In this style of eruption, the accumulation of gas in a capped magma body leads to explosive decompression, and the subsequent emplacement of a pyroclastic deposit around an endogenic source crater. It has been shown that for these types of eruptions, the maximum range of all pyroclasts much larger than 1 cm is up to 4 km, while smaller clasts may be thrown up to tens of kilometers, leaving a well-defined division between the localized deposits of coarse clasts and the widely dispersed deposits of small clasts [25, 26].

Although LDMD may be genetically related and they exhibit many morphologic similarities, spectral reflectance studies have shown that they are spectrally, thus compositionally distinct [7,8,27,30]. Three general compositional types of LDMD have been identified on the basis of the depth, center and overall shape of their ~1.0-μm absorption features as well as their continuum slopes. The spectral characteristics of the various groups are discussed in detail below.

Group 1

Spectra. This group includes spectra from the Grimaldi pyroclastics, the Franklin dark floor deposits, the Atlas dark halo craters, the dark Archimedes south rim deposits, and the pyroclastics on the eastern edge of Mare Nectaris. Spectra for these deposits exhibit 1.0-μm absorption band centers near 0.93-0.95 μm and the depths are approximately 4-5%. These bands are asymmetrical and have been described as "checkmark-like," with a straight, steep short-wavelength edge followed by a shallower straight long-wavelength edge[7]. Some spectra in this group exhibit relatively steep continuum slopes. These Group 1 spectra are similar in many ways to those obtained for typical lunar highlands areas. The Group 1 band parameters indicate the presence of feldspar-bearing rocks with mafic assemblages that are dominated by orthopyroxene. Although major amounts of highland material are present in Group 1 LDMD, the relatively broad, asymmetric, and shallow "1.0-μm" bands indicate the presence of one or more additional components such as volcanic glass, olivine, or clinopyroxene.

Additional information about these deposits is provided by multispectral and albedo images of Group 1 deposits. The 0.40/0.56 μm images indicate that both the Atlas and the Franklin pyroclastic deposits are "blue" (high 0.40/0.56 μm values) relative to the surrounding highlands. In addition, these pyroclastic deposits have very low visible albedoes. This evidence indicates the presence of an exotic, nonhighlands component in these deposits. Based on all the available information, it seems likely that Group 1 pyroclastic deposits are composed of a mixture of highlands-rich wall rock and glass-rich juvenile material with lesser amounts of basaltic caprock material. The available spectral evidence indicates that the deposit composition does vary from place to place on the lunar surface. In fact, some Group 1 deposits (e.g., Archimedes south rim) exhibit low ("red") 0.40/0.56-μm values in the multispectral data set [31]. It is clear that this group is very complex and that additional research will be required to fully understand the composition and origin of all members.

Geology. The geology of two Group 1 members is very similar to the other deposits included in this group. Both Atlas and Franklin floor pyroclastic deposits are associated with vents that occur along fractures on the floor of the craters. The Franklin floor deposit appears to be associated with a series of aligned elongate craters on the eastern side of the crater floor [7]. The dark mantle material covers a horseshoe-shaped area approximately 20-40 km wide by 45 km long. This post-Imbrium deposit was emplaced during a late stage of volcanic activity in the Geminus region of the Moon. Pyroclastic deposits also cover a portion of the floor of Atlas, another Imbrian-aged impact crater. These deposits also occur around vents that are associated with a series of floor fractures in the interior of the crater. Two separate deposits were formed in the crater, one in the

south and one in the north. Both of the deposits are roughly 25 km in diameter. The southern dark mantle deposit is the more pronounced of the two and is associated with an elongate vent (7 km by 5 km) near the intersection of three major floor rille systems. Dark mantling material extends up to 14 km away from the southern vent.

Group 2

Spectra. The group comprises spectra from LDMD east of Aristoteles 1 and 2, Rima Fresnel pyroclastics, and Vitruvius floor. As apparent in the spectra of the LDMD east of Aristoteles 1 and 2, these "1.0-μm" bands are centered at or beyond 0.96 μm. These bands are deeper (7%) and more symmetrical than those in Group 1. These absorption bands indicate the presence of Ca-rich clinopyroxene. Group 2 spectra closely resemble those obtained for mature mare areas (e.g., *McCord et al*[32]), and the deposits in this group contain very large amounts of mare basalt.

Multispectral ratio maps show that most of the Group 2 deposits exhibit low (red 0.40/0.56-μm values and relatively high 0.95/0.56-μm ratios. These deposits appear to be dominated by fragmented basaltic plug rock material with much lesser amounts of highlands debris and juvenile material present. In at least one instance (east of Aritoteles 2) basaltic wall rock may be a major component in the deposit because one of the two major vents is located in the mare.

Geology. The Rima Fresnel LDMD mantles portions of the Apennine Bench formation and adjacent highlands north of the Apollo 15 landing site. The irregularly shaped deposit covers an area of more than 2120 km^2. The distribution pattern, irregular shape, and relatively large extent of this deposit suggest that several source vents may have been responsible for its formation. One source for this deposit is probably an irregularly shaped volcanic crater situated at the junction of Rima Fresnel II, another smaller rille, and a lineament (28° 25'N, 3° 55'E). However, if this feature is the sole source vent, it is not clear why the dark mantle is asymmetrically distributed around the crater, with the vast bulk of the material occurring to the east. This asymmetry could be due to partial vent blockage[31]. Alternatively, some of the deposit may have been erupted from fissure vents associated with faults along Rima Fresnel 1. The mare-type signature of this deposit is probably due to the explosive eruption of basaltic plug rock in association with the mare-filling episode of Imbrium basin.

Two separate localized dark mantle deposits were identified and described in the region east of Aristoteles[21,28,33]. The westernmost deposit (east of Aristoteles 1) is roughly circular and covers a highland area about 45 km in diameter. This LDMD is centered around a northwest-southeast trending chain of endogenic craters; several of these craters appear to have been the source vents for the pyroclastic material. The major vent in this chain measures 4x7 km. The easternmost LDMD (east of Aristoteles 2) is more complex and irregular in shape. This deposit is elongate (~20x40 km) and is superposed on both mare and highlands terrain. Three distinct endogenic crater chains are located in the dark-mantled area. Based on deposit geometry, two large irregular craters appear to have been the primary source vents for the bulk of the pyroclastic debris[7]. One is located in Mare Frigoris and the other is in the adjacent highland terrain. It should be noted that the source vent in the mare would have ejected basaltic wall rock during the explosive eruption that emplaced a portion of the LDMD.

Group 3

Spectra. A typical spectrum for Group 3 is that obtained of the J. Herschel pyroclastics. Other spectra included in this group are from four separate pyroclastic deposits: three on the floor of Alphonsus crater[34] and one on the south flank of Cruger crater[35]. These spectra have moderately deep (5-7%), broad, and asymmetrical absorption bands in the "1.0-μm" region. These bands are clearly composite features with centers at or beyond 1.0 μm. A quantitative analysis of the "1.0-μm band in the J. Herschel deposit spectrum presented by *McCord et al*[32] indicated that this feature could best be explained by a mixture of olivine and orthopyroxene. While in theory this band could be produced by the combination of clinopyroxene, orthopyroxene, and Fe^{2+}-bearing glass, additional band analyses have indicated that this is unlikely. The other members of Group 3 may also contain material rich in olivine and pyroxene. While the basaltic plug rock could be the source of some of the olivine, the very high olivine abundance indicated by the spectral data requires another source. The bulk of this olivine was almost certainly emplaced with the juvenile material. It also seems likely that the bulk of the orthopyroxene in the J. Herschel deposits was present as a component in the highlands-rich wall rock and that it

was eroded and emplaced during the J. Herschel eruption. Spectral data obtained for adjacent highland deposits indicate that the dominant mafic mineral present is orthopyroxene. No evidence for olivine was found in the spectra of these highlands units.

In summary, the J. Herschel pyroclastic deposit is dominated by olivine and pyroxene. The olivine was emplaced with the juvenile material and the bulk of the orthopyroxene was emplaced as a component in the highlands-rich wall rock. The basaltic plug rock could have contributed minor amounts of olivine and pyroxene. Some pyroclastic glass may be present.

Geology. A major deposit of dark mantling material is located on the eastern side of the floor of J. Herschel crater. This deposit was first identified by *Ulrich*[36]. Here, low-albedo material drapes and subdues subjacent highland terrain. Like certain others, this deposit is associated with a major rille system on the floor of the crater. The rille itself appears to be composed, at least in part, of coalesced craters of endogenic origin. Four of these craters appear to have been the major sources of the dark mantling material now spread over the eastern floor of the crater. Vent diameters range in size from 4-8 km with the dark mantling deposit covering an area approximately 60 km by 35 km. The other endogenic craters associated with this rille complex may have been formed by the drainage of debris into the subsurface along faults[7].

The 118-km-diameter crater Alphonsus is located in the highlands of the central nearside. Scattered about the perimeter of the floor are 11 endogenic dark halo craters, each of which is associated with a floor fracture or series of fractures[34]. Several pyroclastic deposits exist in the Cruger region[35]. The largest of these units is located on the southern rim of Cruger crater. This deposit covers an area of roughly 760 km^2. The major portion of the deposit is a tongue-shaped feature that extends straight south from the crater rim. A narrow finger of dark mantle material extends eastward of the main deposit. No source vents have been positively identified for this deposit, but it is possible that several vents were responsible for emplacing such a large, irregularly shaped deposit.

Different depths for the location of the plug rocks may be at least in part responsible for the compositional differences among the various LDMD groups[7]. For example, the highlands-rich deposits of Group 1 suggest that a thin plug rock formed under a thick overburden of highlands material. Likewise, the mare-like composition of the Group 2 deposits suggests the presence of a thicker plug rock at a shallower depth, or that lesser amounts of highlands overburden existed above the conduit prior to the eruption. The mare-like deposits of Group 2 may also have been formed by the eruption of an excessive amount of mare-type material. In addition, in those instances where the source vent formed in preexisting mare terrain (e.g., east of Aristoteles 2), the wall rock emplaced in the pyroclastic deposits would be expected to be composed largely of mare basalt. The abundant olivine component in the Group 3 deposits might be explained in several ways. These include the following (1) the olivine may have existed in the form of phenocrysts in the magma and been emplaced with the juvenile material upon eruption, (2) the olivine now exists as devitrified glass in the localized pyroclastic deposits, (3) olive-rich mantle inclusions might have been present in the melt and now could be found as xenoliths in the pyroclastic deposits, and/or (4) a small amount of olivine could be derived from the basaltic plug rock.

SUMMARY: Regional deposits are the products of strombolian or continuous eruptions while localized deposits are the result of vulcanian eruptions. Some regional deposits contain large amounts of Fe^{2+}-bearing glass while others are dominated by mixtures of black and orange spheres similar to those returned from the Apollo 17 landing site. Localized pyroclastic deposits exhibit three distinct compositions. The first group is dominated by highlands debris and a dark juvenile component. The second group is composed largely of basaltic caprock material with much lesser amounts of highlands-rich wall rock and juvenile material. The final group is dominated by a mixture of olivine and pyroxene. Based upon their compositions, it is very unlikely that regional pyroclastic deposits are the result of coalesced localized dark mantle deposits. Both regional and localized deposits exhibit low-radar returns (3.8-cm), have smooth surfaces and low albedoes. A strombolian or continuous eruption origin of lunar regional pyroclastic deposits is consistent with the characteristics of the volatile-coated spheres returned from the Apollo 17 landing site. The lack of associated lava flows and the small radial extent of the dark-haolos (3-5 km) around the localized dark mantle deposits suggests that they were formed during a short-lived (vulcanian) explosive eruption.

REFERENCES

1. Heiken G. H., McKay D. S., and Brown P. W. (1974) Lunar deposits of possible pyroclastic origin. *Geochim. Cosmochim. Acta*, 38, 1703-1718.
2. Delano J. W. (1979) Apollo 15 green glass: Chemistry and possible origin. *Proc. Lunar Planet. Sci. Conf. 10th*, pp. 275-300.
3. Delano, J. W. (1986) Pristine lunar glasses: Criteria, data, and implications. *Proc. Lunar Planet. Sci. Conf. 16th*, in *J. Geophys. Res.*, 91, D201-D213.
4. Pieters C. M., McCord T. B., Zisk S. H., and Adams J. B. (1973) Lunar black spots and the nature of the Apollo 17 landing area. *J. Geophys. Res.*, 78, 5867-5875.
5. Adams, J. B., Pieters C. M., and McCord T. B. (1974) Orange glass: Evidence for regional deposits of pyroclastic origin on the Moon. *Proc. Lunar Sci. Conf., 5th*, pp. 171-186.
6. Pieters C. M., McCord T. B., Charette M. P., and Adams J. B. (1974) Lunar surface: Identification of the dark mantling material in the Apollo 17 soil samples. *Science, 183*, 1191-11194.
7. Hawke B.R., Coombs C.R., Gaddis L.R., Lucey P.G., and Owensby P.D. (1989b) Remote sensing and geologic studies of localized dark mantle deposits on the Moon. *Proc. Lunar Planet. Sci. Conf. 19th*, pp. 255-268.
8. Coombs C.R. and Hawke B.R. (1989) Explosive volcanism on the Moon: A review. *Proc. Kagoshima Int'l Conf. on Volcanoes*, Kagoshima, Japan, pp. 416-419.
9. Gaddis L.R., Pieters C.M., and Hawke B.R. (1985) Remote sensing of lunar pyroclastic mantling deposits. *Icarus, 61*, 461-489.
10. Howard K.A., Carr M.H., and Muelberger W.R. (1973) Basalt stratigraphy of southern Mare Serenitatis. *Apollo 17 Preliminary Science Report*, NASA SP-330, pp. 29-1 to 29-12.
11. Head J.W. (1974) Lunar dark-mantle deposits: Possible clues to the distribution of early mare deposits. *Proc. Lunar Sci. Conf. 5th*, pp. 207-222.
12. Zisk S.H., Hodges C.A., Moore H.J., Shorthill R.W., Thompson T.W., Whitaker E.A., and Wilhelms D.E. (1977) The Aristarchus-Harbinger region of the Moon: Surface geology and history from recent remote-sensing observations. *The Moon*, 17, 59-99.
13. Pohn H.A. and Wildey R.L. (1970) A photoelectric-photographic study of the normal albedo of the Moon. *U.S. Geol. Surv. Prof. Pap. 599-E*, Plate 1.
14. Cernan E.A., Evans R.E., and Schmitt H. (1972) Apollo 17 technical air-to-ground voice transcription. *MSC-07629*.
15. Lucchitta B. K. (1973) Photogeology of the dark material in the Taurus-Littrow region of the Moon. *Proc. Lunar Sci. Conf. 4th*, pp. 149-162.
16. Lucchitta B.K. and Schmitt H.H. (1974) Orange material in the Sulpicius Gallus formation at the southwestern edge of Mare Serenitatis. *Proc. Lunar Sci. Conf. 5th*, pp. 223-234.
17. Zisk S.H., Pettengill G.H., Catuna G.W. (1974) High-resolution radar map of the lunar surface at 3.8-cm wavelength. *The Moon, 10*, 17-50.
18. Taylor S.R. (1982) Planetary Science: A Lunar Perspective. Lunar and Planetary Institute Houston. pp. 481.
19. Hawke B. R., Coombs C. R., and Clark B. (1990) Ilmenite-rich pyroclastic deposits: An ideal lunar resource. *Proc. Lunar Planet. Sci. Conf. 20th*, in press.
20. Thompson T.W. (1979) A review of Earth-based radar mapping of the Moon. Moon Planets, 20, 179-198. Wilhelms D.E. and McCauley J.F. (1971) Geologic map of the nearside of the Moon. *U.S. Geol. Surv. Misc. Map I-703.*
21. Wilhelms D.E. and McCauley J.F. (1971) Geologic map of the nearside of the Moon. *U.S. Geol. Surv. Misc. Map 1-703.*
22. Lucey P.G., Hawke B.R., Pieters C.M., Head J.W., and McCord T.B. (1986) A compositional study of the Aristarchus region of the Moon using near-infrared reflectance spectroscopy. *Proc. Lunar Planet. Sci. Conf. 16th*, in *J. Geophys. Res., 91*, D344-D354.
23. McCord T.B., Pieters C.M., and Feierberg M.A. (1976) Multispectral mapping of the lunar surface using ground-based telescopes. *Icarus 29*, 1-34.
24. Pieters C., Head J. W., McCord T. B., Adams J. B., and Zisk S. (1975) Geochemical and geological units of Mare Humorum: Definition using remote sensing and lunar sample information. *Proc. Lunar Sci.*

Conf. 6th, pp. 2689-2710.

25. Head J.W. and Wilson L. (1979) Alphonsus-type dark-halo craters: Morphology, morphometry and 25. eruption conditions. *Proc. Lunar Planet. Sci. Conf. 10th*, pp. 2861-2897.
26. Wilson L., and Head J.W. (1981) Ascent and eruption of basaltic magma on the Earth and Moon. *J. Geophys. Res.*, 78, 2971-3001.
27. Coombs C.R., Hawke B.R., and Owensby P.D. (1988) A recent survey of localized lunar dark mantle deposits (abstract). In *Lunar and Planetary Science XIX*, pp. 209-210. Lunar and Planetary Institute, Houston.
28. Hawke B.R. and Head J.W. (1980) Small dark mantle deposits of possible pyroclastic origin: Geologic setting, composition, and relation of regional stratigraphy (abstract). In *Lunar and Planetary Science XI*, pp. 426-428. Lunar and Planetary Institute, Houston.
29. Hawke B.R., McCord T.B., and Head J.W. (1980) Small lunar dark mantle deposits of probable pyroclastic origin. *NASA TM-82385*, pp. 155-157.
30. Lucey P.G., Gaddis L.R., Bell J.E., and Hawke B.R. (1984) Near-infrared spectral reflectance studies of localized dark mantle deposits (abstract). In Lunar and Planetary Science XV, pp. 495-496. *Lunar and Planetary Institute*, Houston.
31. Hawke B. R., MacLaskey D., McCord T. B., Adams J. B., Head J. W., Pieters C. M., and Zisk S. H. (1979) Multispectral mapping of the Apollo 15-Apennine region: The identification and distribution of regional pyroclastics. *Proc. Lunar Planet. Sci. Conf. 10th*, pp. 2995-2934.
32. McCord T. B., Clark R. N., Hawke B. R., McFadden L. A., Owensby P. D., Pieters C. M., and Adams J. B. (1981) moon: Near-infrared spectral reflectance, a first good look. *J. Geophys. Res., 86*, 10883-10,892.
33. Lucchitta B. K. (1972) Geologic map of the Aristoteles quadrangle of the Moon. *U.S. Geol. Surv. Misc. Map I-725*.
34. Coombs C. R. and Hawke B. R., Lucey P. G., Owensby P. D., and Zisk S.H. (1989) The Alphonsus region: A geologic and remote sensing perspective. *Proc. Lunar Planet. Sci. Conf. 20th*, in press.
35. Hawke B. R., Coombs C. R., and Lucey P. G. (1989) A remote-sensing and geologic investigation of the Cruger region of the moon. *Proc. Lunar Planet. Sci. Conf. 19th*, pp. 127-135.
36. Ulrich G. E. (1969) Geologic map of the J. Herschel quadrangle of the Moon. *U.S. Geol. Surv. Misc. Map I-604*.

IMPACT AND VOLCANIC GLASSES OF MARE FECUNDITATIS. Yuequn JIN and Lawrence A. TAYLOR, Dept. of Geological Sciences, Univ. of Tennessee, Knoxville, TN 37996.

Investigations of glasses within the lunar soils have yielded significant information regarding both the impacting processes on the moon and the petrogeneses of mare basalts. Based on their studies of thousands of glasses in lunar soils, Delano and co-workers have proposed 25 different types of lunar volcanic magmas [1,2]. However, their studies were restricted to the sites visited by the Apollo missions. In an attempt to expand the global coverage of studies on lunar samples and to search for possible new pristine magma types from the moon, petrographic examination and microprobe analyses of 116 glass particles have been performed in a Luna 16 sample from Mare Fecunditatis, 21036,15. These analyses were undertaken in order to discern the parental magmas for Mare Fecunditatis and to examine the impact glasses as these might relate to provenance for the soil components. Four types of glass were identified [3]: 1) basaltic (39.6%); 2) ANT (anorthositic- norite-troctolite) suite (55.2%); 3) maskelynite (4.3%); and 4) HASP [4] (0.9%). Notice that none of the Luna 16 glasses plots within the field of the Apollo pristine glass types [Fig. 1]; the Apollo glasses are more primitive.

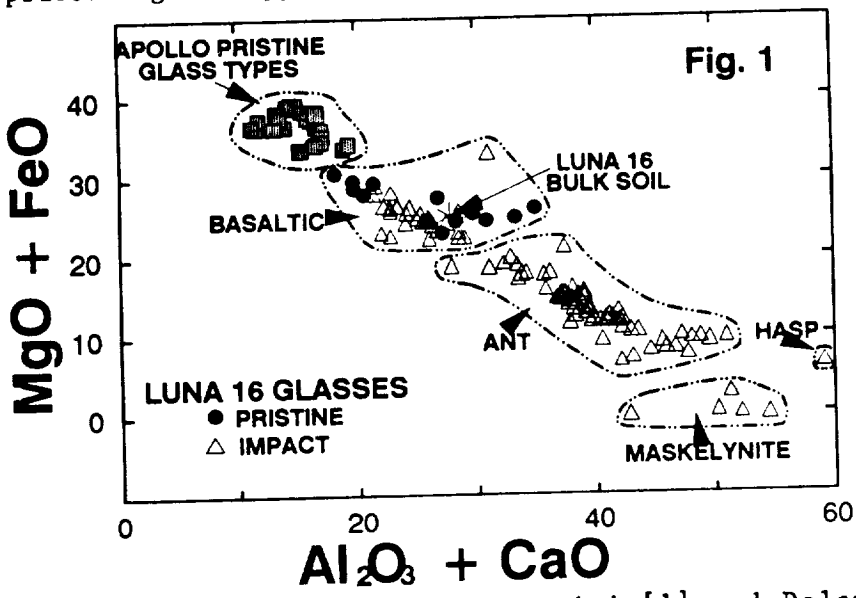

The ANT suite glasses plot well away from the average bulk composition of the soil, which has a composition within the basaltic glass field [Fig 1]. It is possible that the ANT suite glass is foreign to the Luna 16 landing site and could be from the nearby highlands 100 km to the East and to the North, such as that sampled by Luna 20. Alternatively, they could be derived from the highland materials excavated from beneath the relatively thin mare lava flows by meteorite bombardment.

Various criteria have been applied in order to identify the pristinity of the 116 glass particles. According to Delano and Livi [1] and Delano [2], pristine glasses possess intra-sample homogeneity and high Mg/Al ratios, but contain no schlieren and/or exotic inclusions. Only those glasses with CaO/Al_2O_3 (weight) ratio greater than 0.75 are considered to have mare parentage [4]. Applying the collective criteria for volcanic glass, fourteen particles of basaltic glass were identified to be pristine. These pristine glass grains were analyzed for Ni by long (400 sec.) counting times. As has been discussed by Delano [2], the Ni in the lunar magma usually behaves as a lithophile element and will have a positive correlation with MgO. In Figure 2, the Luna 16 pristine glasses occupy a scattered area but generally fall along the trend defined by the Apollo pristine glass types and seem to extend the trend toward the low-MgO end. This trend is cited as evidence to support the volcanic origin of the fourteen glasses. If Ni is a contaminant from meteorite impact, the compositions should follow the arrow in Figure 2 (i.e., siderophile component). In fact, the Luna 16 glass with the highest Ni content (97 ppm) could be interpreted as being of impact origin using this criterion.

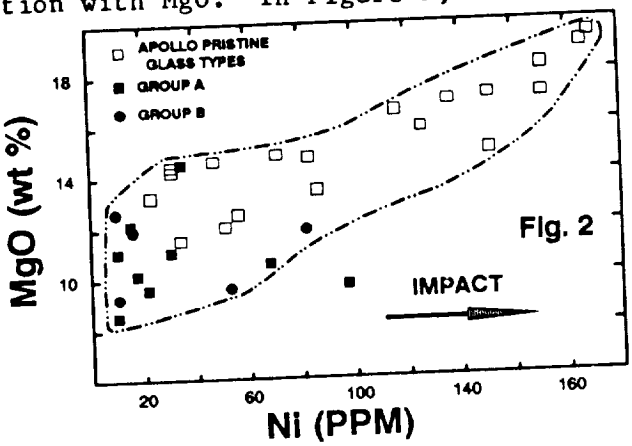

The pristine glasses have similar compositional ranges of FeO, TiO_2, CaO, and Al_2O_3 to those of Luna 16 basaltic fragments [5]. However, the majority

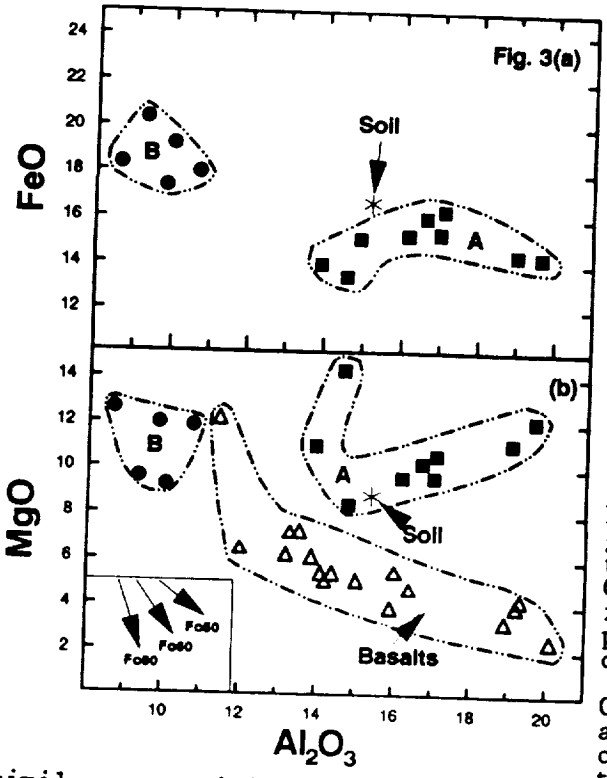

of the pristine glasses have higher MgO contents (7-12 wt.%) and Mg/(Mg+Fe) ratios (0.4-0.7) than the lithic equivalents (2-9 wt.% and 0.2-0.4, resp.) [Fig. 3(b)]. Inspection of the pristine glass chemistry permits division into two groups (A and B) [Fig. 3]. The Group A glass is characterized by high CaO (11.6-15.1 wt.%) and Al_2O_3 (13.9-19.6 wt.%) and low FeO (13.5-16.4 wt.%). This group is similar to Fecunditatis Type A Basaltic Glass of Jakes et al. [6]. The relationship of the Group A glasses with the basalts is difficult to discern. Although some of them could be parental to the Luna 16 basalts by olivine fractionation [Fig. 3b], other element-element plots (e.g., CaO or FeO vs. Al_2O_3) eliminate this possibility. However, as pointed out by Longhi [7], most of the Apollo volcanic glass types do not appear to be parental to the local basalts. Therefore, the Group A glass could justifiably come from an unusual source with high plagioclase content. Without further data, this question cannot be resolved.

The Group B glasses are lower in CaO and Al_2O_3 contents (9.27-10.4 wt.% and 8.64-10.8 wt.%) but higher in FeO content (17.3-20.4 wt.%) than that of the Group A glasses (Fig. 3). They have similar compositions to those of Fecunditatis Type B Basaltic Glass of Jakes et al. [6]. Based on Figure 3(b), it would appear that these glasses can be related to the Luna 16 basalts by simple fractionation of olivine. However, as seen in the TiO_2-MgO plot (Fig. 4), ilmenite or ilmenite + olivine fractionation is required to explain the high-Ti members. Therefore, the Group B glasses may represent the parental magmas of the various types of basalts in Mare Fecunditatis (high-Ti, low-Ti, and aluminous, etc.). Indeed, the Group B glasses probably represent two or more magma types. Here, as with the Group A glass population, there are not sufficient data to draw absolute conclusions.

SUMMARY: **1.** More than half of the glasses (ANT suite) in the Luna 16 soil sample under considerationd are foreign to the Mare Fecunditatis and are impact products of highland components; and **2.** It would appear that **Mare Fecunditatis pristine glasses represent new lunar magma types,.** in addition to the 25 types from the Apollo samples. These new magmas are unusual, compared to Delano's pristine glass [2], being higher in Al_2O_3 (8.64-19.6 wt.% vs. 4.6-9.6 wt.%) and CaO (9.27-15.0 wt.% vs. 6.27-9.40 wt.%) and lower in MgO (8.51-14.4 wt.% vs. 12.1-19.5 wt.%). There is an obvious higher plagioclase component to the Luna 16 magmas.

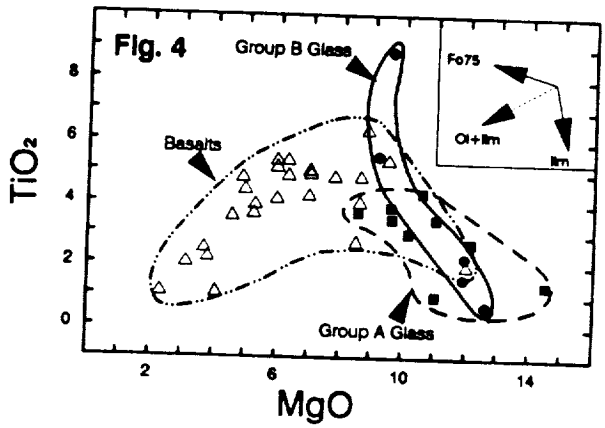

REFERENCES: [1] Delano J.W. & Livi K. (1981) Geochim Cosmochim Acta, 45, p. 2137-2149; [2] Delano J.W. (1986) PLPSC 16th, JGR, 91, p. D201-213; [3] Jin Y. & Taylor L.A. (1989) LPS XX, p. 466-467; [4] Naney M.T., Crowl D.M., & Papike J.J. (1976) PLSC 7th, p. 155-184; [5] Kurat G. et al. (1976) PLSC 7th, p. 1301-1321; [6] Jakes P. et al. (1972) EPSL, 13, p. 257-271; [7] Longhi J. (1989) In Workshop on Lunar Volcanic Glasses: Scientific and Resource Potential, pp. xx-yy, LPI, in press.

MAPPING PYROCLASTIC DEPOSITS AND OTHER LUNAR FEATURES FOR SOLAR WIND IMPLANTED HELIUM

J.L. Jordan, Office of Lunar Base Research, Department of Geology, P.O. Box 10031, Lamar University, Beaumont, TX 77710

In addition to the ubiquitous presence of oxygen in lunar materials, the large amounts of hydrogen and helium of solar wind origin found in returned lunar samples have led to suggestions that the lunar regolith may provide a valuable source of energy for future space exploration as well as assisting in meeting the terrestrial energy demands of the future [1,4,14].

Studies of mineral separates from lunar soils have revealed that the mineral ilmenite ($FeTiO_3$) is the most retentive phase for these solar wind implanted gases [3,12]. Concentrations of solar wind H and He in lunar ilmenites may be more than an order of magnitude greater than in other soil constituents [3,12]. Thus knowledge of the distribution of ilmenite - rich materials can provide insight as to the location of potential H and He reservoirs. In addition, at least one process for extraction of oxygen from the lunar regolith involves the use of an ilmenite separate as a feedstock [4].

There has been the suggestion made in this workshop that regional deposits of ilmenite - rich lunar volcanic glasses could be a valuable lunar resource [2]. The existence of these large scale deposits has been suggested from remote sensing observations [8,13]. Unfortunately the only returned samples that contain lunar volcanic glasses (the Apollo 15 green glass soil, 15426; and the orange soil 74220) were apparently severely outgassed and may have been shielded from further solar wind exposure after their formation [5,7,9]. In regions where soils have been effectively gardened through meteoritic bombardment over a period of a few billion years the exposure of surfaces of grains that originated from depths of several meters is assumed. A quantitative measure of this regolith maturing process is desired since it is a fraction of the solar wind fluence that is ultimately retained.

The "maturity index" that has proven to be very reliable for measuring the degree of solar wind exposure that a soil has experienced is the ratio Is/FeO, which is the fraction of fine metal produced in the surfaces of the grains by solar wind reduction to the total FeO [10,11]. This ratio ranges from 0 to greater than 100 in lunar soils, and if there were no large differences in the trapping efficiency of the mineral phases one may expect the He contents of the soil would correlate with this ratio. Mineralogical differences between and within sites make this correlation generally poor.

Maturity and ilmenite contents can compensate for one another in the role they play in the H and He contents of lunar soils. Thus a correlation between He and the product (Is/FeO)(TiO_2 wt %) should be expected to be global. This correlation is illustrated in Fig.1 for greater than 60 returned Apollo soils for which data on all three parameters exists (references for measurements given in [7]). The linear fit of the trend allows curves of equal He concentration (helium isocons) to be constructed in a plot of Is/FeO versus TiO_2 (wt %) shown in Fig.2. Thus the H and He distribution at the lunar surface may be within the grasp of quantitative assessment if both soil maturity and TiO_2 content of the soil are known.

The suggestion that regional pyroclastic deposits may be enriched in lunar resources could be followed by quantitative assessment if remote means of determining Is/FeO in addition to TiO_2 could be established. Spectral reflectance data on samples for which the Is/FeO has been determined may provide this important link. If there exists a well defined correlation

between these observations, then superposition of this data with remote TiO2 data allows the prediction of H and He - rich zones with a reasonable degree of certainty. These deposits should have (Is/FeO)(TiO2 wt %) products greater than 350 if they are expected to contain greater than average (8 wppb) amounts of 3He.

Fig. 1

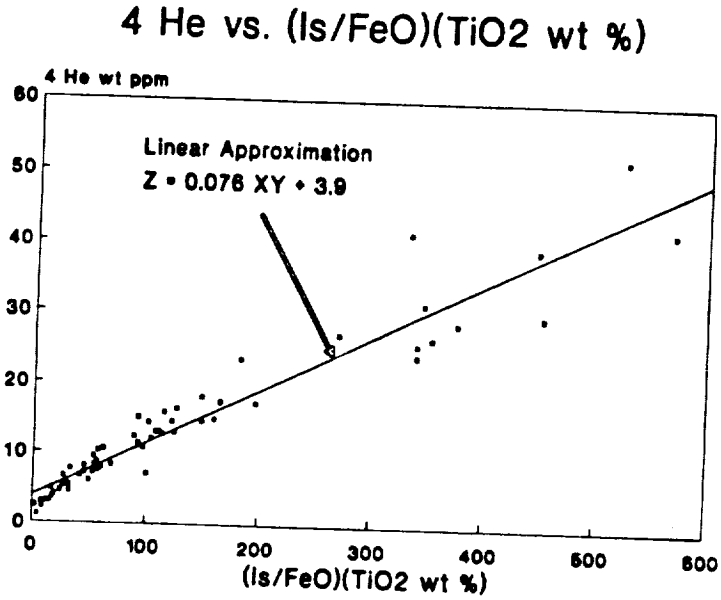

Fig. 2

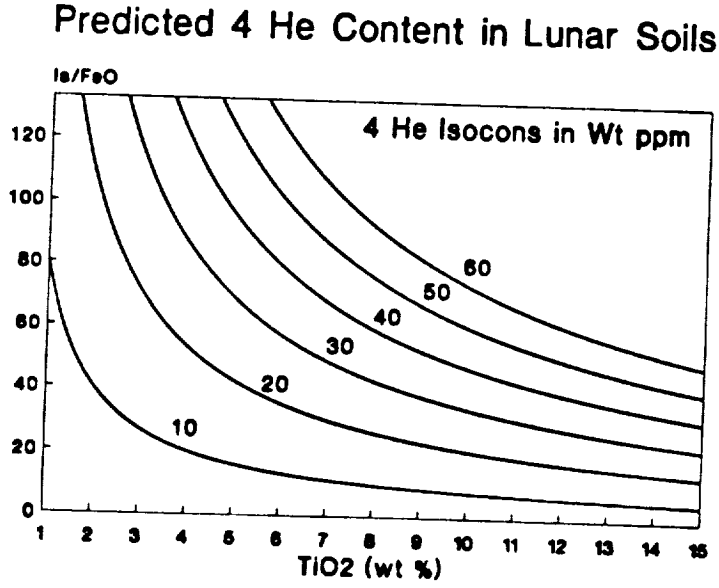

Acknowledgments

This work is supported by a Johnson Space Center Regional Universities Grant NAG9-376.

References

1. Carter, J.L. (1985) Lunar Regolith fines:A Source of Hydrogen,In *Symposium on Lunar Bases and Space Activities of the 21st Century* (W.W. Mendell, ed.), p.571-581. Lunar and Planetary Institute, Houston.
2. Coombs, C.R., Hawke, B.R., Clark, B. (1989) The Optimal Lunar Resource: Ilmenite-Rich Regional Pyroclastic Deposits, In *abstracts* for this workshop, Lunar Planet. Inst., Houston.
3. Eberhardt, P., Geiss, J., Graf, H., Grogler, N., Mendia, M.D., Morgeli, M., Schwaller, H., and Stettler, A. (1972) Trapped Solar Wind Noble Gases in Apollo 12 Lunar Sci. Conf. Vol. 2, p. 1821.
4. Gibson, M.A. and Knudsen, C.W.(1985) Lunar Oxygen Production from Ilmenite, In *Symposium* for Lunar *Bases and Space Activities of the 21st Century* (W.W. Mendell, ed.),p.543-550, Lunar and Planetary Institute, Houston.
5. Hintenberger, H., Schultz, L., and Weber, H.W. (1975) A Comparison of Noble Gases in Lunar Fines and Soil Breccias: Implications for the Origin of Soil Breccias, *Proc. Sixth Lunar Sci. Conf. Conf.*, Vol. 2, p.2261-2270.
6. Jordan, J.L. (1975) Inert Gas Investigations of the Apollo 15 and 17 Landing Sites, *Ph.D. Thesis*, Rice University.
7. Jordan, J.L. (1989) Prediction of the He Distribution at the Lunar Surface, In papers submitted to the *First Ann. Symposium for Space Mining and Manufacturing*, UA/NASA SERC, Tucson.
8. Johnson, T.V., Mosher, J.A. and Matson, D.L. (1977) Proc. Lunar Planet. Sci. Conf. 8th, p.3243-3255.
9. Lakatos, S., Heymann, D., and Yaniv, A. (1973) Green Spherules from Apollo 15: Inferences about their Origin from Rare Gas Measurements, *The Moon*, Vol. 7, p.132.
10. Morris, R. V. (1976) Surface Exposure Indices of Lunar Soils: A Comparative FMR Study, *Proc. Seventh Lunar Sci. Conf.*, Vol. 1, p.315-335.
11. Morris, R.V. (1978) The Surface Exposure (Maturity) of Lunar Soils: Some Concepts and Is/FeO Compilation, *Proc. Ninth Lunar and Planet. Sci. Conf.*, Vol. 2, p.2287-2298.
12. Mueller, H.W., Jordan, J.L., Kalbitzer, S., Kiko, J., and Kirsten, T. (1976) Rare Gas Ion Probe Analysis of Helium Profiles in Individual Lunar Soil Particles, *Proc. Seventh Lunar Sci. Conf.*,Vol. 2, p.937-951.
13. Pieters, C.M. (1978) *Proc. Lunar* and *Planet. Sci. Conf. 9th*, p.2825-2849.
14. Wittenberg, L.J., Santarius, J.F., and Kulcinski, G.L. (1986) Lunar Source of 3He for Commercial Fusion Power, *Fusion Technology*, Vol. 10, No. 2, p.167.

DIFFERENTIATES OF THE PICRITIC GLASS MAGMAS: THE MISSING MARE BASALTS; J. Longhi, Lamont-Doherty Geological Observatory, Palisades, NY 10964

One prediction of the hypothesis that mare basalts are differentiates of more primitive magmas similar in composition to the picritic volcanic glasses (1,2,3) is that there should be mare basalts with compositions spanning the range expected of differentiates of the known picritic compositions. Figure 1 demonstrates that this predicition has not yet been confirmed. Figure 1 shows the TiO_2 and MgO concentrations of fine-grained mare basalts and picritic glasses (2); also plotted are calculated differentiation trends of a few of the picritc glass compositions. It is clear that there are no basalt compositions near the kinked portions of the red and black glass trends. There is also a dearth of basalt compositions corresponding to differentiates of the yellow glasses. Basalts with intermediate and very high TiO_2 concentrations may thus be thought of as "missing", at least from the sample collections. Remote sensing studies (4,5) indicate abundant unsampled flows with intermediate TiO_2, so the non-primary basalt hypothesis is at least consistent with the data in this portion of the composition range and the dearth of the mare basalts with intermediate TiO_2 is apparently a sampling problem. The missing very-high-Ti basalts are more problematical. The same remote sensing studies also describe extensive areas of an unsampled high-Ti basalt type (HDSA) that is similar to Apollo 11 and 17 basalts in TiO_2 concentration,but is apparently more mafic. Taken at face value, the reflectance spectra of these basalts (actually soils) do not correspond the differentiates of the red and black glasses, which should have TiO_2 concentrations in the range of 11(evolved) to 17 (primitive) wt%. So it is not clear whether the very-high-Ti basalts are simply missing from our collections or are simply not present on the Moon.

Given the possibility that a few rare fragments of these intermediate-Ti and very-high-Ti basalts may be present in our collections, it should be useful to describe some the petrographic and chemical characteristics predicted for differentiates of yellow, red, and black glass compositions that might help in their discovery. Accordingly, I have calculated near-perfect fractional crystallization sequences for the Apollo 14 and 15 Yellow, the Apollo 15 Red, and the Apollo 14 Black glass compositions tabulated by (2). Partial results are listed in Table 1 in terms of temperature, volume (approximate) percent crystallized, order of mineral appearance, and silicate mineral composition. The calculations were arbitrarily stopped at 80 mole% crystallization.

Intermediate-Ti Basalts: Calculations show that all picritic glass compositions crystallize olivine and chromite early. The result in fine-grained differentiates should be olivine phenocrysts with chromite inclusions. After olivine and chromite, differentiates of the Apollo 14 and 17 yellow glass magmas should differ only slightly in crystallization sequence. Augite will crystallize next in the Apollo14 magma followed soon after by nearly simultaneous crystallization of plagioclase and ilmenite. The result in fine- to intermediate-grained rocks should be a sub-ophitic texture with ilmenite having the same textural position as plagioclase. Although plagioclase should be the second major phase to crystallize from the Apollo 17 magma (assuming no nucleation delays), plagioclase, augite, and ilmenite should begin to crystallize nearly simultaneously and produce an ophitic groundmass. In general appearance, differentiates of the Apollo 14 and 17 yellow glass magmas will resemble Apollo 12 ilmenite basalts (6), but with 1 to 3 % more ilmenite in the mode.

Very-high-Ti Basalts. Mineralogically, differentiates of the Apollo 15 Red and 14 Black glass magmas should be generally similar to some of the Apollo 11 and 17 basalts: phenocrysts of olivine with chromite inclusions and phenocrysts of ilmenite with cores of armalcolite in groundmasses of intergrown augite, plagioclase, and ilmenite. It is possible that very fine-grained or vitrophyric basalts might have phenocrysts of only olivine (with chromite) and armalcolite. Chemically, these basalts would be readily distinguishable from known mare basalts by their concentrations of TiO_2: up to 15 wt% (Red) or 17 wt% (Black). Petrographically, the total mode of opaques (>25%) would be diagnostic in medium- to coarse-grained rocks, and in fine-grained rocks the amount of armalcolite might approach 10%.

An interesting feature of these calculations is that pigeonite does not appear to crystallize from any of the four magmas modeled. Although pigeonite is the dominant pyroxene in low-Ti mare basalts, it is not a ubiquitous phase in the Apollo 12 ilmenite basalts (6) and in the high-Ti basalts (e.g.,7). Its absence in these latter rocks and in the calculations can be explained in terms of the extent of fractionation which is a reflection of cooling rate. Melting experiments on lunar compositions have shown that pigeonite is unstable with respect to olivine plus silica in highly ferroan ($Mg' < 0.15$) liquids (8). If Mg' in a magma drops below this value before the magma reaches saturation with pigeonite, then no pigeonite will crystallize. This situation is most favorable in magmas undergoing near perfect fractional crystallization that are saturated with augite because augite crystallization will cause Mg' to decrease with minimal increase in SiO_2. The same magma undergoing inefficient fractionation will crystallize pigeonite because Mg' decreases much more slowly per unit of crystallization and the magma is able to reach a sufficiently high SiO_2 content to stablize pigeonite while Mg' is still above 0.15. Thus it is observed that pigeonite is stable predominantly in the more coarsely grained and hence more slowly cooled members of the Apollo 12 ilmenite basalt suite (6) and Apollo 17 high-Ti basalts (7). A related feature of the calculations is the continuous stability of olivine (Table 1). Once augite begins to crystallize the proportion of olivine crystallizing falls almost to zero and then increases once silica begins to crystallize. If pigeonite were to crystallize, then olivine would quickly disappear only to reappear in the latest stages of crystallization when pigeonite became unstable.

REFERENCES

(1) Taylor S.R. (1982) *Planetary Science: A Lunar Perspective*, The Lunar & Planetary Institute. (2) Delano J.W. (1986) *J. Geophys. Res., 91*, D201-D213. (3) Longhi J. (1987) *J. Geophys. Res.*, 92, E349-E360. (4) BVSP (1981) *Basaltic Volcanism on the Terrestrial Planets*, The Lunar & Planetary Institute. (5) Pieters C.M., Head J.W., Adams J.B., McCord T.B., Zisk S., and Whitford-Stark J.L. (1980) *J. Geophys. Res., 85*, 3913-3938. (6) Dungan M.A. and Brown R. W. (1977) *Proc. Lunar Sci. Conf. 8th*, p. 1339-1381. (7) Longhi J. (1974) *Proc. Lunar Sci. Conf. 5th*, p. 447-469. (8) Longhi J. and Pan V. (1988) *J. Petrol., 29*, 115-147.

TABLE 1. Fractional Crystallization of Picritic Magmas

Apollo 14 Yellow

T(°C)	VFX	
1350	0	fo_{78}
1346	1	fo_{78}, crmt
1126	39	fo_{54}, (crmt), $Wo_{35}En_{39}$
1091	46	fo_{48}, $Wo_{34}En_{35}$, An_{88}
1084	50	fo_{46}, $Wo_{34}En_{33}$, An_{87}, ilm
1043	83	fo_{16}, $Wo_{35}En_{14}$, An_{80}, ilm

Apollo 15 Red

T(°C)	VFX	
1254	0	fo_{80}
1248	1	fo_{80}, crmt
1207	10	fo_{77}, crmt, arm
1136	30	fo_{67}, (arm), ilm
1132	31	fo_{66}, ilm, $Wo_{33}En_{46}$
1115	37	fo_{63}, ilm, $Wo_{33}En_{44}$,An_{88}
1049	84	fo_{28}, ilm, $Wo_{36}En_{22}$,An_{78}

Apollo 17 Yellow

T(°C)	VFX	
1292	0	fo_{78}
1287	1	fo_{78}, crmt
1126	28	fo_{62}, (crmt), An_{92}
1123	31	fo_{61}, An_{92},$Wo_{34}En_{43}$
1119	37	fo_{59}, An_{91},$Wo_{33}En_{42}$,ilm
1069	76	fo_{32}, An_{86},$Wo_{34}En_{26}$,ilm, sil
1064	84	fo_{21}, An_{83},$Wo_{33}En_{19}$,ilm, sil

Apollo 14 Black

T(°C)	VFX	
1273	0	fo_{80}
1268	1	fo_{80}, crmt
1244	8	fo_{78}, crmt, arm
1172	36	fo_{67}, (arm), ilm
1129	43	fo_{61}, ilm, $Wo_{34}En_{42}$
1092	56	fo_{52}, ilm, $Wo_{35}En_{36}$,An_{90}
1060	78	fo_{33}, ilm, $Wo_{39}En_{25}$,An_{87}, sil
1047	84	fo_{25}, ilm, $Wo_{39}En_{20}$,An_{86}, sil

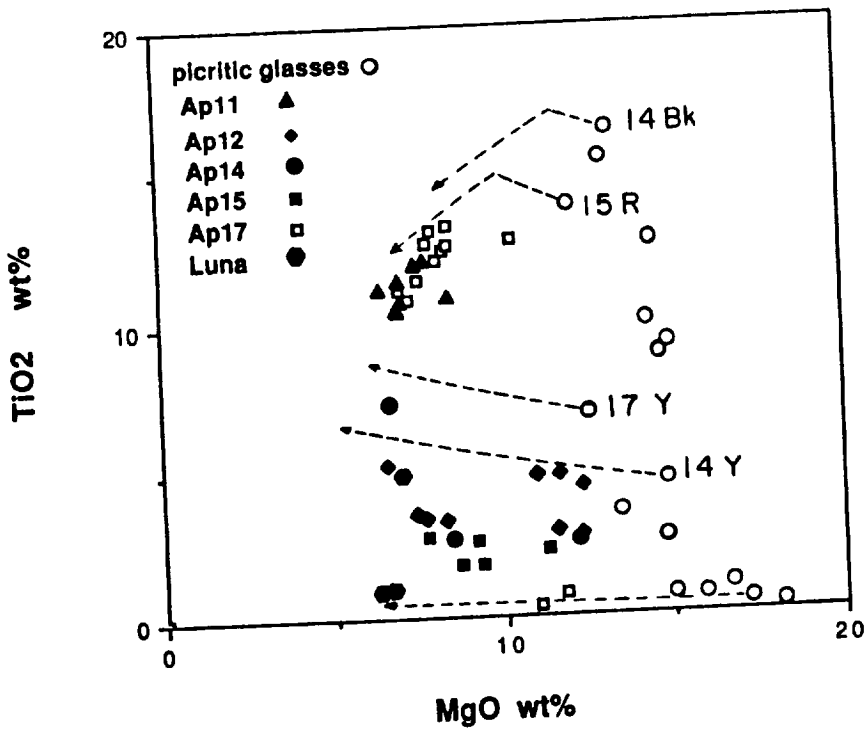

Figure 1. TiO_2 versus MgO in mare basalts and picritic glasses. Dashed lines are partial liquid lines of descent calculated by the method of (3). For green and yellow glasses, liquids are saturated only with olivine and chromite; for red and black glasses, negative slope represents liquids saturated with olivine and chromite, positive slope indicates olivine, chromite, and armalcolite.

REE DISTRIBUTION COEFFICIENTS FOR PIGEONITE: CONSTRAINTS ON THE ORIGIN OF THE MARE BASALT EUROPIUM ANOMALY. G. McKay (SN4, NASA-JSC, Houston, TX,77058) J. Wagstaff, and L. Le (Lockheed ESCO, 2400 NASA Rd. 1, Houston, TX 77058)

Introduction. A long-held paradigm of lunar science is that the complementary REE patterns and Eu anomalies of the lunar crust and mare basalt source regions reflect an early differentiation event of global scale resulting from the crystallization of a lunar magma ocean (MO) [e.g. 1,2]. The positive Eu anomaly of the crust is generally thought to result from plagioclase enrichment, while the negative Eu anomaly in mare basalts is thought to be inherited by the source region from an evolved MO in which prior plagioclase removal had produced a negative Eu anomaly [e.g. 2,3].

Several workers [e.g. 4,5] have called into question the need for prior plagioclase removal, suggesting that the mare basalt Eu anomaly was instead a result of Eu anomalies in the distribution coefficient patterns of the ferromagnesian cumulate minerals in the source regions. However, even some of these workers have recanted their heresy [6], and called for a Eu anomaly in the MO prior to formation of the cumulate source regions.

This issue has again been raised by Brophy and Basu [7] and Shearer and Papike [8]. These authors explicitly addressed the question of whether prior plagioclase removal is required to produce Eu anomalies of the magnitude observed in mare basalts. However, using slightly different approaches, and more importantly, using different values for mineral/melt distribution coefficients for Eu and trivalent REE, these authors arrived at opposite conclusions: Brophy and Basu concluded that prior plagioclase removal is required, while Shearer and Papike concluded that it is not.

Part of the uncertainty in this issue is a result of inadequate mineral/melt partition coefficient data, especially for Eu at lunar oxygen fugacities. The situation is most critical for low-Ca pyroxene (a major carrier of REE among MO crystallization products throughout much of the MO crystallization sequence), but less so for olivine and high-Ca pyroxene. Olivine distribution coefficients are so low [9] that even a small proportion of pyroxene in the source region will dominate REE abundances in both cumulates and their partial melts. High-Ca pyroxene distribution coefficients have been studied by several workers [e.g. 10,11,12] under near-lunar oxygen fugacities, and indicate a significant Eu anomaly (Fig. 1).

The magnitude of the Eu anomaly for Low-Ca PX is less well constrained. OPX distribution coefficients [13] indicate only a very minor anomaly (Fig. 1). However, those results were obtained before the difficulty of measuring very low distribution coefficients on small crystals was appreciated [9], so the magnitude of the anomaly is likely to be unreliable. The goal of this study is to provide reliable values for the partitioning of REE between low-Ca pyroxene and melt under near-lunar fO_2 so that the origin of the mare basalt Eu anomaly can be better constrained.

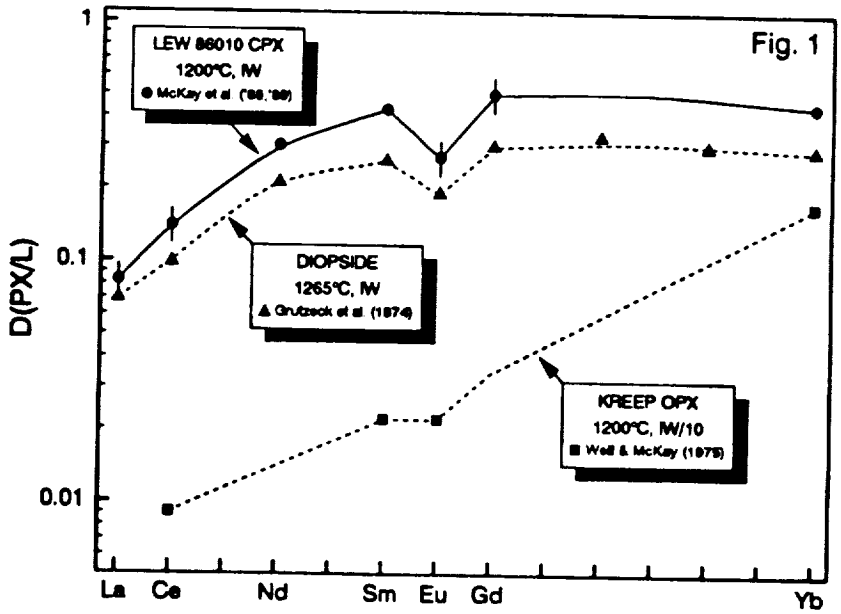

Experiments. McKay [14] reported distribution coefficients for trivalent REE between pigeonite and a melt produced by 15-20% crystallization of a synthetic basalt resembling 12015, but did not study partitioning of Eu. For the present study, we prepared a similar starting composition containing about 1 wt% each of Gd and Eu. Pellets (125mg) of this starting material were suspended on wire loops in a controlled atmosphere (CO/CO_2) furnace at oxygen fugacities near IW, held at 1300°C for four hours, cooled to 1200° in 2 hours, then to 1175° at 0.3°/hr, held for 24 hours, and then air quenched. This multi-stage cooling history permitted growth of large (>200 μm wide) pigeonite crystals for which even very low partition coefficients could be measured without interference from adjacent glass [9].

Resulting charges were sectioned, polished and analyzed with the JSC Cameca microprobe, with no analyzed spot being closer than 100 μm from the nearest glass, to ensure absence of analytical interference.

Table 1.

Xtl	D_{Eu}	D_{Gd}	$D_{Eu/Gd}$
A	.0070	.0225	.321
B	.0077	.0218	.361
C	.0065	.0230	.283
Avg	.0071	.0224	.321

Results. Resulting Eu and Gd partition coefficients for each crystal are given in Table 1, and average compositions of crystals and glass for the current experiments and our earlier experiments [14] are given in Table 2. The partition coefficients showed slight differences among the three charges (Table 1), but values for Eu/Gd are quite consistent. Values for D_{Gd} from the present study differ from our earlier values [14] by nearly 80%, despite the similarity in melt and pyroxene composition and experimental procedures and conditions.

Table 2.

	McKay(1981)		This Study	
	Liq	Px	Liq	Px
SiO_2	46.1	53.2	45.9	53.1
TiO_2	3.43	0.47	3.70	0.48
Al_2O_3	10.5	1.43	10.9	1.43
Cr_2O_3	0.24	0.73	0.23	1.07
FeO	16.6	15.8	16.4	14.4
MgO	7.43	24.5	7.48	25.8
CaO	11.0	3.41	11.7	2.58
Na_2O	0.28	0.00		
K_2O	0.11	0.00		
Eu_2O_3			1.22	0.0085
Gd_2O_3	2.66	0.096	1.25	0.028
mg	0.444	0.734	0.449	0.762
wo		0.068		0.052
D(Gd)		0.036		0.022
D(Eu)				0.0071

Discussion. The major difference between the two sets of experiments is the presence of 0.4 wt% alkalies in the earlier glass, and the slightly more calcic nature of the earlier pyroxene (Table 2). McKay *et al.* [15] noted the strong dependence of CPX distribution coefficients on Ca content, and we suspect that this is at least partially responsible for the difference between our present and earlier results for Gd. We speculate that the presence of alkalies in the earlier melt increased the activity of Ca in that melt, resulting in growth of more calcic pyroxene. Experiments using the new starting composition to which Na has been added are in progress to test this hypothesis.

Because of the absence of alkalies in the present starting composition and the apparent resulting effect on distribution coefficients, for this abstract we rely on the current experiments only to define the magnitude of the Eu anomaly in the pigeonite partition coefficient pattern. We take the absolute values for the trivalent REE from our earlier study, and use the $D_{Eu/Gd}$ ratio from the current study to compute a value for D_{Eu} which is consistent with the earlier trivalent values.

Results are shown in Figure 2, along with the OPX values of [13] for comparison. It is clear from these results that low-Ca pyroxene has a much larger capacity to develop a Eu anomaly than the earlier data suggest. These results are in qualitative agreement with partition coefficients derived by [16] from ion probe analyses of Wo_{12} pyroxenes from lunar mare basalt, but suggest an even larger Eu anomaly for pyroxenes with lower Ca content, in agreement with arguments based on crystal chemistry [8]. Whether the Eu anomaly in low-Ca pyroxene partition coefficients is large enough to explain the Eu anomaly in mare basalt without prior plagioclase crystallization awaits detailed modelling studies which are beyond the scope of this abstract.

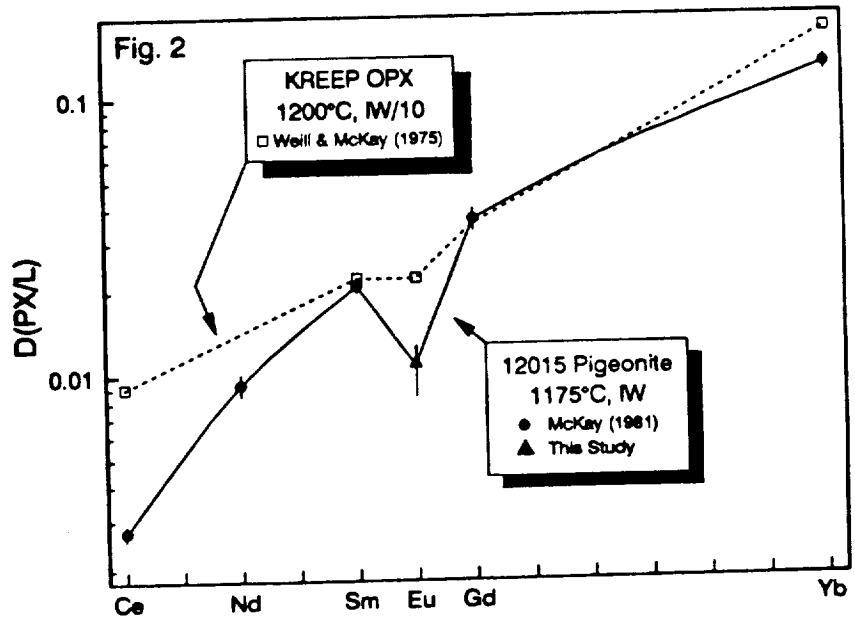

References: [1] Walker *et al.* (1975) PLSC 6th, 1103. [2] Taylor (1982) Planetary Science: A Lunar Perspective. [3] Wood (1975) PLSC 6th, 1087. [4] Shih and Schonfeld (1976) PLSC 7th, 1757. [5] Nyquist *et al.* (1977) PLSC 8th, 1383. [6] Nyquist *et al.*, (1981) EPSL 55, 335. [7] Brophy and Basu (1989) LPSC XX, 115. [8] Shearer and Papike (1989) LPSC XX, 994. [9] McKay (1986) GCA 50, 69. [10] Grutzeck *et al.* (1974) Geophys. Res. Lett. 1, 273. [11] McKay *et al.* (1988) Meteoritics 23, 289. [12] McKay *et al.* (1989) LPSC XX, 677. [13] Weill and McKay (1975) PLSC 6th, 1143. [14] McKay (1981) EOS, Trans. AGU 62, 1070. [15] McKay *et al.* (1986) GCA 50, 927. [16] Shearer *et al.* (1989) GCA 53, 1041

A BRIEF LITERATURE REVIEW OF OBSERVATIONS PERTAINING TO CONDENSED VOLATILE COATINGS ON LUNAR VOLCANIC GLASSES.

C. Meyer, NASA Johnson Space Center, Houston TX 77058

Many studies have been made of the condensed volatile coatings on the Apollo 15 green and Apollo 17 orange glass beads. Lunar samples 15426 and 74220 and adjacent samples contain enrichments in a large number of volatile trace elements when compared to local mare basalts at the same site (see table). Zn, Ge, Cd, ^{204}Pb, Tl, Ag, Au, Ir, Re and Br are enriched by a factor of about 100 and Ga, Cu, Sb, Bi, In, As, Hg?, Se and Te are enriched by a factor of about 10. However, lunar basalts are so very depleted in these elements when compared to terrestrial rocks that these lunar deposits are probably not a significant resource for planning a lunar base.

Leaching experiments (Reed et al 1977, Tatusumoto et al 1987), selective volatilization (Silver 1975, Cirlin et al 1978) and grain-size studies (Wasson et al 1976, Thode and Rees 1976, Krahenbuhl et al 1974, Morgan and Wandless 1984) showed that these volatiles were located on the surfaces of the particles in these glass samples. Depth profiling measurements by Auger electron (Grant et al 1974), ion microprobe (Jovanovic and Reed 1974, Meyer et al 1975) and a resonant nuclear proton-^{19}F experiment (Goldberg et al 1976) directly showed that these were surface deposits. Although there is less sulfur in these glass samples than in the local basalt, the surface deposits appear to be mixed salts of metal sulfides and halides (Meyer et al 1975). Butler and Meyer 1976 found S to be present on the primary surfaces of nearly all spheres. They reported surface concentrations of Zn, K, Cl, Cu, Ni and P. SEM studies by Butler and Meyer 1976, Butler 1978 and Clanton et al 1978 showed that these deposits had a characteristic "micromound" texture. The size of the micromounds is about 30 to 50 angstroms and this would appear to be the thickness of the coating. However, mild leaching does not completely remove the coating so that reaction with the glass surface is probable (Goldberg et al 1976).

Metal halide (Wasson et al 1976) and metal carbonyl (Sato 1979) have been discussed as the volatile species in the volcanic vapor that produced these deposits of glass beads. However, the major component of the volcanic vapor has not been identified.

The presence of trace siderophile elements in these samples is not understood. Some authors (Morgan and Wandless 1984) think these elements came from an added meteorite component. However, the close association with volatile metal halides in these very immature soil samples indicates that the siderophile elements in these samples may have a lunar volcanic origin !

References: Butler P. 1978 PLPSC 9, 1459-1471; Butler P. and Meyer C. 1976 PLSC 7, 1561-1581; Chou C-L. et al 1975 PLSC 6, 1701-1727; Cirlin E.H. et al 1978 PLPSC 9, 2049-2063; Clanton et al 1978 PLPSC 9, 1945-1957; Ganapathy R. et al 1973 PLSC 4, 1239-1261; Gibson E.K. and Moore G.W. 1974 PLSC 5, 1823; Goldberg R.H. et al 1976 PLSC 7, 1597-1613; Grant R.W. et al 1974 PLSC 5, 2423-2439; Jovanovic S. and Reed G. 1974 PLSC 5, 1685-1701; Krahenbuhl U. et al 1977 PLSC 8, 3901-3916; Krahenbuhl U. 1980 PLPSC 11, 1551-1564; Meyer C. et al 1975 PLSC 6, 1673-1699; Morgan J.W. et al. 1974 PLSC 5, 1703-1736; Morgan J.W. and Wandless G.A. 1984 (abs.) Lunar Science XV, 562-563; Reed G. et al 1977 PLSC 8, 3917-3930; Rhodes J.M. et al 1974 PLSC 5, 1097-1117; Sato M. 1979 PLPSC 10, 311-325; Silver L.T. 1975 Lunar Science VI, 738-740; Tatsumoto M. et al 1987 PLPSC 17, E361-371; Taylor S.R. et al 1973 PLSC 4, 1445-1459; Thode H.G. and Rees C.E. 1976 PLSC 7, 459-468; Wanke H. et al 1973 PLSC 4, 1461-1481; Wanke H. et al 1974 PLSC 5, 1307-1335; Wasson J.T. 1976 PLSC 7, 1583-1595.

Condensed Volatile Coatings; Meyer C.

Volatile Enrichment Ratio

	Green Glass 15426	A15 Basalt	RATIO	Orange Glass 74220	A17 Basalt	RATIO
ppm						
Zn	80	1	80	300	2	150
Ga	6	3	2	16	4	4
Ni	96	70	~3	75	3	25
Cu	3.5			26	2	10
S		700		450	2000	0.2
F				~100		
Cl				~100	1-15	
ppb						
Ge	196	3	60	250	1.2	200
Cd	181	1	180	320	2	160
Tl	7	0.2	35	20	0.2	100
Sb	1.6	0.1	16	.6	0.1	6
Bi	2.4	0.12	20	1.4	0.05	30
In	9	0.6	15	29		
Br	136	8	20	520	8	70
Se	174	100	2	640	160	4
Te	16	6	3	62	2	30
As				15	4	4
Hg				6	~3	~2
Sn	.12					
Ag	39	1	40	111	1	100
Au	1.2	0.01	100	1	0.01	100
Ir	0.4	.005	80	0.4	.003	100
Re	.05	.001	50	.05	.001	50

Data are from: **Zn** Duncan, Rhodes, WankeP4 P5, MorganP5, Wasson, Chou; **Ga** Wasson, Taylor, WankeP4; **Ni** WankeP4, Morgan; **Cu** Duncan, Taylor, WankeP4; **S** Gibson, Thode; **F,Cl** Jovanovic, Wanke P4; **Ge** Chou, Wasson, Ganapathy, WankeP4, MorganP5; **Cd** MorganP5 P15, Wasson, Ganapathy; **Tl** Ganapathy, MorganP5; **Sb** MorganP5 P15, Ganapathy; **Bi** MorganP5, Ganapathy; **In** MorganP5, Wasson; **Br** MorganP5, Ganapathy; **Se,Te** MorganP5, Ganapathy; **As** WankeP4 and P5; **Hg** Jovanovic, Krahenbuhl; **Sn** Taylor; **Ag,Au,Ir,Re** MorganP5 P15, Chou, Wasson, Ganapathy.

APPLICATION OF REMOTE-SIMS FOR GLASS AND TRACE-ELEMENT COMPOSITIONS OF LUNAR SOILS;

Y. Miura. Faculty of Science, Yamaguchi University, Yoshida, Yamaguchi, 753, Japan.

The lunar soils can be analyzed by the mass spectral pattern of remote secondary ion mass spectroscopy (i.e. remote-SIMS [1,2,3]). This type of examination can be applied to lunar glasses and trace-element compositions of lunar soils. As a preliminary step at calibrating of this technique, various samples were measured and compared; tektite from Moldau; terrestrial volcanic glass (obsidian); artificial "thin-section" glass; and three simulants of 74220 and portions of 60025 and 14305 lunar rocks.

The main characteristics of the remote-SIMS are summarized as follows [1, 2,3,4]:

(1) Complete compositional data from light (H,He,C etc.) to heavy elements;
(2) Distinction of glassy states and fine-grained textures from crystalline and coarse-grained rocks;
(3) In-situ detection on the lunar surface by reducing the working-distance from 50 m (about 40 cm used in this study);
(4) Investigation of implantation degree of the solar-wind and sedimentation process of the impact-related planetary process.

Ion spectral patterns of the remote-SIMS suggest that glasses and small aggregates (e.g., agglutinates) show comparatively higher peak intensity of the remote-SIMS data than hard crystalline rocks. The glass typically gives a more complex pattern than a given rock.

The following results from this study are summarized and shown in Fig. 1:

(1) Lunar volcanic glass of the 74220-type simulant shows different remote-SIMS pattern when compared with the obsidian, tektite (of higher Na^+ peak intensity) and slide glass plate (of lower peak intensity);
(2) Even in lunar simulant samples, the 74220 glass reveals higher peak intensity than the other simulants (60025 and 14305);
(3) Characteristic remote-SIMS spectral pattern of the 74220-type simulant glass can be applied as remote sensing for the lunar glass;
(4) A data base of real lunar glass, rocks and soils is required for application of the remote-SIMS to the lunar surface.

The research is in part supported by the Grant-in-Aid for Scientific research on Priority Areas (Origin of the Solar System) of the Japanese Ministry of Education, Science and Culture (01611005) of the author.

REMOTE-SIMS

Miura, Y.

References:

[1] Miura, Y. (1989): Lunar and Planetary Science, XX, 705-706.

[2] Sasaki, S., Yamori, A., Kawashima, N., Miura, Y., Ohta, M. and Yokoi R. (1989): 1988 Res. Report of "Origin of the Solar System" (by the Monbusho), 451-461.

[3] Miura, Y., Sasaki, S., Kawashima, N., Yamori, A. and Ohta, M. (1989): ISAS Research Note, 410, 1-30.

[4] Sagdeev, R.Z., Managadze, G.G., Shutyaev, I. Yu., Szege, K., and Timofeev, P.P. (1985), Adv. Space Res., 5, 111-120.

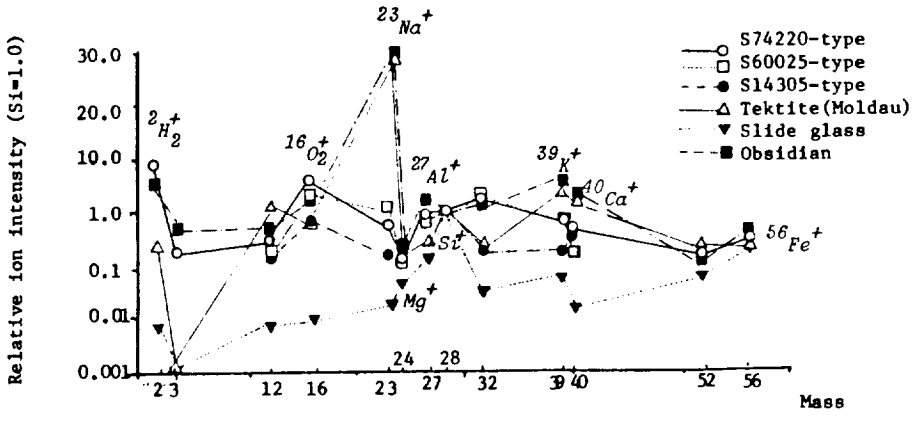

Fig. 1. Remote-SIMS patterns of synthetic lunar simulant 74220, 60025, and 14305, tektite from Moldau, terrestrial volcanic glass of Yatsugatake obsidian and slide glass plate.

A 6-MM SPHERE FROM THE APENNINE FRONT: AN EXCEPTIONAL VOLCANIC GLASS (OR JUST A REMARKABLE IMPACT GLASS?)

Graham Ryder, Lunar and Planetary Institute, 3303 NASA Road One, Houston, TX 77058

15434,28 is a 0.39 g, 6 mm sphere collected in the regolith at Station 7 on the Apennine Front, Apollo 15. It was described by Powell [1] as a spherule with a knobby surface, and included with a group of 26 glass and glass-rich particles (15434,1). The sphere is a yellow/orange glass of intermediate-Ti mare composition (TiO_2 3.2%). The interior is homogeneous and crystal-free, but the exterior is a thin diffuse rind (less than 200 microns) containing debris of mare basalt materials. Major and trace element chemistry suggest that the glass sphere is volcanic, with adhering material.

Petrography: The interior of the broken sphere is shiny black (orange/brown in thin flakes). It is homogenous, with conchoidal fracture. The outer 150 to 200 microns is duller, as if devitrified. The exterior surface is dark gray and slightly bumpy or blistered, and scattered mineral and lithic fragments are embedded in it. One 2 mm fragment is a coarse mare basalt; the mineral fragments are mainly pyroxene and olivine. These embedded fragments have clean surfaces, lacking adhering glass or dust. A chip was taken for two serial thin sections. One (,130) has a yellow/orange glass core with devitrified glass containing some fragmental lithic and mineral debris forming a rind. Towards the interior of the rim tiny crystallites of skeletal olivine are prominent. The embedded fragments coarse enough for identification appear to be solely of mare derivation, and mainly olivines and pyroxenes, though plagioclase, chromite, and ilmenite are present. The largest mineral fragment is about 700 microns across. The second thin section (,131) is almost entirely homogeneous yellow/orange glass, with few fragments (mainly pyroxene) at one edge, and is obviously a more interior portion of the sphere. None of the fragments in either thin section contain any shock features. The thin sections sample only the outer 1/2 mm of the glass sphere, and the rind is grossly over-represented.

Chemistry: Microprobe analyses of the yellow glass were made by Phinney et al. [2] and Vaniman (pers. comm). (The analysis in [2] is reported as ,48 because of a sample misnumbering during thin section making). These analyses are very similar and show that the glass is of mare basalt composition with 21% FeO, 3.5% TiO_2, and 9.3% Al_2O_3. I acquired 144 mg as two chips for chemical analysis. One fragment of 66 mg lacking conspicuous fragments was ground into a homogeneous powder for microprobe fused bead and INAA analyses; the other is preserved for future studies. The analysis is reported in the table and the figure, with other compositions for comparison.

The major element analysis is similar to those previously reported for the yellow/orange glass, and within the realm of other intermediate-TiO_2 compositions glasses from the Apollo 15 site, including the yellow volcanic glass and the yellow impact glasses [3-5, and others]. It differs from the volcanic glass mainly in being lower in MgO and Cr_2O_3, and higher in alkalis. It differs from most of the impact glasses in having lower TiO_2 and SiO_2, and higher FeO.

The trace elements show that 15434,28 is an exceptional glass. For a mare basalt composition it has high rare earth elements, although not as high as Apollo 11 high-K basalts. Most of the incompatible elements are 3 to 4 x those in the Apollo 15 olivine basalts and 2 x those in the A15 yellow volcanic glass. 15434,28 is a little more enriched in the lighter rare earths than the heavier ones compared to those two groups, but the pattern is certainly not KREEP-like (Fig. 1). The incompatible elements are less than half as abundant as those in the 15010 yellow impact glass, which has a much more KREEP-like slope of rare earths. U and Th are less than 1/5 as abundant as in the yellow impact glass. Sr, Sc, Co, Ni, and Ni/Co are similar to those in the volcanic glass. Ir and Au abundances do not exceed the INAA detectability limits of about 4 ppb.

Origin of the glass: The glass is exceptional in both structure and chemistry. Most impact glasses are more heterogeneous, with at least flow-banding if not schlieren. In impact glasses, fragments are not confined to the outermost few hundred microns, but occur throughout; they generally include shocked varieties. Many impact glasses are vesicular or hollow, but 15434,28 is neither. The chemistry gives no indication of meteoritic contamination, whereas most impact glasses are formed from contaminated regolith (yellow impact glass 15010 for instance contains 26 ppb Au). The unusual bulk composition cannot be manufactured by mixing materials known among lunar samples. Any hypothetical mixture contains a high proportion of a mare basalt with an unusual composition; the elevated rare earths are not a result of KREEP contamination, but are inherent in the mare material (as was concluded for the 15010 impact glass [4]).

15434,28 differs from lunar volcanic glass beads in its large size and its adhering material. Accepted lunar volcanic beads are smaller, no larger than 1 mm and most are less than 300 microns. Although lunar volcanic beads include composites, none have so far been described that have rinds similar to 15434,28, which is more like some terrestrial volcanic beads in size and structure. However, if 15434,28 were broken up and its fragments analyzed, it would form a cluster that would certainly be identified as a volcanic glass group. It would be mildly unusual; its Mg/Al would be the lowest of any volcanic group, although not much lower than A15 yellow volcanic glass. On most element-element plots it would plot at the edge of or within volcanic glass compositions. It lacks vesicles, schlieren, banding, and meteoritic contamination.

Conclusions: I find no evidence that 15434,28 was produced in an impact, and its features are entirely compatible with those of a fire fountain product. Therefore I conclude that 15434,28 is an exceptional (size, rind, composition) volcanic glass. It remains possible that it is a remarkable impact glass. Isotopic and more detailed siderophile data for the glass are desirable, and the ramifications of intermediate Ti glasses in the evolution of the Imbrium area remain to be explored. If the sphere is volcanic, why is it so large? and whatever its origin, why does it have adhering crystals? The adhering mare materials are of petrologic and geologic interest.

Split	15434 ,28,202	A15 Yell volc	15010 impact
wt %			
SiO_2	43.6	42.9	(47)
TiO_2	3.19	3.48	4.2
Al_2O_3	9.1	8.3	9.5
Cr_2O_3	0.45	0.59	0.31
FeO	21.3	22.1	18.9
MnO	0.28	0.27	0.24
MgO	10.7	12.1	9.3
CaO	9.0	9.0	9.5
Na_2O	0.59	0.45	0.32
K_2O	0.13	0.08	0.22
P_2O_5	0.37		0.22
ppm			
Sc	38	42	39
Co	57	69	41
Ni	78	85	
Sr	174	165	
Zr	323		460
Hf	8.1	5.3	12.6
Ba	167		410
Th	1.39		8.3
U	(.3)	0.3	3.0
La	21.6	8.55	48.2
Ce	62	24.6	106
Sm	13.0	6.4	20.3
Eu	2.1	1.47	1.61
Tb	2.5	1.4	4.1
Yb	6.4	4.3	15.6
Lu	0.90	0.48	2.4

Table: Composition of 15434,28 (this study; INAA, MFB) and other Apollo 15 yellow glasses [3-5].

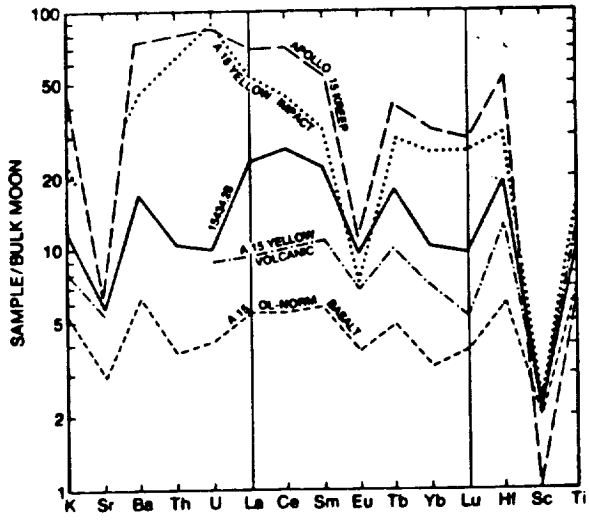

Figure. Trace elements in 15434,28 and comparitive materials, normalized to bulk Moon composition.

[1] Powell B. (1972) NASA MSC 03228, 91pp. [2] Phinney W. et al. (1972) Apollo 15 Lunar Samples, LPI, p.149 [3] Delano J. (1985) PLPSC 16th, p. D201. [4] Delano J. et al. (1982) PLPSC 13th, p. A159. [5] Hughes S. et al. (1988) Geochim. Cosmochim. Acta 52, 2379.

APOLLO 17 ORANGE SOIL: INTERPRETATION OF GEOLOGIC SETTING; H.H. Schmitt, Consultant, Albuquerque, NM, 87191

The discovery of the orange soil in the rim of Shorty Crater during the Apollo 17 Mission to the Valley of Taurus-Littrow (1), and subsequent recognition of orange materials as a major component of mantling deposits at the southwestern edge of Mare Serenitatis (2), added excitement, puzzles, and critical new information to our studies of the moon. The excitement came from the discovery of what, at the time, appeared to be volcanic material the science team had speculated might be found at Shorty. The puzzles came when, after the soil had be examined carefully on Earth, we had to conclude that somehow 3.6 aeons old (3) orange glass beads of pyroclastic origin, underlain by their black devitrified equivalent, had been emplaced in the rim and ejecta blanket of an 80 m. diameter impact crater with only minor contamination by other material (4). The critical new information came when it became clear that the source region for the orange soil magma must be the deep interior of the moon, below the region included in the original melted shell (5).

An explanation of the geologic setting of the orange and black soils comes from the writer's personal observations of the effects of the explosion of 500 tons of ammonium nitrate (1971 DIAL PACK event) near Medicine Hat, Alberta. This explosion caused the pressurization of underlying water saturated sand strata and the eruption of the water-sand mixture along conduits in radial and circumferential fractures cutting the rim and ejecta blanket of the explosion crater. By analogy and further logic, the following sequence of events may have taken place in the vicinity of Shorty Crater:

1. Eruption of the mare basalt flows that partially filled the Valley (3.7 aeons (3)).
2. Pyroclastic eruption (4) of orange glass beads and black devitrified glass beads (3.6 aeons (3)).
3. Immediate covering of the pyroclastic deposits by a basalt flow of sufficient thickness to protect the orange and black glass from significant contamination by regolith materials.
4. Avalanche from the north side of the South Massif (1) to form the Light Mantle.
5. Meteor impact that created Shorty Crater (5) which penetrated below the Light Mantle and into the basalt flow overlying the pyroclastic deposits (19 My (7)).
6. Instantaneous release and pressurization of adsorbed gases and the fluidization of pyroclastic deposits immediately beneath Shorty Crater.
7. Eruption of gas/bead mixtures along conduits in the radial and circumferential fractures around Shorty Crater.

8. Continuous sorting of the less dense orange glass beads toward the top of the gas column to give the sharp separation of orange and black beads observed in and on the core tube (1).

9. Development of thin regolith on the exposed top of each orange and black bead deposit.

The primitive nature of the gases adsorbed on the surfaces of the orange and black beads (8) indicate a source region in the deep interior of the moon, below the zones affected by the degasing of the magma ocean (9). This in turn suggests that these deep source materials remained relatively cool during the processes that formed the moon and had not been subject to significant earlier differentiation. The existence of a necessary density reversal below 200-300 km., the probable depth of differentiated crust and mantle, to maintain the average density of the moon supports this conclusion. Both these constraints on lunar composition and structure severely limit possible mechanisms for the formation of the moon and suggest formation as a contemporaneous partner to Earth rather than derivation from the early, already differentiated Earth as suggested by others (10).

References:
(1) Schmitt, H.H. (1973) Apollo 17 report on the Valley of Taurus-Littrow. Science, 182, 680-690.
(2) Lucchitta, B.K., and Schmitt, H.H. (1974) Orange material in the Sulpicius Gallus Formation at the southwestern edge of Mare Serenitatis. LSCP 5, 1, 223-234.
(3) Wilhelms, D.E. (1987) The geologic history of the moon. USGS Prof. Paper 1348, 237.
(4) Heiken, G.H., and others (1974) Lunar deposition of possible pyroclastic origin. Geochim. Cosmochim. Acta 38, 11, 1703-1718.
(5) Schmitt, H.H. (1975) Evolution of the moon: The 1974 model. Space Sci. Rev., 18, 259-279.
(6) Wolfe, E.W., and others (1981) The geologic investigation of the Taurus-Littrow valley: Apollo 17 landing site. USGS Prof. Paper 1080, 280p.
(7) Eugster, O. (1977) The cosmic ray exposure history of Shorty Crater samples: The age of Shorty Crater. LSCP 8, 3, 3059-3082.
(8) Taylor, S.R. (1982) Planetary science: The lunar perspective. LPI, Houston, 298-299.
(9)Warren, P. (1985) The magma ocean concept and lunar evolution. Ann. Rev. Earth Planet. Sci., 13, 201-240.
(10) Hartmann, W.H., and others (1986) Origin of the Moon. LPI, Houston, TX.

SECONDARY ION MASS SPECTROMETRIC ANALYSIS OF GLASSES, TRACE ELEMENT CHARACTERISTICS OF LUNAR PICRITIC GLASSES AND IMPLICATIONS FOR THE MANTLE SOURCES OF LUNAR PICRITIC MAGMAS; C.K. Shearer, J.J. Papike, K.C. Galbreath, H. Yurimoto (SDSM&T, Rapid City, SD 57701) and N. Shimizu (MIT, Cambridge, MA 02139).

Introduction. Trace element analysis of microvolumes of geologic materials using secondary ion mass spectrometry (SIMS) has a wide range of applications to terrestrial and lunar petrogenetic problems. SIMS involves bombardment of the microvolume by energetic ions (O^-), ejection of material by a process known as sputtering and analysis of ionized sputtered material by mass spectrometry. Complexities in the secondary ion mass spectra of geologic materials greatly slowed the quantitative application of SIMS. These complexities involved the generation of molecular ions during sputtering resulting in isobaric interferences, unknown effects caused by matrix variations, lack of quantification of secondary-ion intensities and lack of numerous, well-documented standards. However, within the last ten years most of these problems have been resolved. Molecular ionic interference may be largely removed by kinetic energy filtering (1,2) and isobaric corrections (2,3). Matrix effects are commonly resolved by comparing unknowns with standards of the same major element chemistry (4) or empirical relationships between ion yield and matrix (5). Empirical relationships between concentration and relative intensity in a variety of silicate matrices have been documented (3,4,6).

Experimental technique. Our current work on lunar glass beads (volcanic, impact) involves establishing working curves for appropriate silicate glass compositions and trace element analysis of lunar glasses. Trace element analyses (REE, Ba, Sc, Sr, Co, V, Zr, Cr*, Zn*, Cu*, and Rb*) are being conducted with Cameca IMS 3f ion probes located at MIT and the University of Tsukuba (*). A primary beam of O^- ions is focused to a spot of 15-25 μm in diameter for REE and 8-15 μm in diameter for the other set of trace elements. Molecular ion interferences are virtually eliminated from the mass spectra by reducing the secondary ion accelerating voltage (1,2,6). Secondary positive ions are analyzed with combined electrostatic and magnetic analyzer sectors. Secondary ions are detected by an electron multiplier in pulse counting mode. Interference of BaO ions on Eu(^{151}Eu-$^{135}Ba^{16}O$ and ^{153}Eu - $^{137}Ba^{16}O$) is corrected by empirical relations among $^{151}Eu/^{153}Eu$, $^{135}Ba/^{137}Ba$ and BaO/Ba ratio observed in silicate glasses ($\sim$0.1). Similar empirical relations were used to correct other interferences (i.e. $^{151}Eu^{16}O$ on ^{167}Er).

For our studies, three sets of well-documented glass standards were used to investigate matrix effects on ion yield in calculating working curves; synthetic glasses produced from GSJ standards, A-15 Green Glass and A-17 Orange Glass. Secondary intensities (I) of REE were normalized to ^{30}Si to produce I(REE)/I(^{30}Si) vs. REE (concentration) working curves. Working curves for other trace elements were normalized to a constant Si content. Concentrations were then recalculated based on SiO_2 content of the individual glass beads. Using these working curves, A-17 Orange, A-15 Green and A-15 Yellow glasses were analyzed as secondary standards. These standards were analyzed at the beginning and during each analytical session. To monitor both reproducibility and drift over a single analytical session (8-24 hours), a single glass bead is used as an "internal standard". Every 3 to 5 analyses, the operator returns to the "internal standard".

Based on the major element classification scheme of Delano (7), the glass beads thus far analyzed in this study are: A-14 Green B, Green A, VLT, Yellow, Orange, Red/Black; A-17 Orange I (preliminary), Orange II (preliminary), Orange 74220-type; A-15 Green A, B, C (preliminary), D, E, Red (preliminary) and All Orange (preliminary). In addition, A-16 Ultra Mg glasses (8) and the A-14 LAP glass (9) have been analyzed. REE patterns and selected trace element characteristics of the various glass types show wide to subtle variation among glasses of similar composition from different sites (i.e. A-14 VLT vs A-17 VLT), wide variation among glass types (i.e. high-Ti vs. low-Ti glasses) and wide (A-14 Red/Black) to subtle (A-15 Green) variations within a glass type.

Variations among glasses of similar composition from different sites. REE patterns for the low-Ti glasses from A-14 (Green A, Green B, VLT) are commonly light-REE enriched with (Ce = 14-70 x chondrite) Sm/Eu = 6-14, Ba/Sr > 1.4 and Zr content between 66-508 ppm. In contrast, the

SIMS ANALYSIS OF GLASSES: Shearer et al.

low-Ti glasses at the A-17 site (VLT) have flat REE patterns, lower REE abundances (Ce = 6-9 x chondrite), slight (-) to No Eu anomaly, Ba/Sr < 0.5 and Zr=20-50 ppm. Relative to the A-17 low-Ti glass, the A-14 glasses have a trace element signature which suggests a KREEP component. Regardless of possible models, the glass compositions indicate that mantle characteristics at the two sites are intrinsically different.

Trace element differences among glasses of contrasting major element chemistry. Comparisons of glasses from individual sites (A-14, A-17) indicate that the low-Ti glasses (Green, VLT) are depleted in incompatible elements (REE, Ba, Sr, Zr, Zn, Cu) and enriched in compatible elements [Co, Ni (7)] relative to the high-Ti glasses (Red/Black, Orange). These data are generally consistent with various lunar mantle cumulate and hybridization models (i.e. 7,10,11,12) which predict that high-Ti basalts represent a more evolved source. However, the evolved cumulate mantle source appears to be compositionally variable (A-17 Orange 74220 and Type I; A-17 Orange Type II; A-14 Red/Black; A-14 Orange).

Compositional variations within individual glass groups. Trace element variations within individual glass groups (i.e. Red/Black, A-15 Green) confirm their compositional heterogeneity observed by major element studies (i.e. 7). The Red/Black glasses display a large range of Ba, Rb, Na_2O, K_2O whereas REE and Zr show limited enrichment. These variations may be attributed to selective assimilation or volatile exchange during eruption. More subtle are the compositional variations observed in A-15 Green Glass. Cluster analyses of the trace element data delineates five groups (A-E), equivalent to those previously defined (7). Two trends are defined on trace element variation diagrams (Zr, Ba, REE vs. Co); a high-Co trend composed of groups A and D and a low-Co trend composed of groups B, C, and E. REE abundances of groups A, B, D and E overlap (Ce 3.3 to 8.5 x chondrite), whereas abundances in the more MgO-rich group C are slightly lower (Ce = 2.7 - 3.1 x chondrite). Trace element variation trends (e.g. positive correlations of Zr, Ba, Sr and REE with Co) are difficult to reconcile in terms of fractionation or partial melting processes involving a single, chemically distinct mantle source. Magma mixing and very subtle compositional differences in mantle source are being evaluated to explain the complex chemical trends.

Trace element characteristics of Ultra Mg glasses. Wentworth and McKay (8) identified a suite of minute Ultra Mg glasses in A-16 regolith breccias. The wide major element compositional range and Ultra-Mg character (atomic Mg/Mg+Fe $\geq$ .90) of the glasses suggest a variety of possible origins from complex impact processes to complex volcanic processes involving rather exotic and primitive magmatism. Trace element data show a wide range of concentrations (La_N = 25-290, Yb_N = 16-120, Ba = 80-1000, Zr = 182-800 and Sr = 70-230) but with distinct trace element characteristics Ba/Sr > 1, $(La/Yb)_N$ = 1.5-2.5, $(Eu/Sm)_N$ = 0.1-0.3, and low siderophile element concentrations (Co = 2-10 ppm). Low Co and high incompatible element concentrations eliminate the possibility that these glasses are a product of lunar komatiitic volcanism. The low siderophile concentrations suggest a complex, impact melt process.

Continuing studies. These initial SIMS generated trace element data indicate that picritic glasses represent partial melts derived from numerous compositional distinct sources. In addition, the data are useful in distinguishing volcanic process from impact related phenomena. Continuing SIMS studies on lunar glass beads will emphasize further work on A-17 (additional VLT, Orange I and II, Green), A-14 (further studies of chemical variations within glass groups) and A-15 (Yellow and Red), and new studies involving A-11, A-12 and A-16, new volcanic types, calibration of a new trace element package and SIMS analyses of surface coatings.

References: 1) **Shimizu, N.** (1978) EPSL 39, 395-406. 2) **Humeke et al.** (1983) GCA 47, 1635-1640. 3) **Jolliff et al.** (1989) GCA 53, 429-441. 4) **Ray** and **Hart** (1982) Int. J. Mass. Spec. Ion Phys. 44, 231-255. 5) **Shimizu** (1986) Int. J. Mass. Spec. Ion Phys. 44, 231-255. 6) **Shimizu et al.** (1978) GCA 42, 1321-1334. 7) **Delano** (1986) PLSC 16, D201-D213. 8) **Wentworth** and **McKay** (1988) PLSC 18, 67-77. 9) **Papike et al.** (1988) LPS XX, 818-819. 10) **Hughes et al.** (1988) GCA 52, 2379-2392. 11) **Ringwood** and **Kesson** (1976) PLSC 7, 1697-1722. 12) **Taylor** and **Jakes** (1974) PLSC 5, 1287-1305.

YOUNG DARK MANTLE DEPOSITS ON THE MOON; Paul D. Spudis, U.S. Geological Survey, Flagstaff, AZ 86001

Dark mantling deposits were recognized and postulated to be of volcanic origin during the geologic mapping of the Moon (e.g, [1]). Based on a general belief that "dark" = "young" (see [1,2]), they were considered to be the youngest products of lunar volcanism. The Apollo 17 mission was sent to the Taurus-Littrow Valley to sample the extensive dark mantle deposits in this region that were inferred to be young [3-5]. Samples returned from that mission showed that the Taurus-Littrow dark mantle was the product of pyroclastic volcanism that occurred over 3.7 billion years ago [6]. Since then, it has been widely assumed that lunar pyroclastic volcanism was confined to the "main phase" of mare volcanism, i.e., from around 3.8 to 3 billion years ago. Subsequent reinterpretations of other lunar dark mantle deposits [7], the stratigraphy of Mare Serenitatis [8], and crater densities in the Apollo 17 region [9] all concluded that lunar pyroclastic deposits are old (> 3 Ga) and that "young" dark mantling deposits probably do not exist.

Estimating the age of dark mantle deposits on the Moon is difficult. Because these units are fine-grained, unconsolidated debris in which craters are eroded very rapidly, crater densities are of little value [9]. The only way to estimate the age of unvisited dark mantle deposits is to bracket them stratigraphically with units that can be dated by crater densities. I here discuss two dark mantle deposits on the eastern limb of the Moon that occur in different geological settings and attempt to determine their ages. Although of small extent, their presence suggests that explosive volcanism on the Moon continued to as recently as about 1 billion years ago.

Dark mantle deposits of Mare Smythii. Mare Smythii is a circular mare on the equatorial eastern limb of the Moon [10, 11]. Several dark deposits are evident on high-sun illumination photographs of the region. In particular, dark mantle deposits occur around the margins of the inner basin ring (370 km dia.) near the craters Haldane, Kiess, and McAdie. These deposits are closely associated with the mare fill of the Smythii basin. Within the basin, the dark mantle material underlies the mare in some places (e.g., western rim of McAdie at 3 N, 93 E) while it overlies mare basalt elsewhere (e.g., near a volcanic vent north of Haldane at 0, 83 E). It thus appears that eruption of mare basalt in the Smythii basin was accompanied by eruptions of dark mantling material; such a relation is similar to that found at the Apollo 17 site, where dark mantle pyroclastics are of similar age (and composition) to the local mare basalts.

Dark mantle deposits within Taruntius crater. The crater Taruntius (5.6 N, 46.5 E; 55 km dia.) is a floor fractured impact crater [12] of Copernican age. A low albedo deposit is associated with irregularly shaped craters and fractures on the floor of Taruntius; these deposits are similar to localized dark mantle deposits [13] that occur within crater floors elsewhere on the Moon. They probably represent deposits from vulcanian eruptions [13] associated with the injection of magma beneath the crater floor, floor uplift, and fracturing [12]. The Taruntius dark mantle deposits are also associated with minor mare basalt flooding of portions of the crater floor. All of these volcanic events post-date the formation of the crater Taruntius, which appears to be about the same age as Copernicus.

Ages of the Smythii and Taruntius dark mantle deposits. I have attempted to determine the ages of these two deposits by measuring the crater densities on units that have a clear stratigraphic relation to the dark mantle (Figure 1; after [14]). The Smythii mare basalts (point "Mare Smythii" in Fig. 1) are among the youngest on the Moon; an estimate based on known ages of the Apollo mare sites and inferred ages of Copernicus and Tycho (850 Ma and 100 Ma respectively; [15]) suggest an age of about 1.2 $\pm$ 0.3 Ga for the basalts of

YOUNG DARK MANTLE DEPOSITS; Paul D. Spudis

Mare Smythii. Because the dark mantle deposits of the Smythii basin are contemporaneous with the basalts, a similar age for the dark mantle is inferred, i.e., from about 1.5 Ga to less than 1 Ga. Similarly, the crater density and inferred absolute age of Taruntius suggests that it is about the same age as the crater Copernicus (about 1 Ga; [15]). The dark mantle on the floor of Taruntius post-dates the crater; thus, these volcanic deposits must be younger than 1 Ga. The dark mantle deposit within Taruntius is the youngest recognized volcanic unit on the Moon, possibly younger than the mare flow that embays Lichtenberg crater [14].

While these dark mantle deposits are not extensive, their existence indicates that very late volcanism on the Moon exhibited the same styles of eruption and emplacement operative during earlier epochs of mare volcanism. Both of the two major types of occurrence determined for explosive volcanic deposits on the Moon [13] are displayed by these two pyroclastic deposits.

References. [1] Wilhelms D.E. and McCauley J.F. (1971) USGS Map I-703. [2] Mutch T.A. (1970) Geology of the Moon. Princeton Univ. Press, 324 pp. [3] Carr M.H. (1966) USGS Map I-489. [4] Scott D.H. et al (1972) USGS Map I-800. [5] Greeley R. and Gault D.E. (1973) EPSL 18, 102. [6] Taylor S.R. (1982) Planetary Science, LPI Press, 481 pp. [7] Head J.W. (1974) PLSC 5th, 207. [8] Howard K.A. et al. (1973) Apollo 17 PSR, NASA SP-330, p. 29-1. [9] Lucchitta B.K. and Sanchez A. (1975) PLSC 6th, 2427. [10] Wilhelms D.E and El-Baz F. (1977) USGS Map I-948. [11] Spudis P.D. and Hood L.L. (in press) Lunar Bases II. [12] Schultz P.H. (1976) Moon 15, 241. [13] Hawke B.R. et al. (1989) PLPSC 19, 255. [14] Schultz P.H. and Spudis P.D. (1983) Nature 302, 233. [15] BVSP (1981) Basaltic Volcanism, Pergamon Press, Ch. 8.

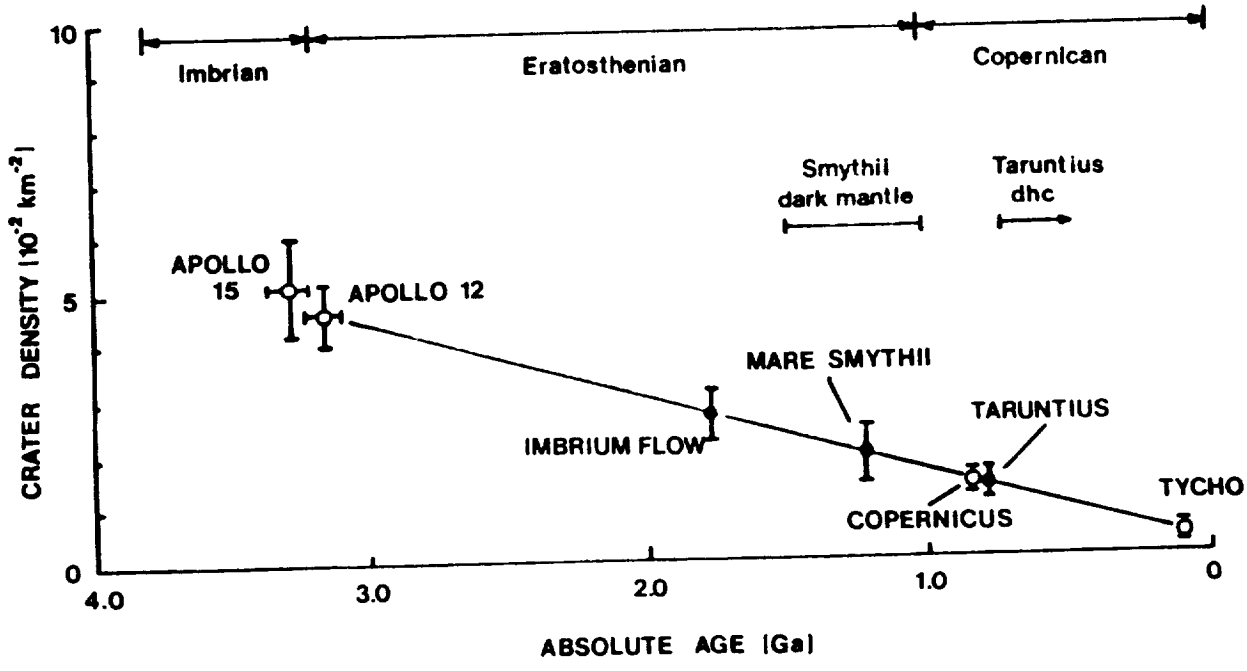

Figure 1. Crater densities and absolute ages for sampled units (open circles) and inferred ages for unsampled units (solid circles) on the Moon. Dark mantle deposit ages (above curve) are inferred from stratigraphic evidence. Lunar stratigraphic divisions shown at top. After [14].

APOLLO 15 GREEN GLASS I: NEW COMPOSITIONAL AND PETROGRAPHIC INSIGHT.

Alison M. Steele, Randy L. Korotev, and Larry A. Haskin, Dept. of Earth and Planetary Sciences, Washington University, St. Louis, MO 63130.

Introduction: Because the petrogenesis of the Apollo 15 green glasses is still enigmatic, we are currently examining a suite of them using a variety of techniques, which include determining both major and trace element abundances for individual spherules, assessing both green glass vitrophyres and vitric samples together, and utilizing petrographic observations. We hope that by characterizing individual particles at this level of detail we will provide additional constraints on their formation.

Materials and Procedure: Green glass particles were handpicked from splits 15426,9012 and 15426,154. The matrix (unconsolidated material <1 μg) of 15426,9012 is light green in color and is composed mainly of pulverized green glass. It is also relatively rich in larger (>50 μg) green glass particles. In contrast, 15426,154 is fine grained and brown/grey with sparse large green glasses and contains a variety of lithologies. Glasses were chosen from these two diverse splits of 15426 so that we could evaluate whether green glass compositional spread was related to host material or split.

Three hundred sixty-five glass particles were analyzed by INAA. Following radioassasy, petrographic examinations were made of each, with the following features noted: crystallinity (vitric/vitrophyric); droplet shape where determinable (sphere/spheroid/elongate); presence or absence of surface coating; contamination (i.e. adhering regolith); and, in the case of broken spherules, the approximate percentage of the original droplet remaining, where determinable. Although continua exist among some of these criteria, each particle was described as objectively as possible so that physical features could be compared with compositions.

Finally, 41 of the 365 particles were analyzed by electron microprobe. These 41 spanned the entire compositional range indicated by INAA, and all were vitric. In addition to several well-characterized probe standards, one of our own green glasses was used as an "internal standard" for all probing sessions.

Results and Discussion: Relative elemental abundances determined by INAA are precise for the elements plotted in Figures 1-3 and limited only by "counting statistics." However, the accuracy of the absolute abundances is limited by the accuracy with which the sample masses can be determined, and this is the largest source of uncertainty for these small samples (range: 36-3800 μg, mean: 120 μg). Errors in mass determination lead to correlated errors in element concentrations along diagonal lines intersecting the origin on 2-element plots such as Figs. 1-3. To compensate for weighing errors (and other correlated errors, if present), INAA data for the 41 glasses we have probed to date have been normalized to microprobe results using FeO concentration, which is determined by both techniques. Figures 1a and 1b compare data for Sc and FeO before and after normalization and show that the two positive trends in the unnormalized INAA data are artifacts induced by weighing errors, and that the samples in the trends actually form tight compositional clusters (Figure 1b). Furthermore, the suite having the greatest range in FeO (squares; Figure 1a), rather than being of variable Sc concentration, actually exhibits nearly constant Sc concentration (Figure 1b).

Major element data for 41 glasses indicate that the Sc-FeO divide we observe (Figure 1a, 1b) corresponds to the major compositional hiatus described by Delano [1]. In general, we agree with the group divisions suggested by Delano [1] and will thus retain the established names of A though E for the green glass groups, although we will not presently separate E from D or C from B, and we will elaborate on A.

Figure 2 illustrates that there is a split in Group A and that glasses on either side of this split show significant petrographic and morphological differences. These suggest that Group A actually consists of two subgroups that formed under different eruptive conditions. On plots involving compatible elements (e.g., Figure 1b) these subgroups, which we will call High-Sm Group A and Low-Sm Group A, are not entirely resolved although the amount of overlap is minor. The compositions of individual spherules within each of these clusters appear to be nearly identical within analytical uncertainty for FeO and Sc (Figure 1b), but trends are still present for Na and probably for REE (Figure 2).

Figure 3 illustrates how Group B-C differs from the other green glass groups. On all plots we have examined to date, Group B-C forms apparent trends rather than clusters as the other groups do. In addition, although it is often ambiguous on major-element plots whether or not Groups A, B, and C form a compositional continuum (e.g., [1, Figure 2-8]), trace element data indicate that they do not. There is a definite compositional break between A and B-C on Figure 3, and this is evident on other plots as well (e.g. Sm vs. Na_2O for Group B-C, not shown). Furthermore, Figure 3 suggests that Group B-C *itself* might consist of three clusters aligned to resemble a single trend. We offer the suggestion that all Apollo 15 green glasses may belong only to discrete, tight compositional groups, of approximately the extent of compositional variability exhibited by the High- and Low-Sm Group A clusters, but that some are sufficiently similar in composition to overlap or in some cases produce apparent compositional trends. This hypothesis is essentially an extension of previous suggestions that, like many other kinds of lunar glass such as the Apollo 17 orange glass [2], Apollo 15 green glass occurs as compositional clusters [1; 3]. Individual clusters could represent material from discrete eruptive events or phases, each from a slightly different source or vent, but how those sources might be related still has to be explained. We cannot be certain, however, whether the B-C group consists of obvious discrete clusters or a single, continuous trend because we have not yet analyzed enough samples from this group.

Conclusions. Combined major and trace element data reinforce previous indications [1] that the Apollo 15 green glasses belong to several distinct compositional groups. Furthermore, incompatible trace element data indicate that one additional division (High-Sm vs. Low-Sm Group A) not evident on plots involving compatible elements is present, and that other analogous divisions may also exist within Group B-C. Not only are the long-ignored green glass vitrophyres members of these previously defined groups, their distribution, along with other petrographic criteria, help to distinguish such clusters having only slight compositional differences.

REFERENCES: [1] Delano, J.W. 1979. PLPSC 10: 275-300. [2] Hughes, S.S., Delano, J.W. and Schmitt, R.A. 1988. PLPSC XIX: 517-518. [3] Delano, J.W. 1986. PLPSC XVI: D201-D213.

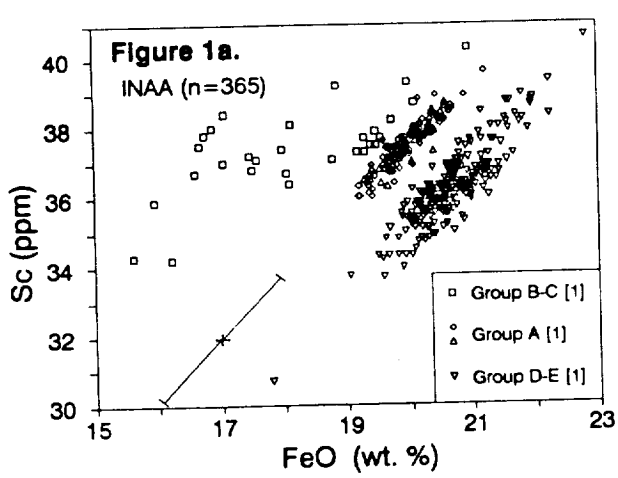

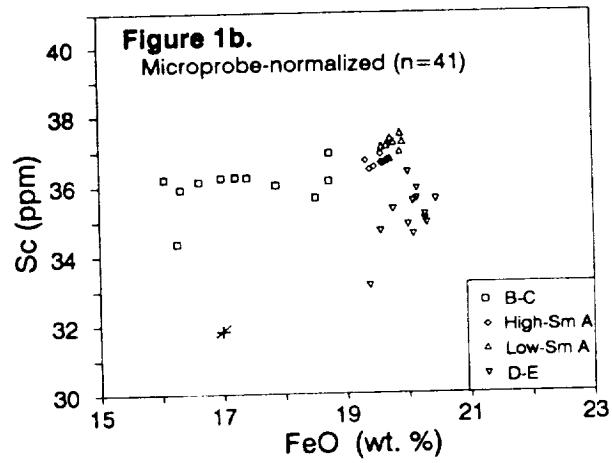

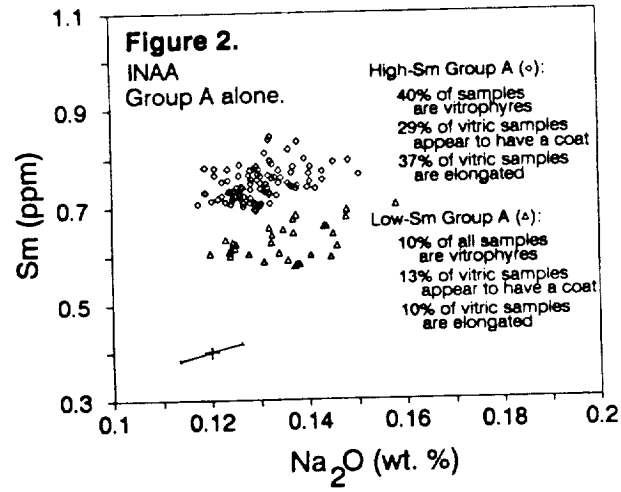

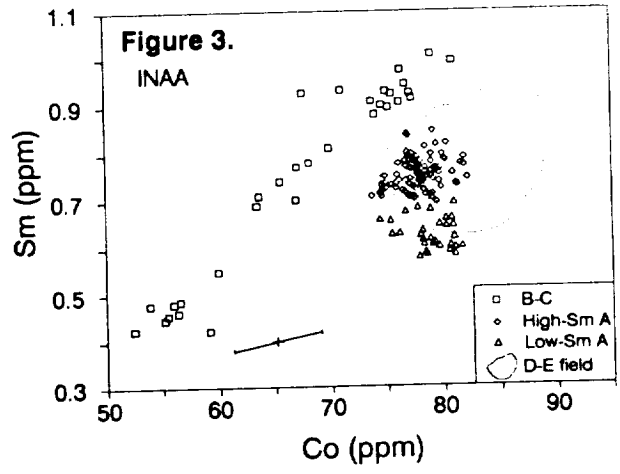

Notes on Figures 1-3. Small crosses represent one sigma uncertainties in the relative abundances of the elements in question. The larger diagonal bars emanating from the small crosses on the INAA plots (Figure 1a, 2, 3) represent our estimate of the correlated random uncertainties in absolute concentration if we add (1) an estimate of a correlated random uncertainty from INAA, and, (2) a weighing error of ±4%, which is what we have observed for replicate weighings. When one corrects for correlated errors by normalizing to microprobe FeO values, the only serious remaining correlated error is that for FeO by microprobe, which is what is represented by the much smaller diagonal bar on Figure 1b.

APOLLO 15 GREEN GLASS II: GROUP PROPORTIONS AND THE CLUSTER HYPOTHESIS.
Alison M. Steele, Randy L. Korotev, and Larry A. Haskin, Dept. of Earth and Planetary Sciences, Washington University, St. Louis, MO 63130.

Despite the exceedingly small sizes of the Apollo 15 green glasses and the corresponding difficulty in obtaining precise analyses of individual spherules, several studies have successfully illustrated and confirmed their compositional variability [1, 2, 3, 4]. However, most workers have approached the green glass problem by using a database limited to either major elements [1, 3] or minor and trace elements [2]; only one study [4] has combined both types of compositional data with petrographic information. The development of petrogenetic explanations for green glass has previously been influenced by data that do not illustrate complete green glass compositional characteristics.

Ma *et al.* [2] used INAA procedures similar to ours to analyze green glasses from an unspecified split of 15426. Figure 1 superimposes Sc-FeO data for the spherules they analyzed on the compositional range we found [4]; the difference in distribution is striking. Some compositions (e.g. Group B-C; E) are relatively rare. Ma *et al.* [2] attempted to sample the entire compositional range of green glasses by choosing 55 particles that covered the full range of Mn and Na_2O concentrations, which they determined first for a larger number of particles. While not exactly random, this procedure should not cause gross discrimination between Groups A and D-E, since both groups have comparable ranges in Mn and Na_2O. However, most of their samples belong to Group A (Figure 1), suggesting that the split of 15426 they were allocated did not have the same ratio of Groups A to D-E as either of ours; based on our results, we would have expected a preponderance of Group D-E (Table 1). As only four of their glasses plot in the D-E field, these authors were not able to distinguish D-E as a separate group, and their interpretations reflect this. In addition, we presume that since their INAA data span a slightly larger range in Sc and FeO than ours and lie along the same correlated error line (Figure 1) the trends in their data probably result largely from correlated errors, as ours do [4]. Thus, we find it difficult to support their suggested petrogenetic explanation of fractional crystallization lines lying orthogonal to a general mixing trend (e.g. [2, Figure 3b, 4b]).

Similarly, workers who examined only major element data [1, 3] could not observe that Group A should be subdivided into the two discrete clusters that are fully evident on plots of incompatible trace elements [4, Figure 2]. That this division is fully evident only in incompatible trace elements illustrates how compositionally similar some green glass groups can be. It seems reasonable, then, that other clusters with compositions that differ only slightly from one another might exist and are as yet unidentified, such as within Group B-C [4]. Furthermore, some clusters could overlap in composition with respect to *all* elements, so they would be visually inseparable on any given 2-element plot. This might be the case for Group D-E, because it forms a noticeably larger, looser cluster than Group A [4, Figure 2], and thus might be composed of several overlapping or superimposed clusters (we will subject Group D-E to statistical analyses to test this possibility).

Differences among subsplits of 15426 in the proportions of the different compositional groups, such as those between our study and that of Ma *et al.* [2], have been reported previously (e.g. [3]). A compilation of studies done since the groups were first designated as A-E [1] is presented in Table 1. Group proportions we find [4] contrast with Delano's [1] initial findings, and those of both Ryder [3] and Ma *et al.* [2] differ even more in having a predominance of Group A. Curiously, even though we deliberately chose our samples from two dissimilar splits of 15426, one very green-glass rich (,9012) and the other poor (,154), our splits show essentially the same percentages of the various groups. We take the results presented in Table 1 at face value. These differences suggest that green glass of all compositions was not deposited simultaneously. At the very least, emplacement of the two groups on either side of the Sc-FeO hiatus (Figure 1) appears to require a number of discrete events. The differences shown in Table 1 also support the extended clustering hypothesis [4] in which each identified cluster would represent a single pyroclastic event. It would follow that, since different portions of a clod contain different proportions of the various compositional clusters, the green glass clods may retain some of the stratigraphy of a volcanic field where multiple pyroclastic events occurred. At one extreme, there may have been a single vent emitting different material at different times, at the other extreme, a series of different vents each emitting materials of a single group. We plan to investigate mechanisms to see how the compositions of the various clusters might relate to one or a few sources.

REFERENCES: [1] Delano, J.W. 1979. PLPSC 10: 275-300. [2] Ma, M.-S., Liu, Y.-G. and Schmitt, R.A. 1981. PLPSC 12B: 915-933. [3] Ryder, G. 1986. LPS XVII: 738-739. [4] Steele, A.M., Korotev, R.L. and Haskin, L.A. 1989: this volume.

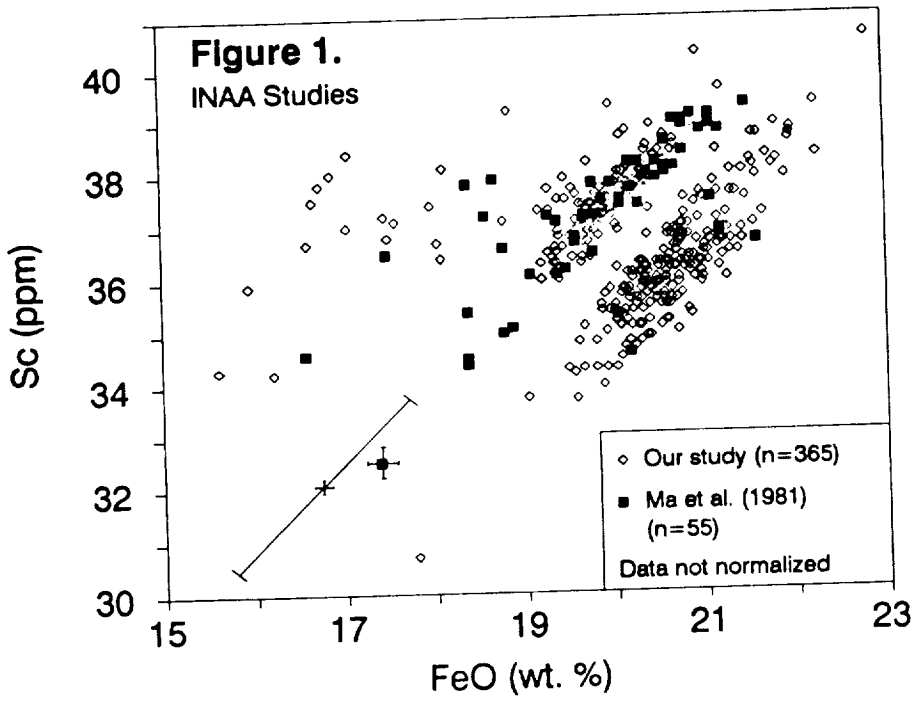

Figure 1. See [4] for explanation of error expressions for our data. Error estimates for the data of Ma et al. [2] are taken from their Appendix.

Table 1.

Comparison of Apollo 15 Green Glass Studies

Author	Split(s)	# analyses	% samples group A-C	% samples group D-E	analytical method(s)
Delano (1979)	15425,15 15426,72 15427,26	416	65%	35%	probe
Ma et al. (1981)	15426,?	55	93%	7%	INAA
Ryder (1986)	15426,26	113	83%	17%	probe
Steele et al. (1989)	15426,154	142	39%	61%	INAA+probe
Steele et al. (1989)	15426,9012	223	33%	67%	INAA+probe

Table 1. Comparison of the green glass group proportions found by different workers. Our percentages [4] have been recalculated on a vitrophyre-free basis for the comparison, since the other workers examined only vitric particles.

THERMODYNAMIC CALCULATIONS OF TRACE SPECIES IN VOLCANIC GASES: THE POSSIBLE APPLICATIONS OF NEW COMPUTER MODELS TO LUNAR VOLCANIC GASES AND SUBLIMATES; R. B. Symonds and W. I. Rose, Dept. of Geological Engineering, Geology, and Geophysics, Michigan Technological University, Houghton, MI 49931 (906-487-2714)

Over the past several years, we have studied metal transport in volcanic gases sampled from volcanoes on Earth. Our approach has consisted of using a variety of field sampling techniques at high-temperature volcanic fumaroles followed by thermochemical modeling of the resulting data. We have found the thermochemical modeling to be particularly useful in understanding chemical processes in terrestrial volcanic fumaroles. Here we will present some of our results of the thermodynamic calculations for terrestrial volcanic gases. We are now looking for new applications of our programs and propose to apply the models to lunar volcanic gases. Several possible applications will be discussed as well as the necessary inputs to our programs to complete the modeling. A major purpose of this presentation is to obtain feedback on the best possible input parameters for our computer models.

SOLVGAS and GASWORKS (our thermochemical models) are computer programs for calculating homogeneous and heterogeneous (GASWORKS) equilibrium in gaseous systems. They accommodate minor and trace components (e.g. Na, As, Cu, Zn, Pb, Mo) and species in addition to the major ones (those in the C-O-H-S-Cl-F system), and provide for strict oxygen mass balance, allowing calculation of the oxygen fugacity at any P and T. The programs calculate the distribution of hundreds of gas and solid (GASWORKS) species in a system of 30-40 components as a function of temperature and pressure using the basic formulations of equilibrium calculations for aqueous systems (1) modified for gases. The calculations consist of solving simultaneously a series of mass balance and mass action equations using a Newton-Raphson method.

By calculating the most stable gas species out of the hundreds possible, SOLVGAS and GASWORKS determine the molecular form in which elements are actually transported in the gas phase. The programs have been applied to trace element transport studies at terrestrial volcanoes. Examples of applications to Merapi Volcano, Indonesia (2) and Augustine Volcano, Alaska will be discussed. In both cases, the calculations show that (on Earth): 1) the concentration of most elements in high-temperature volcanic gases can be explained by equilibrium volatilization from magma, 2) most metals are transported as chloride gas species, and 3) sublimates at these fumaroles form in an order predicted by their equilibrium saturation temperatures.

SOLVGAS and GASWORKS are potentially applicable to a variety of lunar volcanological problems: 1) the speciation of major and trace components in lunar volcanic gases, 2) prediction of the concentration of trace elements in a lunar volcanic gas, and 3) the speciation and origin of lunar volcanic sublimates.

THERMODYNAMIC CALCULATIONS OF TRACE SPECIES IN VOLCANIC GASES: THE POSSIBLE APPLICATIONS OF NEW COMPUTER MODELS TO LUNAR VOLCANIC GASES AND SUBLIMATES; R. B. Symonds and W. I. Rose

To attack these problems, we need help to obtain (or derive a best estimate of)

1) the elemental composition of the lunar volcanic gases (C, O, H, S, Cl, F, Br),
2) the pressure and temperature conditions during degassing,
3) the range of compositions and mineralogy of the lunar basalts, and
4) the composition and mineralogy of the lunar volcanic sublimates.

This proposed study would improve on previous work (3-5) on lunar volcanic gases and sublimates by 1) considering more possible gas species than was done by (3), 2) providing a theoretical model for the origin of sublimates on the moon, and 3) predicting possible sublimate phases not described by (3-5).

(1) Reed M. H. (1982) Geochimica et Cosmochimica Acta, **48**, p. 513-528.
(2) Symonds R. B., Rose W. I., Reed M. H., Lichte F. E., Finnegan D. L. (1987) Geochimica et Cosmochimica Acta, 51, p. 2083-2101.
(3) Naughton J. J., Hammond D. A., Margolis S. V. and Muenow D. W. (1972) Proceedings of the Third Lunar Science Conference, p. 2015-2024.
(4) Meyer C. Jr., McKay D. S., Anderson D. H., and Butler P. Jr. (1975) Proceedings of the Sixth Lunar Science Conference, p. 1673-1699.
(5) Chou C. L., Boynton W. V., Sundberg L. L., and Wasson J. T. (1975) Proceedings of the Sixth Lunar Science Conference, p. 1701-1727.

PHENOCRYST CONTENT OF MARE VOLCANICS: INFERENCES FOR MAGMA MIGRATION MECHANISMS ON THE MOON G. Jeffrey Taylor, Institute of Meteoritics and Department of Geology, University of New Mexico, Albuquerque, NM 87131

A striking feature of lunar volcanic deposits is the rarity of phenocrysts grown at depth. Mare basalts have no more than a few percent of phenocrysts; pyroclastic glasses have less than one percent. Observed phenocrysts, such as those in Apollo 15 pyroxene-phyric basalts, formed when the basalts erupted (1,2). Even in Apollo 15 olivine basalts, among the basalts richest in phenocrysts, the phenocrysts seem to have grown in thick flows on the surface (3). This is in sharp contrast to terrestrial basalts, which are rarely free of phenocrysts (4); most basalts from the Aleutians, for example, contain 25 to 55% phenocrysts. Basalts associated with rifts, such as MORBs, contain fewer phenocrysts, (typically < 10%), but few are completely aphryic (A. M. Kudo, personal communication). I argue below that this difference in phenocryst content between typical terrestrial and lunar basalts is caused mostly by differences in migration rates due to differences in magma viscosities, and by the rarity of magma chambers on the Moon.

Magma migration

As Marsh (4) points out, it is improbable to observe terrestrial magmas near their liquidi, so they contain phenocrysts. Thus, it seems that mare basalt magmas had quite different thermal histories than did terrestrial basalts. This implies that they moved more rapidly from their source regions or traveled through hotter rock, or both. They also could not have spent significant time in subsurface holding chambers.

Transit time. The velocity of a magma moving by porous flow is directly proportional to the gravitational acceleration (g) and inversely proportional to viscosity (5). Lunar gravity is one-sixth of that on Earth; mare basaltic viscosities are about ten times less than those of terrestrial basalts. Thus, lunar magmas will flow from their source regions about 50% faster than terrestrial basaltic magmas. Once they reach the colder, more solid lithosphere (and perhaps even before), magmas cease migrating by porous flow and probably move by fluid fracture (5), essentially making their own dike-like conduits. As shown by Turcotte (e.g., 5) for laminar flow the velocity is proportional to g and h^2 (the conduit width), and inversely proportional to the viscosity. Because the conduit width is proportional to $g^{-1/3}$, the velocity of crack propagation (and hence magma migration) is directly proportional to $g^{1/3}$ and inversely proportional to viscosity. Therefore, magmas will move a factor of ten faster on the Moon because of the lower viscosities of lunar basaltic magmas and the weak dependence on gravity. It appears that there was less time available for cooling lunar magmas, so there would be fewer phenocrysts in magmas reaching the lunar surface. In addition, regional stress fields are proportional to gravity, leading to wider conduit widths and greater eruption rates on the Moon than on Earth (6).

Cooling rates during migration. A consequence of the larger conduit size is a slower cooling rate, leading to a greater time spent near the liquidus. The greater volume of magma coursing through a given conduit also would have led to greater heating of the surrounding wall rocks, thus limiting cooling of magmas in the channels. This, of course, would have led to fewer phenocrysts and less fractionation.

Magma chambers. Magma chambers are crystal factories. In them, magma ceases to migrate through the crust and cools by conduction, mainly through the top and bottom. Crystals form and sink or float. Although most are captured by the solidification front (7),

some escape and are mixed by convection or dissolved. If the fluid portion of the magma erupts, it will contain phenocrysts, their abundance increasing as the chamber crystallizes. Frequent eruption and replenishment might lead to a substantial amount of basalt erupted with low phenocryst contents, but eventually the system would produce some lavas laded with phenocrysts. The lack of phenocrysts in mare basalts indicates that magma chambers were rare on the Moon. This is supported by the absence of collapse structures in lunar volcanic regions (8), evidence for the absence of near-surface magma chambers. The general intensely brecciated nature of the upper lunar crust is consistent with the rarity of large magma chambers. It also suggests that mare basalt magmas might form extensive networks of dikes.

Where did mare basalt fractionation take place?

Suites of mare basalts show clear evidence for low-pressure fractional crystallization (e.g., 9); for example, calculations indicate that up to 25 wt.% of olivine and Fe-Ti oxides fractionated from Apollo 17 high-Ti basalts. If the basalts erupted without phenocrysts, where did this fractionation take place? There are two possibilities: First, it could have occurred in conduits as the magmas migrated through the crust. Some crystallization would have occurred along the walls, especially early in a magmatic cycle when the walls were cold. The crystals might nucleate on the walls, thus removing them from the flowing magma. Continued build up of such crystals would increase the viscosity of a zone near the walls, eventually reaching a point where the viscosity increases so much that the material behaves as a solid, i.e., a rheological locking point (4). Alternatively, much of the differentiation could have occurred in flows. Some thin mare basalt flows traveled for hundreds of kilometers (8), during which substantial amounts of differentiation could have taken place. As Walker et al. (3) showed, thick flows can also differentiate. Fractionation processes in thick, flowing, low viscosity lavas ought to be studied.

Implications

The unique rheological properties of lunar magmas and the tectonic environment in which they operated have several consequences. The rarity of magma chambers suggests that magma recharge was less effective on the Moon than it might be on Earth, although it could occur to some extent in a complex system of dikes. It seems unlikely that vast layers of ilmenite-rich cumulates were produced from mare basalt magmas, though such cumulates might have formed in lava lakes. For example, ilmenite-rich cumulates could exist in the bottom of the crater Jansen in Mare Tranquillitatis. If magma chambers were rare for mare volcanism, perhaps the magmas that produced highland rocks also rarely occupied them. If so, most pristine highland rocks formed in dikes, not large plutons. The presence of large exsolution lamellae in the pyroxenes in some of them might simply be a record of the depth of their emplacement, not the size of the magma bodies in which they formed.

References: 1) Dowty, E. et al. (1974) *J. Petrol.* **15**, 419-453. 2) Lofgren, G. et al. (1974) *PLSC 5th*, 549-567. 3) Walker, D. (1976) *PLSC 7th*, 1365-1389. 4) Marsh, B.D. (1981) *Contrib. Mineral. Petrol.* **78**, 85-98. 5) Turcotte, D. (1987) In *Magmatic Processes: Physicochemical Processes*, 69-74. 6) Wilson, L. and Head, J.W. (1988) *LPSC XIX*, 1283-1284. 7) Marsh, B.D. (1988) *Geol. Soc. Am. Bull.* **100**, 1720-1737. 8) Head, J.W. (1976) *Rev. Geophys. Space Phys.* **14**, 265-300. 8) Papike, J.J. et al. (1976) *Rev. Geophys. Space Phys.* **14**, 475-540.

IN SEARCH OF ANCIENT LUNAR PYROCLASTICS. S. J. Wentworth[1], D. J. Lindstrom[2], D. S. McKay[2], and R. M. Martinez[1]. [1]Lockheed, 2400 NASA Rd. 1, Houston, TX 77058; [2]NASA Johnson Space Center, Houston, TX 77058.

Background During previous studies of glass clasts in Apollo 16 regolith breccias, we found traces of mare and ultra Mg' (atomic Mg/Mg + Fe $\geq$0.90) glasses in the ancient (~4 Gy) regolith breccias [1,2]. Some of the ultra Mg' glasses have compositions similar to that of the hypothetical lunar komatiite proposed by [3], suggesting a pyroclastic origin for the ultra Mg' glasses. Trace element data for ancient mare glasses would be very important in understanding the systematics of the earliest mare volcanism, and the identification and characterization of lunar komatiitic glasses would be of great benefit in deciphering the history of the moon as a whole. Therefore, we have undertaken a search for individual mare and ultra Mg' glass spherules in ancient regolith breccias in order to characterize their major and trace element compositions.

Methods Samples included ancient regolith breccias 60016,165 and 66075,16. Splits of these samples had previously been disaggregated by both freeze-thaw (FT) and ultrasonic (S) techniques and sieved into standard lunar soil size fractions [2]. For this study, spherules were picked from the 150-250, 90-150, and 45-90 micrometer fractions of 60016,165FT, 60016,165S, 66075,16FT, and 66075,16S, and the 20-45 micrometer fraction of 60016,165S. Scanning electron microscopy and energy dispersive X-ray analysis (SEM/EDS) were used to identify possible mare or ultra Mg' glasses. Spherules of interest were analyzed by INAA according to methods similar to those previously tested for individual highland impact glasses from Apollo 16 regolith breccias [4]. The final step is electron microprobe major element analysis of flat polished surfaces of the glasses in order to obtain more accurate FeO contents than those determined by EDS; these numbers can be compared with INAA Fe data so that absolute abundances can be calculated for the INAA data (the spheres were not weighed because of their small sizes).

Results A total of 282 spherules was picked from 60016,165 and 66075,16 and analyzed by SEM/EDS. Most of the spherules are heterogeneous (recrystallized or devitrified) rather than homogeneous glass. This predominance of heterogeneous glass is consistent with our earlier results for the Apollo 16 ancient regolith breccia glasses [2]. Most of the spherules seem to have compositions typical of common highlands glasses. Quantitative EDS indicated that only two spherules, both from 60016,165S, had unusual compositions. Based on the EDS data, one sphere, 208A (from 60016,165S 20-45 μm), had a high FeO content, which is characteristic of mare glasses; the other unusual spherule, A-8 (from 60016,165S 150-250 μm), had a high Mg' value (0.89 by EDS).

The two unusual spheres and four typical highlands-type spheres were analyzed by INAA. Trace element data (Table 1) indicate that all of the spherules, with the possible exception of high Mg' glass A-8, are probably highlands impact glasses. The REE patterns (Fig. 1) for all but A-8 are typical of highlands impact melts, including the pattern for 208A, which had high FeO according to EDS. High Mg' glass A-8 has a similar pattern but lower abundances; most other trace element abundances in the high Mg' glass are also very low (Table 1). Electron microprobe major element data for high Mg' glass A-8 are given in Table 2. Spherule A-8 is not an ultra Mg' glass (microprobe Mg' = 0.86) but it has a major element composition similar to that of troctolitic-noritic ultra Mg' glass (Table 2). Both glasses have norms that consist mostly of olivine, orthopyroxene, and plagioclase (Table 2).

Several possible origins have been proposed for the ultra Mg' glasses. Possibilities include preferential removal of Fe (by impact volatilization or reduction of FeO to Fe during impact), mixing of lunar materials with very high Mg' meteoritic material, and derivation from high Mg' lunar material by impact or volcanic processes [1]. Of the different compositional types of high and ultra Mg' glass, troctolitic-noritic glasses 60016 A-8 and 65715,5-4 (Table 2) are the most likely candidates for a volcanic origin because of their similarities to the composition proposed by [3] for a lunar komatiite (Table 2). The trace elements in high Mg' glass A-8 do not clearly indicate a volcanic origin for the glass, however; e.g., a pristine volcanic glass would be expected to have much higher Ni and Co abundances.

Summary One of the most significant results of this study is that none of the 282 glasses analyzed by EDS have a definite mare composition, illustrating the extreme rarity of mare glasses in the ancient regolith breccias. High Mg' bead 60016,165S 150-250 μm A-8 is not an ultra Mg' glass as defined in [1], but it seems to be closely related to troctolitic-noritic ultra Mg' glass. The origins of these troctolitic-noritic glasses are still uncertain.

References: [1] Wentworth and McKay (1988) *Proc. LPSC 18th*, 67-77. [2] McKay et al. (1986) *Proc. LPSC 16th*, D277-D303. [3] Ringwood et al. (1987) *EPSL 81*, 105-117. [4] Wentworth et al. (1989) *LPS XX*, 1195-1196.

TABLE 1: INAA trace element abundances for Apollo 16 spheres. For A-8, absolute abundances are scaled to microprobe FeO. For other spherules, absolute abundances are based on masses (estimated from sizes).

	60016 A-8	60016 A-2	60016 208A	66075 C-1	66075 C-10	66075 D-12
	22.0 µg.	42.0 ng.	17.0 ng.	540. ng.	750. ng.	250. ng.
Na2O	0.280 ± 0.004	1.073 ± 0.024	0.149 ± 0.007	1.005 ± 0.015	0.0898 ±0.0016	0.853 ± 0.013
K2O	0.055 ± 0.006	———	———	0.37 ± 0.09	———	0.59 ± 0.09
CaO	6.0 ± 0.4	———	<20.	10.8 ± 2.3	8.6 ± 1.4	5.2 ± 2.0
FeO	8.94 ± 0.10	5.89 ± 0.16	10.24 ± 0.24	6.53 ± 0.08	6.49 ± 0.08	4.49 ± 0.07
Sc	5.96 ± 0.06	14.74 ± 0.25	21.9 ± 0.4	15.53 ± 0.18	13.22 ± 0.15	9.53 ± 0.12
Cr	1965. ± 24.	1460. ± 30.	1770. ± 40.	1470. ± 20.	1426. ± 19.	1116. ± 16.
Co	20.46 ± 0.23	10.7 ± 0.9	40.3 ± 1.9	23.5 ± 0.4	12.68 ± 0.24	30.0 ± 0.5
Ni	71. ± 4.	340. ± 100.	610. ± 160.	460. ± 40.	182. ± 20.	400. ± 40.
Rb	<1.2	<60.	<50.	<41.	5.7 ± 2.2	23. ± 7.
Cs	<0.07	<1.9	<2.9	0.66 ± 0.21	<0.31	1.39 ± 0.27
Sr	71. ± 8.	<500.	<1100.	110. ± 60.	110. ± 40.	240. ± 60.
Ba	92. ± 5.	430. ± 190.	<1600.	500. ± 50.	390. ± 30.	410. ± 60.
La	11.28 ± 0.13	48.8 ± 2.9	26.1 ± 1.7	69.7 ± 1.0	33.6 ± 0.5	33.7 ± 0.6
Ce	38.2 ± 0.5	119. ± 8.	55. ± 9.	187. ± 3.	106.3 ± 1.9	90.1 ± 2.5
Nd	19.7 ± 1.6	<110.	<120.	137. ± 14.	72. ± 8.	52. ± 13.
Sm	4.46 ± 0.17	15.7 ± 0.8	9.2 ± 0.7	25.8 ± 1.0	12.5 ± 0.5	11.6 ± 0.5
Eu	0.72 ± 0.03	<3.6	<5.	1.97 ± 0.22	1.65 ± 0.15	2.01 ± 0.23
Tb	0.966 ± 0.020	3.2 ± 0.5	<2.4	5.99 ± 0.18	3.53 ± 0.11	2.41 ± 0.15
Yb	2.94 ± 0.06	12. ± 3.	<27.	19.0 ± 0.9	11.2 ± 0.5	9.1 ± 0.8
Lu	0.359 ± 0.010	4.7 ± 1.1	<2.4	2.51 ± 0.18	1.52 ± 0.09	1.95 ± 0.15
Zr	183. ± 13.	<1100.	<1400.	970. ± 120.	550. ± 70.	350. ± 100.
Hf	4.00 ± 0.07	14.9 ± 1.3	8.7 ± 1.7	23.1 ± 0.5	14.1 ± 0.3	9.9 ± 0.4
Ta	0.58 ± 0.04	2.8 ± 1.4	<4.	2.6 ± 0.3	1.38 ± 0.18	1.23 ± 0.27
U	0.624 ± 0.026	<10.	<13.	2.8 ± 0.4	1.11 ± 0.20	1.8 ± 0.4
Th	1.05 ± 0.03	6.4 ± 0.9	4.3 ± 1.0	10.48 ± 0.30	6.19 ± 0.18	4.98 ± 0.28
As	0.056 ± 0.024	<10.	<23.	<1.3	<0.4	———
Se	1.2 ± 0.4	<31.	<50.	<7.	<6.	<8.
Sb	<0.007	<2.7	<3.	<0.21	<0.09	<0.30
W	0.89 ± 0.05	3460. ± 50.	38700. ± 500.	142.7 ± 2.6	71.6 ± 1.2	36.1 ± 1.3
Ir	<0.006	<0.15	<0.39	<0.06	<0.023	<0.028
Au	0.0021 ±0.0006	3.3 ± 0.3	1.1 ± 0.4	<0.033	<0.019	0.86 ± 0.04
Ag	<0.7	<26.	<40.	<6.	<3.1	<5.
Zn	5.9 ± 0.7	71. ± 24.	210. ± 50.	24. ± 6.	9. ± 4.	29. ± 7.
Br	0.41 ± 0.07	<11.	<13.	<5.	<0.7	<3.1

TABLE 2: Major element compositions.

	(1)	(2)	(3)
SiO_2	45.2	47.4	45.4
TiO_2	0.54	1.33	0.86
Al_2O_3	6.61	12.6	9.56
Cr_2O_3	0.40	0.24	0.28
FeO	14.8	3.15	9.05
MnO	0.19	0.03	0.11
MgO	26.9	28.7	30.4
CaO	5.31	5.86	5.25
Na_2O	0.10	0.08	0.23
K_2O	n.d.	0.20	0.02
P_2O_5	n.d.	0.07	0.17
TOTAL	100.0	99.6	100.0
Mg'	0.76	0.90	0.86
Major normative minerals (wt%):			
Feldspar	18.4	30.6	27.1
Olivine	43.4	25.0	47.3
Diopside	7.0	0.0	0.0
Hypersthene	29.5	39.3	24.6

(1) Proposed komatiite [3].
(2) Ultra Mg' glass 65715,5-4 [1].
(3) High Mg' glass 60016,165S 150-250 µm A-8.

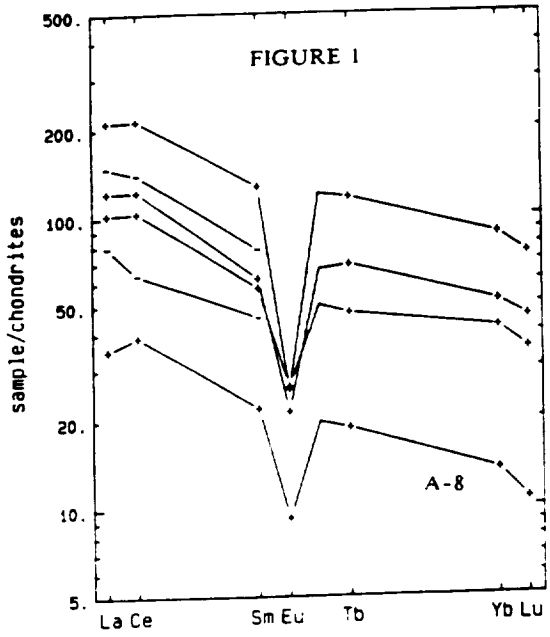

List of Workshop Participants

Judy Allton
Mail Code C23
Lockheed ESCO
2400 NASA Road 1
Houston, TX 77058

Robert Andres
Department of Geological Engineering
Geology and Geophysics
Michigan Technological Institute
Houghton, MI 49931

Jafar Arkani-Hamad
McGill University
Montreal, Quebec
Canada

Abhijit Basu
Department of Geology
Indiana University
Bloomington, IN 47405

Paul Buchanan
Department of Geosciences
University of Houston
Houston, TX 77004

Mark J. Cintala
Mail Code SN21
NASA Johnson Space Center
Houston, TX 77058

Cassandra Coombs
Mail Code SN15
NASA Johnson Space Center
Houston, TX 77058

Donna K. Dawson
Alcoa/Goldsworthy Engineering
23930 Madison Street
Torrance, CA 90505

Shan DeSilva
Lunar and Planetary Institute
3303 NASA Road 1
Houston, TX 77058

John Delano
Department of Geological Sciences
State University of New York
Albany, NY 12222

Tammy Dickinson
Mail Code SN2
NASA Johnson Space Center
Houston, TX 77058

John Dietrich
Mail Code SN2
NASA Johnson Space Center
Houston, TX 77058

Darryl Futrell
6222 Haviland
Whittier, CA 90601

Everett Gibson
Mail Code SN2
NASA Johnson Space Center
Houston, TX 77058

B. Ray Hawke
Planetary Geosciences Division
Hawaii Institute of Geophysics
University of Hawaii
Honolulu, HI 96822

Grant Heiken
Geology Group, D462
Los Alamos National Laboratory
Los Alamos, NM 87545

Odette James
U. S. Geological Survey
959 National Center
Reston, VA 22092

Yuequn Jin
Department of Geological Sciences
University of Tennessee
Knoxville, TN 37996

John Jones
Mail Code SN2
NASA Johnson Space Center
Houston, TX 77058

Jim Jordan
Department of Geology
Lamar University
P.O. Box 10031
Beaumont, TX 77710

Derrick Kong
E. C. Box 236
Massachusetts Institute of Technology
3 Ames Street
Cambridge, MA 02139

David J. Lindstrom
Mail Code SN2
NASA Johnson Space Center
Houston, TX 77058

Marilyn Lindstrom
Mail Code SN2
NASA Johnson Space Center
Houston, TX 77058

Gary Lofgren
Mail Code SN2
NASA Johnson Space Center
Houston, TX 77058

John Longhi
Lamont-Doherty Geological Observatory
Palisades, NY 10964

David McKay
Mail Code SN14
NASA Johnson Space Center
Houston, TX 77058

Gordon A. McKay
Mail Code SN2
NASA Johnson Space Center
Houston, TX 77058

Charles Meyer
Mail Code SN2
NASA Johnson Space Center
Houston, TX 77058

Yas Miura
Department of Mineral Sciences
Faculty of Sciences
Yamaguchi University
Yoshidai
Yamaguchi 753, Japan

Don Morrison
Mail Code SN2
NASA Johnson Space Center
Houston, TX 77058

A. V. Murali
Lunar and Planetary Institute
3303 NASA Road 1
Houston, TX 77058

Dennis Nelson
National Research Council
NASA Johnson Space Center
Houston, TX 77058

Larry Nyquist
Mail Code SN2
NASA Johnson Space Center
Houston, TX 77058

William Phinney
Mail Code SN2
NASA Johnson Space Center
Houston, TX 77058

M. N. Rao
Mail Code SN2
NASA Johnson Space Center
Houston, TX 77058

Arch Reid
Department of Geosciences
University of Houston
Houston, TX 77004

Graham Ryder
Lunar and Planetary Institute
3303 NASA Road 1
Houston, TX 77058

Harrison (Jack) Schmitt
P.O. Box 14338
Albuquerque, NM 87191-4338

Ben Schuraytz
Lunar and Planetary Institute
3303 NASA Road 1
Houston, TX 77058

C. K. (Chip) Shearer
Institute for the Study of Mineral Deposits
South Dakota School of Mines and Technology
Rapid City, SD 57701

Chi-Yu Shih
Lockheed ESCO
2400 NASA Road 1
Houston, TX 77058

Paul Spudis
U. S. Geological Survey
2255 N. Gemini Drive
Flagstaff, AZ 86001

Alison Steele
Department of Earth and Planetary Sciences
Campus Box 1169
Washington University
St. Louis, MO 63130

Robert Symonds
Department of Geology and Engineering
Geology and Geophysics
Michigan Technological Institute
Houghton, MI 49931

G. Jeffrey Taylor
Institute of Meteoritics
University of New Mexico
Albuquerque, NM 87131

Larry Taylor
Department of Geological Sciences
University of Tennessee
Knoxville, TN 37996

Ann Therriault
Department of Geosciences
University of Houston
Houston, TX 77004

Peter Thy
Mail Code SN2
NASA Johnson Space Center
Houston, TX 77058

Susan Wentworth
Mail Code C23
Lockheed ESCO
2400 NASA Road 1
Houston, TX 77058